GAME THEORETIC APPROACH TO RADIO RESOURCE MANAGEMENT ON THE REVERSE LINK FOR MULTI-RATE CDMA WIRELESS DATA NETWORKS

by

Wiklom Teerapabkajorndet

B.Eng., Prince of Songkhla University, Thailand 1991

M.B.A., Prince of Songkhla University, Thailand 1996

M.Eng., University of Colorado at Boulder, 1998

Submitted to the Graduate Faculty of

School of Information Science in partial fulfillment

of the requirements for the degree of

Doctor of Philosophy

University of Pittsburgh

2004

UNIVERSITY OF PITTSBURGH

FACULTY OF INFORMATION SCIRNCE AND TELECOMMUNICATIONS

This dissertation was presented

by

Wiklom Teerapabkajorndet

It was defended on

November 17, 2004

and approved by

Dr. Richard Thompson, PhD, Professor

Dr. David Tipper, PhD, Associate Professor

Dr. Marwan Simaan, PhD, Professor

Dr. John Duffy, PhD, Professor

Dr. Prashant Krishnamurthy, PhD, Assistant Professor
Dissertation Director

GAME THEORETIC APPROACH TO RADIO RESOURCE MANAGEMENT ON THE REVERSE LINK FOR MULTI-RATE CDMA WIRELESS DATA NETWORKS

Wiklom Teerapabkajorndet, PhD

University of Pittsburgh, 2004

This work deals with efficient power and rate assignment to mobile stations (MSs) involved in bursty data transmission in cellular CDMA networks. Power control in the current CDMA standards is based on a fixed target signal quality called signal to interference ratio (SIR). The target SIR represents a predefined frame error rate (FER). This approach is inefficient for data-MSs because a fixed target SIR can limit the MS's throughput. Power control should thus provide dynamic target SIRs instead of a fixed target SIR. In the research literature, the power control problem has been modeled using game theory. A limitation of the current literature is that in order to implement the algorithms, each MS needs to know information such as path gains and transmission rates of all other MSs. Fast rate control schemes in the evolving cellular data systems such as cdma2000-1x-EV assign transmission rates to MSs using a probabilistic approach. The limitation here is that the radio resources can be either under or over-utilized. Further, all MSs are not assigned the same rates. In the schemes proposed in the literature, only few MSs, which have the best channel conditions, obtain all radio resources. In this dissertation, we address the power control issue by moving the computation of the Nash equilibrium from each MS to the base station (BS). We also propose equal radio resource allocation for all MSs under the constraint that only the maximum allowable radio resources are used in a cell. This dissertation addresses the problem of how to efficiently assign power and rate to MSs based on dynamic target SIRs for bursty transmissions. The proposed schemes in this work maximize the throughput of each data-MS while still providing equal allocation of radio resources to all MSs and achieving full radio resource utilization in each cell. The proposed schemes result in power and rate control algorithms that however require some assistance from the BS. The performance evaluation and comparisons with cdma2000-1x-Evolution Data Only (1x-EV-DO) show that the proposed schemes can provide better effective rates (rates after error) than the existing schemes.

TABLE OF CONTENTS

PREFACE xi
1.0 INTRODUCTION 1
1.1. BACKGROUND OF RADIO RESOURCE MANAGEMENT IN CELLULAR NETWORKS 1
1.2. CURRENT LIMITATIONS OF EXISTING RRM SCHEMES 5
1.3. RESEARCH GOALS AND PROBLEM STATEMENT 7
1.4. ESSENCE OF THE PROPOSED SOLUTION 9
1.5. RESEARCH CONTRIBUTIONS 10
1.6. ORGANIZATION 11
2.0 A SURVEY OF LITERATURE 12
2.1. INTRODUCTION 12
2.2. POWER AND RATE ALLOCATION STUDIES IN THE RESEARCH LITERATURE 13
2.2.1. Power control 13
2.2.1.1. Power control studies based on the SIR balancing approach 15
2.2.1.2. Power control based on game theory 17
2.2.1.3. Open research issues of power control for bursty traffic 20
2.2.2. Rate control 20
2.2.2.1. Distributed rate control 24
2.2.2.2. Network assisted rate control 24
2.2.2.3. Centralized rate control 25
2.2.2.4. Evolving rate control in 1x-EV-DV revision D 26
2.2.3. Joint rate and power allocation 26
2.3. CONCLUSIONS 29
3.0 PROBLEM FORMULATION AND SOLUTION APPROACHES 31
3.1. INTRODUCTION 31
3.2. NASH EQUILIBRIUM COMPUTATION AT MS 32
3.3. NASH EQUILIBRIUM COMPUTATION AT BS 37
3.4. OTHER LIMITATIONS IN THE LITERATURE AND SOLUTION APPROACHES 39
3.5. ASSUMPTIONS AND LIMITATIONS OF THIS WORK 43
3.6. CONCLUSIONS 43
4.0 ANALYSIS OF UTILITY FUNCTION FOR POWER CONTROL 44
4.1. INTRODUCTION 44
4.2. UTILITY FUNCTION EXPRESSIONS 45
4.3. UTILITY FUNCTION ANALYSES 51
4.4. CONCLUSIONS 56
5.0 POWER CONTROL ALGORITHMS 57
5.1. INTRODUCTION 57

5.2. PROPOSED POWER CONTROL ALGORITHM 58
5.2.1. Adaptive pricing algorithm 62
5.3. RUNNING TIME OF THE ALGORITHM 65
5.4. NUMERICAL ANALYSIS FOR CONTINUOUS TRANSMISSIONS 66
5.4.1. Experimental design 66
5.4.2. Numerical results for the effect of feedback information 69
5.4.3. Numerical results for the effect of the number of cells and shadow fading 72
5.4.4. Conclusions of power control for continuous transmissions 74
5.5. NUMERICAL ANALYSIS FOR BURSTY TRANSMISSIONS 75
5.5.1. Experimental design 75
5.5.2. Convergence analysis 76
5.5.3. Performance evaluation 78
5.6. CONCLUSIONS 85
6.0 RATE AND POWER CONTROL ALGORITHMS 86
6.1. INTRODUCTION 86
6.2. PROPOSED RATE AND POWER CONTROL SCHEMES 87
6.2.1. Overall design 87
6.2.2. Problem formulation based on game theory 89
6.2.3. A controllable Nash equilibrium using the adaptive pricing algorithm 90
6.2.4. Equal rate control 90
6.2.5. Complexity analysis 93
6.3. NUMERICAL ANALYSIS 94
6.3.1. Experimental design 94
6.3.2. Rate allocation comparisons 95
6.3.3. Analysis of the sentitivity of the convergence of the proposed schemes to Δ 97
6.3.4. Simulation analysis of bursty and multi-rate transmissions 99
6.3.5. Performance evaluation 105
6.4. CONCLUSIONS 113
7.0 SUMMARY 114
APPENDIX A 117
BIT ERROR RATE EXPRESSION 117
APPENDIX B 121
DERIVATION OF THE FEASIBLE RANGE OF THE PRICING COEFFICIENT 121
APPENDIX C 123
INTRODUCTION TO GAME THEORY 123
BIBLIOGRAPHY 125

LIST OF TABLES

Table 2.1 Supported power control options for each reverse link channel type of cdma2000 and UMTS 23
Table 2.2 Comparison of pptimal power and rate assignment schemes 30
Table 4.1 The equilibrium SIR (not in dB) for different pricing coefficients for different utility functions 54
Table 4.2 The equilibrium SIR for different pricing coefficients and a pricing index for the utility in bps in Equation (4.19) 54
Table 5.1 Average SIR results (dB) 79
Table 6.1 SIR threshold (γ_{th}) in dB for each data rate (R in kbps) 93
Table 6.2 Allocated rates (R in kbps) and average SIRs (γ in dB) in the case of employing the MC approach in the proposed schemes 101
Table 6.3 Allocated rates (R in kbps) and average SIRs (γ in dB) in the case of employing the VSF approach in the proposed schemes 102
Table C.1 Prisoner's dilemma 123

LIST OF FIGURES

Figure 1.1 Cellular network architecture 2
Figure 2.1 Reverse link power control in CDMA systems 13
Figure 2.2 Classification of power control for wireless data networks 14
Figure 2.3 Graphical illustration of the optimum transmitter power [2] 16
Figure 2.4 Classification of rate control 24
Figure 3.1 Utility function with different values of pricing coefficients 35
Figure 3.2 Utility of MS1 35
Figure 3.3 Utility of MS2 36
Figure 3.4 The Nash Equilibrium 36
Figure 3.5 Utility when computing the equilibrium at a MS as Equation (3.1) and at a BS as Equation (3.10) 38
Figure 3.6 Required transmit power for different levels of extra-cell interference when a single MS is in a cell at 500 m from a BS 41
Figure 3.7 Intra-cell interference results from a single MS in a cell at 500 m from a BS for different extra-cell interference levels 41
Figure 3.8 SIR results from a single MS in a cell moving farther away from a BS when the extra-cell interference is -167 dBm and the maximum allowable transmit power is 1 mW. 42
Figure 4.1 Concavity illustrations 47
Figure 4.2 Utility in bits per joule (bpj) 49
Figure 4.3 Utility in bits per second (bps) 49
Figure 4.4 Sensitivity of the utility function in Equation (4.16) with the pricing coefficient 51
Figure 4.5 Sensitivity of the utility function in Equation (4.17) with the pricing coefficient 52
Figure 4.6 Sensitivity of the utility function in Equation (4.18) with the pricing coefficient 52
Figure 4.7 Effect of the pricing index (n) on the utility function in Equation (4.19) when c=1 55
Figure 4.8 Effect of the pricing index (n) on the utility function in Equation (4.19) when $c=10^8$ 55
Figure 4.9 Effect of the pricing index (n) on the utility function in Equation (4.19) when $c=5\times10^8$ 56
Figure 5.1 Equal received SIR allocation for 9.6 kbps given the maximum allowed interference level 60
Figure 5.2 Block diagram of power control for bursty transmission 61
Figure 5.3 Adaptive pricing algorithm 64
Figure 5.4 A two-cell scenario 67
Figure 5.5 A seven-cell scenario 68
Figure 5.6 Interference level for 2-cell case 70
Figure 5.7 Average transmit power of each MS for 2-cell case 71
Figure 5.8 SIR for 2-cell case 71
Figure 5.9 FER for a 2-cell case 72
Figure 5.10 Interference for 2 and 7 cells with/without shadow fading 73

Figure 5.11 SIR for 2 and 7 cells with/without shadow fading 73
Figure 5.12 FER for 2 and 7 cells with/without shadow fading 74
Figure 5.13 Effective rates for 2 and 7 cells with/without shadow fading 74
Figure 5.14 On-off traffic source model 75
Figure 5.15 Average convergence rates in the case of 8 MSs in each cell for a 7-cell scenario without shadow fading 77
Figure 5.16 Convergence rates in the case of 8 MSs in each cell for a 7-cell scenario with shadow fading 77
Figure 5.17 Convergence rates for different numbers of MSs when shadow fading is considered 78
Figure 5.18 Average SIR for each number of active MSs (bursts) 80
Figure 5.19 Average interference for each number of active MSs (bursts) 80
Figure 5.20 Average effective rate for each number of active MSs (bursts) 81
Figure 5.21 Average effective rate in cell no. 1 (the center cell) 82
Figure 5.22 Average effective rate in cell no. 2 82
Figure 5.23 Average effective rate in cell no. 3 83
Figure 5.24 Average effective rate in cell no. 4 83
Figure 5.25 Average effective rate in cell no. 5 84
Figure 5.26 Average effective rate in cell no. 6 84
Figure 5.27 Average effective rate in cell no. 7 85
Figure 6.1 Block diagram of the proposed rate and power control schemes 88
Figure 6.2 Equal SIR allocations when the rate adaptation is based on the MC approach 92
Figure 6.3 Equal SIR allocations when the rate adaptation is based on the VSF approach 92
Figure 6.4 Flowchart of the equal rate control algorithm 93
Figure 6.5 Sample simulation results of assigned rates in 1x-EV-DO 96
Figure 6.6 Sample simulation results of equal rate assignments (bps) based on MC in the proposed scheme 96
Figure 6.7 Sample simulation results of equal rate assignment (bps) based on VSF in the proposed scheme 97
Figure 6.8 Sample simulation results for observing the convergence of interference to the threshold (-167 dBm) in the MC case when Δ=1dB 98
Figure 6.9 Sample simulation results for observing the convergence of interference to the threshold (-167 dBm) in the MC case when Δ=10dB 98
Figure 6.10 Sample simulation results for observing the convergence of interference to the threshold (-167 dBm) in the MC case when Δ=20dB 99
Figure 6.11 Average effective rate of each MS in the under-utilization case when the standard deviation of shadow fading is 0 dB 102
Figure 6.12 Average interference in the under-utilization case when the standard deviation of shadow fading is 0 dB 103
Figure 6.13 Average effective rate of each MS in the under-utilization case when the standard deviation of shadow fading is 7.5 dB 103
Figure 6.14 Average interference in the under-utilization case when the standard deviation of shadow fading is 7.5 dB 104
Figure 6.15 Average effective rate of each MS in the over-utilization case 104
Figure 6.16 Average interference in the over-utilization case 105

Figure 6.17 Average effective rates per MS in cell no. 1 (the centered cell) – all MS are moving at 50 kmph..... 106
Figure 6.18 Average effective rates per MS in cell no. 2 – all MS are moving at 50 kmph 106
Figure 6.19 Average effective rates per MS in cell no. 3 – all MS are moving at 50 kmph 107
Figure 6.20 Average effective rates in cell no. 4 – all MS are moving at 50 kmph 107
Figure 6.21 Average effective rates in cell no. 5 – all MS are moving at 50 kmph 108
Figure 6.22 Average effective rates per MS in cell no. 6 – all MS are moving at 50 kmph 108
Figure 6.23 Average effective rates per MS in cell no. 7 – all MS are moving at 50 kmph 109
Figure 6.24 Average effective rates per MS in cell no. 1 – Mixture of pedestrians and moving MSs 110
Figure 6.25 Average effective rates per MS in cell no. 2 – Mixture of pedestrians and moving MSs 110
Figure 6.26 Average effective rates per MS in cell no. 3 – Mixture of pedestrians and moving MSs 111
Figure 6.27 Average effective rates per MS in cell no. 4 – Mixture of pedestrians and moving MSs 111
Figure 6.28 Average effective rates per MS in cell no. 5 – Mixture of pedestrians and moving MSs 112
Figure 6.29 Average effective rates per MS in cell no. 6 – Mixture of pedestrians and moving MSs 112
Figure 6.30 Average effective rates per MS in cell no. 7 – Mixture of pedestrians and moving MSs 113
Figure A.1 *FER* and P_e relationship for different M..... 118
Figure A.2 BER as a function of the SIR..... 120

PREFACE

I would like to thank both the Thai government and Prince of Songkhla University for giving me a chance to pursue my Ph.D. education.

My thanks to the Graduate Program in Telecommunications at the University of Pittsburgh: I have been profoundly able to learn the subject of Telecommunications from foundations all the way to system aspects. Additionally, I would like to thank the program for the financial support during my study in the program.

This dissertation has developed under the guidance of my dissertation adviser: Dr. Prashant Krishnamurthy. He has taught me how to do research and helped me in many aspects. Without his intellectual guidance, I might not have been able to learn how to do research in such a short period of time.

I also gratefully acknowledge the support and insightful comments from my dissertation committee: Dr. Richard Thompson, Dr. David Tipper, Dr. Marwan Simaan and Dr. John Duffy.

My sincere thanks to all my friends in Pittsburgh: they have made my life here so spectacular. Even in my rough times, they were always there to comfort me. I cannot imagine how lucky I was to be here with all of them.

Last but not least, this dissertation would not have been possible without the loving care of my family in Thailand. Thank you.

1.0 INTRODUCTION

The existing voice cellular networks have been very successful and have resulted in widespread use thorough the world. Due to the remarkable growth of the Internet, the next generation cellular networks are being developed to offer new services for data users as the concept of *anywhere* and *anytime* communications becomes close to reality. With this new paradigm of wireless networks, the question of how to design wireless communications for data traffic has to be revisited. Radio resource management (RRM) is an essential element that has to be explored for this transformation. Wireless cellular networks require RRM to provide communication services over the air interface to a mobile user. Since radio resources are scarce and have to be shared by all users, efficient RRM is needed so as to completely utilize the available radio resources and to satisfy all mobile users' service requirements. To fulfill this objective of RRM, this dissertation investigates a new approach to RRM that maximizes each mobile data user's satisfaction while using the available radio resources to the greatest possible extent.

This chapter is intended to provide an overview of this dissertation. Firstly, background material related to RRM is explained to provide some basic concepts for readers who are not familiar with this area. Next, the limitations of the current RRM for wireless data networks are discussed and the problem statement focused on in this dissertation is given. Then a brief explanation of the proposed solution approach in this dissertation is provided and major research contributions are listed. At the end of this chapter, the organization of this dissertation is presented.

1.1. BACKGROUND OF RADIO RESOURCE MANAGEMENT IN CELLULAR NETWORKS

With the success of code division multiple access (CDMA) in the IS-95 standard (one of a second generation wireless network), CDMA is the predominant technology being implemented for the next generation wireless networks. Examples of standards being developed for the next generation cellular networks are Wideband CDMA (developed by Universal Mobile Telecommunication Services - UMTS), cdma2000, cdma2000-1x-Evolution for Data Only (1x-EV-DO), High Speed Downlink Packet Access

(HSDPA) and cdma2000-1x-Evolution-Data and Voice (1x-EV-DV) [1]. CDMA employs spread spectrum technology, which allows multiple users to access the entire frequency bandwidth at the same time. Like other cellular technologies, CDMA cellular networks basically consist of a wired backbone part and a radio access part as shown in Figure 1.1. The backbone provides interconnections among radio access ports or base stations (BSs). Each BS provides radio communications to mobile stations (MSs) in different coverage areas. The BSs communicate with each other through a base station controller (BSC) and a mobile switching center (MSC) or a General packet radio service Support Node (GSN) that are further connected to the backbone network that can be the public switched telephone network or the Internet. Before a MS can send its information (e.g., voice and data) to a BS, radio communication between the MS and the BS must be established first. Three key *radio resources* that must be assigned to the MS in order to setup the radio communication are the BS, a waveform channel, and transmitted power [2]. Loosely speaking, the process of making decisions related to these radio resource assignments is called radio resource management (RRM).

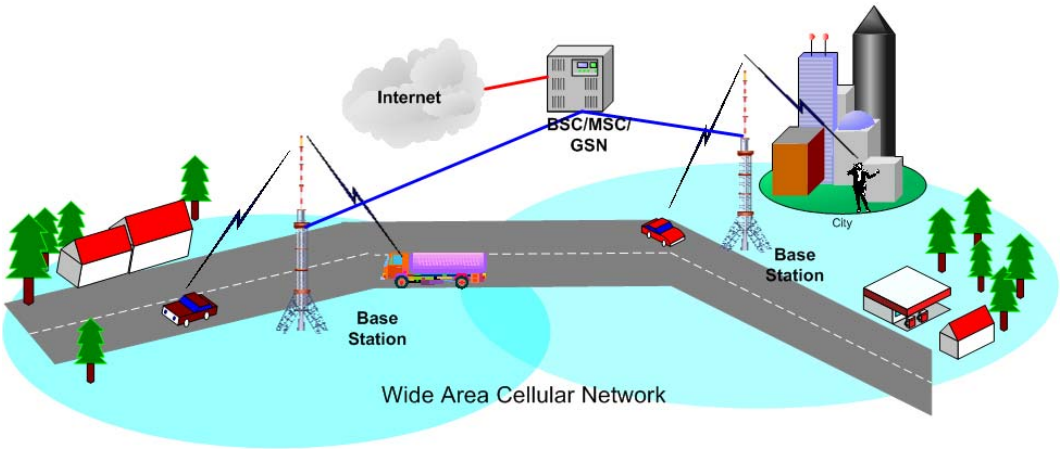

Figure 1.1 Cellular network architecture

RRM encompasses the protocols and mechanisms enabling each MS to use the best radio communications channel available as well as to maintain the proper transmit powers (power control). The objective of radio resource management is two-fold – to enable good communications over a radio link and to eliminate unnecessary interference between radio transmissions at the same or nearby frequencies. *Power management* (PM) overlaps with radio resource management in that it involves strict control of the transmit power and also includes algorithms, protocols and strategies to reduce the power consumption in a MS at all levels. Radio resource management and power management form very important components for efficient and smooth operation of any wireless system [3]. Radio resource management is strongly tied to the quality of service received by a mobile station. In a system where radio resource management is not

properly implemented, certain mobile stations may be denied service or obtain poor service at best and the entire system may be rendered unstable at worst.

RRM consists of three tasks: power control, waveform assignment (or rate control in multi-rate wireless networks since the waveform influences the rate) and handoff (BS assignment). Radio resource management continually manages and changes the radio resources such that a MS has the best communication channel all the time. The definition of the *best* in this context is ambiguous, but for voice cellular networks, this implies providing a fixed target signal-to-interference ratio (SIR) denoted by γ in (1.1).

$$\gamma_i = \frac{W}{R_i} \frac{h_i p_i}{\sum_{j \neq i} h_j p_j + \sigma^2} \tag{1.1}$$

The SIR or energy per bit to interference density ratio of MS i (γ_i) can be found from the transmitted power of MS i (p_i), the path loss from the MS i to the BS (h_i), the spread spectrum bandwidth (W), the data transmission bit rate of the MS i (R_i) and the variance of the AWGN noise at the receiver of the BS (σ^2). The SIR can be mapped to the quality of a radio communication channel in terms of the probability of successfully receiving packets at the receiver. For a given data rate R, a corresponding packet error rate (PER), and a given radio propagation condition, the target SIR that achieves this PER is fixed. Due to the changing radio propagation conditions, the target SIR may have to be adjusted periodically.

The SIR changes as MSs move and so, a MS's transmitted power will also need to be continually updated to maintain an acceptable SIR. This mechanism is called power control. In current CDMA systems, open-loop and closed-loop power control are used [4]. In open loop power control, the MS measures the signal quality of a *reference channel* from the base station. There may be a variety of metrics (such as the received signal strength (RSS), the SIR or the frame or bit error rate) for determining the appropriate power control action. For example, if the RSS, the SIR or the bit error rate (in the standards of CDMA systems, this metric is the SIR) is better than the target acceptable value, the mobile station will automatically reduce it's transmit power. If the signal quality is not good, the mobile station will increase the transmit power. Open loop power control is not very accurate as the characteristics of the waveform or channel used by the MS will be different from those of the reference channel. Closed loop power control eliminates the disadvantages of open-loop power control by implementing a feedback mechanism between the BS and the MS. The BS measures the quality of the signal received from the mobile station and indicates what actions the mobile terminal should take via control signaling on the forward channel.

Another aspect of RRM is base station and channel assignment (this is in addition to the control of the transmitted power at the MS and the BS). The BS covers a geographical area that is referred to as a cell. In most cases, each BS has a preset number of waveforms or channels that cannot be changed. Usually, one or more of the channels are allocated to a MS within the cell for communication. As much of the traffic on the air becomes data, the next generation wireless networks are evolving towards all data networks that can provide multi-rate services by applying rate adaptation techniques to the waveform channel. Accordingly, the simple waveform and channel assignment with a single transmission rate in the traditional voice cellular networks is evolving into a more complicated task called *rate control* [5, 6]. Recently, fast rate control has been developed in 1x-EV-DO to assign transmission rates on a per frame basis instead of slow rate control on a per packet burst basis in cdma2000. This fast rate control can provide better radio resource utilization than slow rate control. In this research, we also focus on the rate control scheme in 1x-EV-DO and use it for comparison with our approach.

As MSs move away from a BS, their ability to communicate with the current BS degrades even with the changes in the transmit power. This is primarily due to the limited maximum transmit power at both the BS and the MS and the MSs will need to switch their connections to neighboring base stations (handoff). At some point of time, a decision has to be made to handoff [7] from one base station to another. Handoff can be classified into two types: hard handoff and soft handoff. In hard handoff, only one BS, which has the best signal quality, is assigned to a MS. In soft handoff, several BSs, which can provide better signal quality than a threshold level, are assigned to a MS at the same time. *In this research, handoff is not considered.*

In summary, RRM requires (a) selection of a base station (b) assignment of a waveform or channel to the MS for transmission (c) assignment of a transmit power to each channel/rate assigned to each MS continually to reduce system-wide interference while maintaining adequate signal quality (d) possibly changing the transmit power and rates used by the MS depending on the global usage of the radio resources.

A lot of research has been done in this area for voice-oriented systems but only a little has been done for mobile data networks. Due to the different characteristics of data and voice, RRM for mobile data networks, which is composed of power control, rate control and handoff, requires more investigation such that it can utilize the scarce radio resources efficiently. RRM on the reverse link (the communication link where the transmitter is the MS and the receiver is the BS) and on the forward link (the communication link that has the opposite direction to the reverse link) are different. On the forward link, there is only one transmitter (the BS) and the cellular standards for data traffic such as cdma2000-1X-EV-DO (the evolution of cdma2000) and high speed downlink packet data access (HSDPA-the evolution of

UMTS) have recognized these issues for data traffic and *schedule* packet transmissions based on the requirements of mobile stations (MSs) such that there is almost no interference *within* a single cell [8, 9]. However, on the reverse link of mobile data networks, MSs have asynchronous transmissions and continue to use the traditional RRM from voice cellular networks. Therefore, the focus of this research is radio resource management on the reverse link for wireless data systems.

1.2. CURRENT LIMITATIONS OF EXISTING RRM SCHEMES

The existing RRM schemes in both current cellular systems and research literature are not efficient for the evolving wireless data networks. The major issues that cause this inefficiency are discussed in this section.

In practice, the traditional power control in RRM is based on fixed target SIR schemes to achieve a certain packet error rate (PER) level. In the case of voice cellular networks, the target PER is typically 1%. The corresponding SIR is 6-7 dB depending on the channel conditions [10]. A PER that is lower than this target does not improve the voice quality in a way that the human ear can perceive[11]. In contrast, a larger number of successfully transmitted packets at a receiver, as a result of a low PER, can improve the transmission throughput in mobile data networks. If voice traffic experiences a PER that is more than 1%, we can notice the deterioration of natural voice. In comparison, data traffic can tolerate longer transmission delays than voice and packet retransmission can be employed in the case of a high PER. Therefore, there is no single target PER that a data-MS needs to absolutely keep all the time like in the case of a voice-MS [11-13]. Accordingly, we see the limitation of the existing power control schemes when used in mobile data networks in that they cannot utilize the available radio resources efficiently. The different characteristics of data compared to voice traffic provide a challenge in designing more flexible and more efficient power control schemes rather than reusing the existing ones that are more suitable for voice traffic.

The power control problem is quite complicated as increasing the SIR of one MS will hurt the SIR of another MS. The actions of other MSs will affect the actions and strategies of a given MS making this problem suitable for modeling by using a game theoretic approach (see Appendix C for introduction). In the literature, non-cooperative game theory has been applied to model power control in wireless data networks [14, 15]. The basic idea here is that every MS in a cell tries to maximize its satisfaction, which is defined by a utility function, by adjusting its transmitted power. The utility function in [14, 16] is not defined in terms of throughput (bits per second) but in the unit of bits per joule. One main limitation of

this literature is the requirement that each MS in a system needs to know information related to all other MSs as common knowledge in order to solve for its own transmit power. Also the results in current literature have not been applied to a real system, nor have they been compared to existing power control schemes. This makes it very hard to evaluate the benefits of these power control schemes.

The major characteristic of data that is different compared to voice traffic is the discontinuous or bursty transmission. Random arrivals of transmission bursts and random periods of on and off transmissions cause dynamic changes of interference levels (interference here is the summation of the received power of all MSs at a BS). As a result, the signal quality of data transmission fluctuates and the estimations of the communication quality are difficult. These estimations are important in making the RRM decisions. Additionally, quick RRM decisions are required [17] because of the brief duration of transmission of each data burst. Only few papers consider this bursty nature of data traffic when they address RRM issues in mobile data networks. Lueng addresses this problem by using a Kalman filter to predict the interference in TDMA (time division multiple access) systems [18]. TDMA is different from CDMA systems, therefore this prediction might require some modification if it has to be used in CDMA systems. The prediction technique is based on a statistical approach and it is at a preliminary state of research. A more sophisticated statistical estimation might be required in order to have a highly accurate prediction of interference for random bursty transmissions [18]. In summary, RRM algorithms have to consider bursty transmissions to assure proper operations in mobile data networks.

Power and rate assignments affect both quality of service and radio resource utilization. A measure of the amount of radio resources and quality of service obtained by each MS is the signal-to-interference ratio (SIR) for that MS. The amount of usage of the radio resources by all MSs is limited by the maximum allowable interference at the BS [19]. Power and rate assignments are dependent on each other because the transmit power of MSs determines the SIR seen by each MS which then is translated into the rate. Transmitting data at a high rate can increase the throughput; nevertheless, high transmit power levels are required to obtain low PERs at high data rates. Moreover, this high amount of power can cause interference to other MSs in the systems impacting power control. Consequently, if a large number of MSs wish to transmit data at the high rates, then *very few* of them can transmit because the number of admitted MSs is limited by the incurred system interference level. On the other hand, if there are only few MSs transmitting data, then power and rate should be assigned to the MSs such that the highest throughput can be obtained. Consequently, integrated power control and rate assignment in mobile data networks needs to be investigated. The problem of power and rate assignments should be formulated to account for dynamic target SIRs and not a single target SIR (even for the MSs that have the same

transmission rates) in order to *completely* utilize the radio resources, maximize each MS's throughput (or effective rate) and support as many MSs as possible in a cell.

The fast rate control and the traditional power control schemes in cdma2000-1x-EV-DO standard can achieve a predetermined and fixed target SIR but they cannot ensure the full utilization of radio resources. While the power control scheme provides sufficient energy per bit to each active MS such that the minimum SIR requirement at a given data rate is met, the radio resource can be either under or over-utilized. In a lightly loaded situation, the interference can be much lower than the maximum allowable level after rate and power are assigned to the MSs. However, the power and rate control schemes can exacerbate problems by increasing the interference to neighboring cells by sometimes over-utilizing the radio resources in an overloaded situation. The resulting resource utilization depends on the assigned rate, which is controlled in a probabilistic way in 1x-EV-DO.

In the literature, optimal power and rate assignments are studied theoretically in [19, 20]. The results suggest that the MS that has a better channel condition than others should get most of the radio resources. In such a case, only few MSs can transmit data. In [21], the issue of fairness in multi-rate wireless packet networks is addressed and a generalized processor sharing (GPS) approach is applied in the proposed rate assignment. However, this approach is quite complex and requires several changes to other functions such as the MAC protocol and signaling protocols [21]. In addition, a continuous range of rate variations and power control based on a fixed target SIR are assumed in this work. A gap in knowledge of power and rate assignments that can provide fairness to MSs still exists. We believe that both rate and power should be assigned equally to all MSs even if some MSs have better channel conditions or have prior admissions. This equal resource allocation issue is not addressed in the employed rate and power control schemes in 1x-EV-DO. Further, the research work in [19-21] has not been evaluated in comparison with real systems such as 1x-EV-DO.

1.3. RESEARCH GOALS AND PROBLEM STATEMENT

In light of the limitations of the existing schemes in the current cellular networks and in the research literature, a new approach for power and rate control that can efficiently handle data traffic, which has different requirements and characteristics compared to voice traffic, will be investigated in this work. The basic idea of this research is a power control and rate control scheme based on *dynamic target SIRs* for multi-rate mobile data networks that can handle *bursty data traffic* and can *completely utilize and equally*

assign the radio resources. In the literature, there is no work that has investigated all these issues together. Consequently, the research goals of this dissertation can be established as follows.

The first goal is to consider full utilization of radio resources. By this we mean provision of high throughput to each MS by increasing the assigned rate and power as long as the interference is lower than the allowable maximum level. In the CDMA standards, the interference is mostly considered in admission control but not in power control. RRM on the reverse link in the 1x-EV-DO standard assigns power based on a fixed target SIR and assigns rate based on the interference threshold [8]. In the literature, the peak interference is also included in the study of optimal power and rate assignment [19]. Traditional power control based on fixed target SIRs assigns power to a MS such that it can obtain the SIR at the target level. When all the received SIRs at the BS are equal to the target levels at given rates, radio resources in the cell can be under-utilized if the incurred interference is less than the maximum allowable level. Rate control in 1x-EV-DO increases or decreases a MS transmission rate in a probabilistic manner. Therefore, radio resources can be under or over utilized. The remaining radio resources (if any) should be assigned such that each MS obtains a high effective rate (transmission rate after errors) by increasing both rate and power until the interference is close to the acceptable threshold level (full utilization). The full utilization aspect is important in RRM because it can increase data throughput if the traffic is *bursty* (important from both user's and service provider's perspectives) and it maximizes the radio resource utilization near the allowable level (important from the service provider's perspective).

Secondly, RRM for data traffic can be more flexible than in the case of voice. For example, a situation could arise where all MSs in a cell transmit at the basic rate (the lowest rate) and yet all of the received SIRs at the BS are lower than the target level. The radio resources in the cell are over-utilized in this situation. In this case, the interference level is being maintained lower than the threshold level to prevent the deterioration of the capacities of other cells; thus the MSs cannot transmit at higher power levels. If admission control is employed, some MSs may be rejected from the network. Since retransmissions are possible in wireless data communications, RRM schemes can have some flexibility in providing services to a number of data-MSs that already transmit data at the basic rate but there is over-utilization of radio resources. In this situation, the MSs can be supported by keeping their transmit power such that all of their SIRs are as high as possible but the incurred interference is not higher than the threshold. No work has considered such flexibility of power assignments in wireless data communications before. RRM based on this power control approach is interesting for the service provider because it can support more numbers of MSs with a tradeoff in increasing retransmissions. However, the acceptable number of retransmissions is not investigated in this research.

Finally, radio resources should be assigned equally to all MSs. This is different from the solutions being developed in the evolving standards (such as HSDPA for the forward link and cdma2000 1x-EV-DV Revision D for the reverse link) and presented in the literature [19, 20] where a MS that has a better channel quality than others obtains most of the radio resources. We believe that obtaining equal radio resources is important from the user's perspective. The GPS approach [21] tries to assign the highest rate to the MSs whenever there are idle radio resources left. However, the most important assumption of GPS is that the granularity of rate that can be assigned to each MS is infinitesimal (fluid model). In practice, the offered rates are discrete and each rate level is a multiple of the basic rate. Accordingly, it is our goal to design study simpler and more practical algorithms that can assign radio resources equally to all MSs.

The **problem statement** of RRM investigated in this research is how to assign power and rate to MSs based on dynamic target SIRs for bursty transmissions in order to maximize the throughput of each data-MS on the reverse link while still providing equal allocation of radio resources to all MSs and achieving full radio resource utilization in each cell in a decentralized manner.

1.4. ESSENCE OF THE PROPOSED SOLUTION

The essence of our proposed RRM solution is to assign the same rate and different transmit powers to each active MS to achieve the same received power such that the highest possible SIR exists based on the available radio resources in a cell. Thereby, we provide equal resource allocation under the constraints of the maximum allowable interference level. By an active MS, we mean any MS that wants to transmit a burst of data traffic at that time. With the motivation of decentralized control, we use game theory to analyze user needs and to understand how systems work and how algorithms can be developed or adapted, to meet those needs of data-MSs. Game theory has been used in modeling power control on the reverse link in the literature [13, 14]. Totally non-cooperative power control among MSs favors the MSs that are closer to a BS than others [14]. Furthermore, an important assumption in applying game theory for modeling power control in the literature is that common knowledge of parameters of all MSs is known to everyone. This limitation has to be addressed in practical implementations because it is very difficult for each MSs to be aware of the path loss and transmit powers of all other MSs. Where appropriate, we apply the game theoretical model to the problem and adjust the algorithms in order to satisfy the constraints of the MS and the system regarding the availability of such common knowledge. Our study results in decentralized power and rate control algorithms with assistance from a BS and it performs the

function to meet the concepts of equal allocation and fully flexible utilization of radio resources. The proposed algorithms are simple and do not require additional signaling compared to existing standards.

1.5. RESEARCH CONTRIBUTIONS

The following is the list of the research contributions of this dissertation:

1) Power control has been studied by using game theory in the literature in an abstract manner without connection to practical aspects and comparisons of the performance with real systems. This research investigates a practical power control scheme that uses a game theoretical approach to provide higher SIRs (lower bit error rate) than power control based on a fixed target SIR. The common knowledge requirement (in the literature of reverse link power control based on game theory) is a problem for practical implementation. Moving the computation of the Nash equilibrium from a MS to the BS in this research is one approach that can address this limitation.

2) Power control in this research is based on the constraints of SIR and interference. No previous work in the literature has considered interference in power control. This power control approach is appropriate for wireless data networks since a MS can obtain high SIR without causing interference higher than the specified level.

3) Joint power and rate control studied in the literature assigns all radio resources to only a few MSs that have better channel conditions than others in a cell. This research proposes joint power and rate control for complete utilization and equal allocation of radio resources in wireless data networks. The concept of the joint power and rate control uses the maximum allowable interference level and the number of active MSs in each cell in dividing the radio resources to each MS equally.

4) When the network is over-utilized, all MSs cannot attain the target SIR and the interference can be higher than the tolerable level. Traditional radio resource management overcomes this problem by admitting only a certain number of MSs. However, data communications is error sensitive but delay tolerant. Additional numbers of MSs can be supported with the cost of high transmission delay. Power control in this research considers this property to provide flexibility in radio resource management for wireless data networks without causing higher interference than a predefined level.

1.6. ORGANIZATION

The organization of this dissertation is as follows. Chapter 2.0 provides a literature review of radio resource management for wireless data networks focused on power control, rate control and joint power and rate control. Chapter 3.0 addresses the problem of common knowledge requirement in the literature by moving the computation of the Nash equilibrium from a mobile station to the base station. Since this dissertation is based on a game theoretical approach, i.e., each user tries to maximize its own satisfaction which is called a utility function, the properties of utility functions in the literature are studied and the selection criteria of the utility functions to be used in power control are discussed in Chapter 4.0. The problem formulation and development of the proposed power control algorithms for wireless data networks are discussed in Chapter 5.0. Bursty transmissions are also considered in the design of the proposed algorithms in Chapter 5.0. Both the running time and the performance of the proposed algorithms are examined under bursty transmissions. Performance evaluation in a multi-cell scenario is provided. The performance is compared with the traditional fixed target SIR power control. Only a single rate is considered in this chapter. Chapter 6.0 presents proposed rate and power control algorithms for wireless data networks. The performance of the proposed algorithms is compared with the traditional rate and power control in cdma2000-1x-EV-DO standard. The summary of the dissertation is discussed in Chapter 7.0.

2.0 A SURVEY OF LITERATURE

2.1. INTRODUCTION

Efficient RRM is required on both forward and reverse links. On the forward link, the BS/MSC/GSN, which is a central controller, can assign the radio resources efficiently. In comparison, on the reverse link, each MS does not have information related to other MSs in the system. Therefore, RRM approaches on the reverse link and the forward link require different strategies to efficiently assign the radio resources. RRM on the forward link for wireless data networks has been studied more extensively than on the reverse link. The current standards of 1x-EV-DO, 1x-EV-DV release C and 3GPP release 5 (HSDPA: high speed downlink packet access) manage the radio resources to maximize the throughput on the forward link by providing all resources to each MS in a time slot fashion [22-24]. In contrast, RRM on the reverse link just has received more attention lately. For example, the standards of 1x-EV-DV release D or 1x-EV-DV RL (reverse link) [25] and 3GPP release 6 (EUL: enhanced uplink) [26, 27] are being developed to improve the performance of RRM on the reverse link. This literature survey focuses on RRM on the reverse link of wireless data networks.

Power control studies have been extensively reviewed in [4]. However, the previous survey of power control in [4] is outdated since most of the literature is for voice traffic. Very little description of new power control schemes for data traffic is provided in [4]. In addition, wireless systems beyond the second generation can provide multi-rate service to a data MS. No work has provided a survey of such rate assignment. Recently, joint power and rate assignment for data has been investigated to maximize data throughput. The organization of this chapter is as follows. The review of power and rate allocations in the literatures is provided in Section 2.2. Conclusions are given in Section 2.3.

2.2. POWER AND RATE ALLOCATION STUDIES IN THE RESEARCH LITERATURE

2.2.1. Power control

The current power control algorithms in CDMA systems employ a combined open loop and a closed loop scheme as shown in Figure 2.1. In the open loop power control, the MS measures the signal strength of a reference channel (the pilot channel in CDMA systems) from the BS. If the received signal strength of the pilot channel is higher than the target, which is specified in the access parameter message sent from the BS, the MS will automatically reduce its transmitted power to achieve that target. Otherwise, the MS will increase its transmitted power in order to meet the target [28]. This process is repeated every 20 ms [10]. The transmitted power of the traffic channel is then adjusted according to the gain of the traffic channel compared to the pilot channel [29]. The characteristics of the traffic channel on the reverse link are different from those of the pilot channel on the forward link since the forward and reverse links occupy different frequency ranges. Therefore open loop power control is not very accurate for controlling the transmitted power on the reverse link [4].

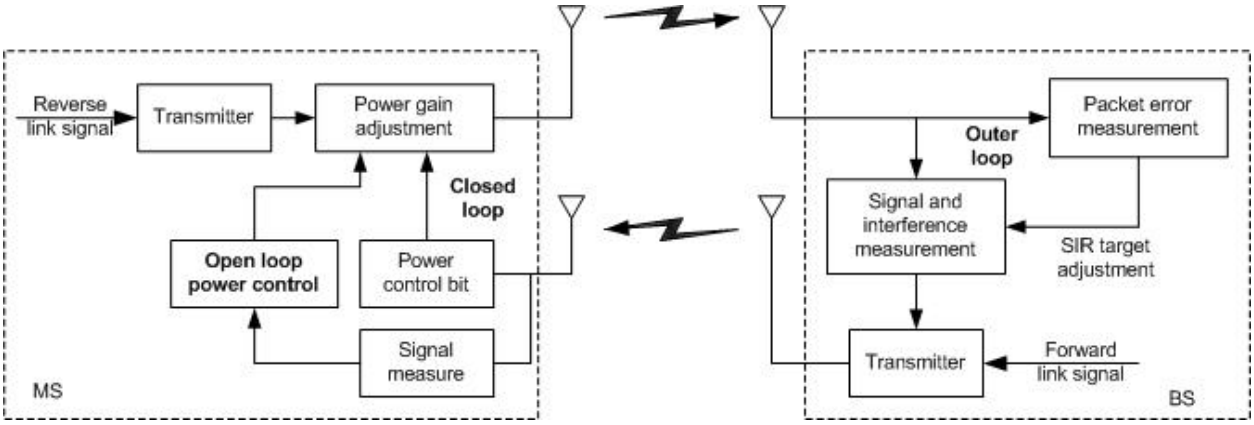

Figure 2.1 Reverse link power control in CDMA systems

The closed loop power control assists the open-loop power control by implementing a feedback mechanism between the BS and the MS [10]. The fast closed loop power control that is implemented on the reverse link is a crucial element in maintaining the signal quality at the BS's receiver. In both IS-95 and cdma2000, the rate of closed loop power control is 800 Hz (this rate is nearly doubled in WCDMA.) The closed loop power control operates every 1.25 ms ($1/800\ Hz^{-1}$), which is faster than the 20 ms interval of the open loop power control [10], in order to correct the power adjustment of the open loop at the MS [4].

Two basic operations of this fast closed loop power control are as follows. First, the serving BS compares the SIR of the received signal with a target SIR. Second, the power control bit (up/down) is sent to the MS based on the result of the SIR comparison. When the MS receives the up/down power control bit, it increases/decreases the transmitted power by a fixed amount of power determined by a predefined value called *power step size* [4].

Fast closed loop power control can adapt to the rapid changes of received signal strength caused by radio propagation and interference levels caused by other MSs to achieve a predefined target SIR (this target SIR is a mapping from a certain level of PER.) However, the feedback of the closed loop power control might be insufficient to compensate for the multi-path fading effect. An additional component called an *outer loop power control* assists the closed loop power control in compensating for the effects of multi-path by measuring the PER at the receiver and adjusting the target SIR of the closed loop power control to meet the required PER [30]. This target SIR is periodically adjusted by the outer loop power control every 20 ms (16 times slower than the rate of the closed loop power control in IS-95).

In the research literature, several papers have investigated the new properties of power control for mobile data networks. The general categories of power control for wireless data networks in the literature can be classified as shown in Figure 2.2 based on different criteria.

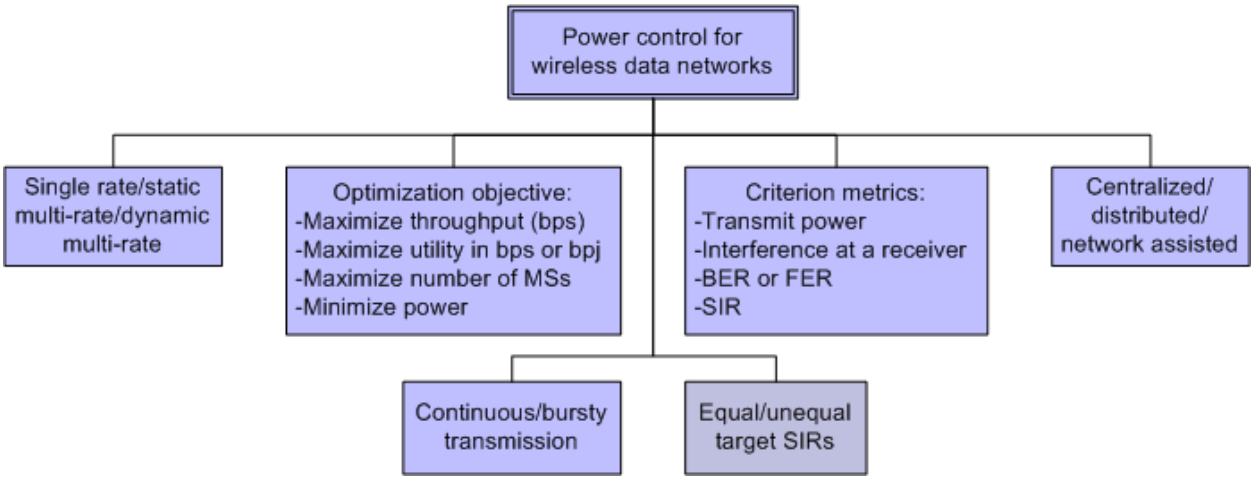

Figure 2.2 Classification of power control for wireless data networks

In this section, only some of the literature of power control is reviewed with a focus on SIR balancing power control, distributed power control, and the bursty transmission issue. The remaining topics are discussed in Section 2.2.3. The next subsection first reviews the power control studies based on the SIR

balancing approach for voice and data traffic. Then distributed power control based on game theoretical models is explained. After that, research issues of power control for bursty traffic are discussed.

2.2.1.1. Power control studies based on the SIR balancing approach

In the literature, the optimal power control problem for voice communications is formulated as the maximization of the number of users (by minimizing the transmit power) subject to the minimum required SIR. The solution of this problem called "optimal balanced SIR" is the highest equally received SIR where the transmit power of all MSs is minimized [31]. The concept of this SIR balancing approach can be illustrated as shown in Figure 2.3. In this scenario, the minimum SIR requirement is γ_{min}. MS1 and MS2 find their own transmit power levels that should be used such that they can be supported by the system. Each line in the figure indicates the power level that a MS should use in order to obtain the required SIR when the other MS's power level is known. These two plots divide the transmit power operating region into four areas: A, B, C and D. Region A/C is where only MS2/MS1 can be supported because its SIR is lower than γ_{min}. In region B, both MSs' SIRs are lower than γ_{min} so neither of them is supported. Region D covers the range of transmit power levels of both MSs that can be supported in the system. However, both MSs should transmit at the optimum operating point (as shown in the figure) where both SIR requirements are met and the sum of the transmit power (i.e. system interference level) is minimized. Note that the SIRs of both MSs at the optimum operating point are equal. Thus, this approach of assigning the transmit power is called SIR balancing. In this figure, it is assumed that both MSs suffer the same path loss.

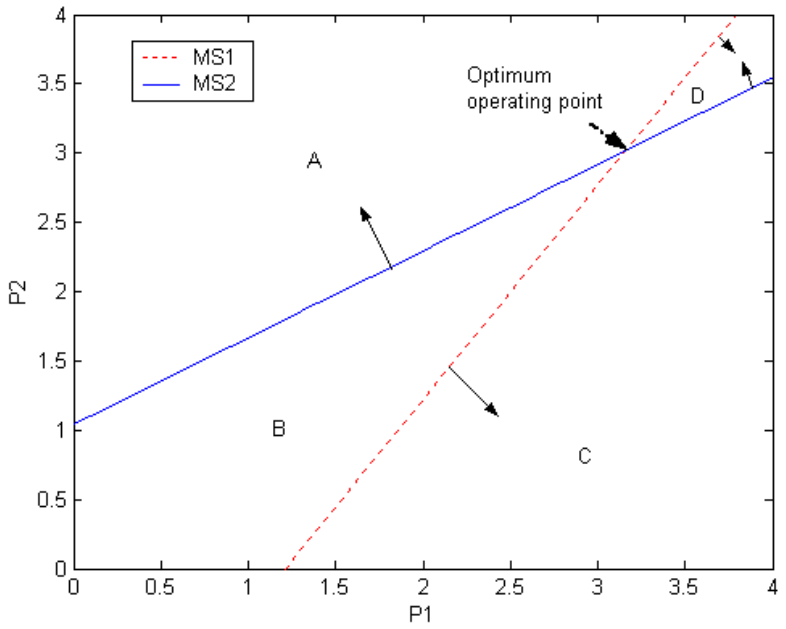

Figure 2.3 Graphical illustration of the optimum transmitter power [2]

The highest achievable balanced SIR is based on the link gains of all MSs in the systems. Let us denote this highest balanced SIR as γ^*. If γ^* is higher than γ_{min}, then all MSs can be supported. γ^* can be found by computing the largest eigenvalues (λ^*) of the normalized uplink path gain matrix [31-33]. In the case that γ^* is higher than γ_{min}, the MSs' transmit powers that can achieve γ^* corresponds to the eigenvector $\mathbf{P}^*$ corresponding to λ^*. If γ^* is lower than γ_{min}, then as few MSs as possible have to be removed (to minimize the outage probability, i.e., to maximize the number of users) until γ^* is greater than γ_{min}. This is the centralized optimum power control approach in [31-33]. The practical limitation of these optimally centralized power control approaches [31-33] is the requirement of available information. The global information of all link "path gains" is required for finding the highest balanced SIR (γ^*). This requirement is too costly to implement [2]. Additionally, this γ^* has to be broadcast to all users so that each MS can know how much power it has to adjust. The concept of SIR balancing has been developed in a distributed manner in [34-36]. Although the global information of the transmit power of all users is not required for these distributed power control algorithms, other practical limitations still exist. 1) It is difficult to find the suitable number of iterations during operations required for converging to the minimum target SIR, especially in the dynamically changing cellular environments (e.g. radio propagation conditions and mobile speed). 2) The signaling requirement for transmitting the exact SIR information from the receiver to the transmitter. In addition, this SIR balancing approach for voice is to meet the target SIR and

minimize the interference level. This objective is not appropriate for data communications where high SIRs are required so that a MS can transmit data as fast as possible.

In the literature, it has been shown that the optimal power control for maximizing aggregate throughput at a BS in a single-rate mobile data network does not have the optimal balanced SIR solution [37]. Goodman *et al.* examine whether the equally received power approach is the optimal power control scheme for data if the objective is the system throughput and how the number of MSs affects the optimal throughput [37]. Path gains are assumed to be known and all MSs are assumed to have the same fixed transmission rate. The constraints of the interference and the bit error rate on the uplink are not considered in [37]. The throughput in [37] is defined as a function of the frame success rate. This frame success rate function is derived from the properties of the employed physical layer modulation and coding. For the analysis of optimal received power (whether they are equal or not), the important parameters are the outer-cell interference and noise. When the outer-cell interference and noise are neglected, the analytical result shows that the received power levels of all MSs should be equal at the BS in order to maximize the system throughput. In addition, the authors find that the maximum throughput level is different for a different number of admitted MSs in a cell. For a given modulation and coding scheme, the number of admitted MSs that the system can provide the highest maximum throughput is called the optimal number of MSs. Accordingly, the networks should limit the number of admitted MS to be less than this optimal value in order to maximize the system throughput. These results are similar to the case of the optimal voice power control. In contrast, received power balancing does not result in the optimal throughput when the outer-cell interference and noise are considered. The authors believe that the received power balancing approach is attractive for implementation; therefore, they suggest two options to reduce the effect of noise and outer-cell interference. The first option is to limit the number of supported MSs. The systems admit an additional MS only when the BS can assure each MS's throughput as in the noiseless systems. The second option is the expansion of the system bandwidth (W) to increase the processing gain (W/transmission rate). The bandwidth has to increase until each MS can obtain throughput that is the same as in the noiseless systems.

2.2.1.2. Power control based on game theory

Centralized power control is not practical [2]. Some research groups have started investigating power control for data communications from a distributed approach based on game theory. Game theory is a powerful tool for modeling conflict interactions of various *objective* participants or players in a system. The result of a game theoretical analysis provides an *action* that each player should use to meet its objective requirements. A basic assumption of game theory is that each player is selfish (rational) and

wants the outcome that maximizes its preference by selecting the action (strategy) appropriately based on the rules of the game. To model a problem as a game, we need players, a set of actions or strategies, and each player's payoff or utility function. The utility function maps the set of actions of all players (outcome) to a real number. The value of utility represents *a satisfaction quantity* of that set of actions. Note that the actions of one player affect the utility of all other players. The results of the pioneering work in applying game theory to the power control problem in CDMA like systems are reported in [14]. The basic idea here is that every MS in a cell tries to maximize its own satisfaction, which is called utility, by adjusting its transmitted power. The utility in [14] is defined as the number of information bits received successfully per joule of energy expended. The convergence of the utility maximization process by all MSs is to the Nash equilibrium where no single MS can improve its utility by changing its strategy. The authors also show that the Nash equilibrium of this game is Pareto inefficient (i.e. the utility of everyone can be improved compared to the equilibrium utility). Pricing can be applied to move MSs from the equilibrium towards a more efficient set of strategies. The pricing coefficient in the pricing term is selected such that all MSs reduce their power incrementally until at least one MS's utility level is decreased. In [14], a gradient search is used for solving for the equilibrium SIR [38]. A snapshot analysis is provided. A single rate and continuous transmission are assumed. Each MSs' information is assumed to be known by all other MSs as common knowledge. This work considers only a single cell. The numerical results show that all MSs have improved utility when pricing is employed. Additionally, the MS that is closer to a BS gets higher utility than the MS that is farther away.

In [39], the concepts of game theory in a single cell case in [14] are extended to a multicell case. Two methods of BS assignments are studied in [39]. The first is based on the received signal strength (RSS) and the second on the SIR. First the authors consider the utility function without pricing. When the BS assignment based on RSS is studied, a BS that has the highest RSS is assigned to a MS. Because fading is not considered in [39], the BS that provides the highest RSS is the closest BS. Next the power control game as explained previously is used to assign the equilibrium power to the MS. In a manner similar to the single cell case, all MSs adjust their power to achieve the same equilibrium SIR at the closest BS. In contrast, a MS with the SIR based approach finds a BS that can provide the highest utility based on the equilibrium transmitted power that can achieve the equilibrium SIR (this value is 12.4, the same as the single cell case). A power control game with pricing in a multicell network is also considered in [39]. In this work, two pricing schemes are considered: global pricing and local pricing. The global pricing scheme uses the same pricing coefficient for all MSs in every cell. The local pricing scheme uses a different pricing coefficient for each cell based on the traffic load in a cell. In this game, each MS tries to maximize its utility. The equilibrium SIR can be computed by solving the nonlinear system of equations. When the BS assignment based on RSS is employed, the closest BS is assigned. Next the MS

adjusts its power to attain the equilibrium SIR. In the second BS assignment approach, the BS is assigned based on the highest equilibrium SIR. Therefore, the BS assignments with and without pricing coefficient are possibly different.

The power control problem studied in [14, 39] is modeled as a one shot game, i.e., there is no consequence after a MS makes a decision. A refereed game and repeated game are introduced as alternatives in power control on the reverse link in [15]. The utility function in bits per joule (the same as in [14]) is employed. However, the pricing term is not considered in [15]. To assign the radio resources to all MSs fairly, the goal of this power control game is to achieve equal received power levels (i.e. equal SIR levels) at the BS. The equilibrium power can be computed either at the BS or the MSs. The latter requires the BS to send all information to the MSs for computation. In the refereed game, the BS punishes a MS that transmits at a power level higher than that suggested by the Nash equilibrium by randomly changing the MS's information bit with a certain probability. This probability is a function of the received power at the BS. In their proposed repeated game, the punishment is performed by all MSs instead of the BS. The assumption of the repeated game is that each MSs knows the received power of all other MSs in the previous time slot. If any MS transmits at higher than the Nash equilibrium power, then the other MSs can increase their transmitted power to punish that MS. The performance comparisons between power control based on a one shot game and a repeated game are given. Both power control games are designed to meet the desired equal received power at the BS. The evaluation scenario assumes single rate transmission, a single cell and no mobility. Global information is assumed as common knowledge. The results show that the power control based on the repeated game provides higher utility and lower transmit power than the one shot game.

Sung and Wong formulate a noncooperative power control game for multi-rate CDMA data networks [13]. The utility function is formulated as data throughput using an information theoretic approach. Information theory is used in deriving the bound of the probability of a correctly received bit at a receiver without requiring the knowledge of the modulation and coding. Thus, each MS in this power control game tries to maximize its own data throughput which is different from other work such as [14]. Pricing is also included in the utility function. This pricing function consists of a pricing parameter and a ratio of the received power from the tagged MS at the BS over the total received power. The pricing parameter is very important because it determines how the power control game performs. Additionally, this pricing parameter is required to be global information for everyone. Only a single cell is considered and a single rate is evaluated in this work. The effect of the pricing parameter is studied. However, how to properly set this pricing parameter remains a research issue.

2.2.1.3. Open research issues of power control for bursty traffic

The bursty nature of data traffic makes the power control scheme employed in traditional voice cellular networks inefficient [40]. The bursty characteristic makes the estimation of communication quality difficult. Due to the unreliable estimation of the signal quality, it is hard to assign the radio resources efficiently. To the best of our knowledge, there is only a little work has been devoted to the design of power control for bursty transmissions. Next, the literature review of this work is provided.

In [41], power control in spread spectrum cellular networks is designed by taking the bursty nature of data traffic into consideration. The design issue is that the traditional power control scheme cannot dynamically adapt to the rapid fluctuations of interference levels which happens because of the short burst transmissions. Accordingly, the power is statistically adjusted to meet the SIR requirement on average based on the randomness and burstiness of data transmissions by including the mean and variance of interference from measurement in the power control algorithms. However, there is no numerical analysis in this work.

The problem of bursty data traffic for power control is also recognized in [18] and predictive power control is suggested for packet data transfer in TDMA-like systems. Unlike voice calls where the transmit power is continually adjusted through closed-loop power control, in data transmission it has to be adjusted for the burst of data, preferably once. The argument in this work is that depending on the size of the message, it is likely that a MS will reserve contiguous time slots for transmission of data. Depending on the interference observed in the first few slots, the MS can increase or decrease it's transmit power to achieve the target SIR for subsequent time slots by predicting the future interference. This prediction is performed using Kalman filters. It is shown by simulation that this scheme performs only about a dB or so worse than the distributed power control method used in [35] for this situation especially when the message consists of at least 10 time slots on average.

2.2.2. Rate control

In IS-95B, only dedicated traffic channels are offered for data transmissions [42]. High transmission rates can be achieved through code channel aggregation (multi-code). There are two types of traffic code channels to serve this purpose: fundamental and supplemental code channels. In both cdma2000 and UMTS, there are two types of traffic channels: dedicated and common channels [10, 24]. The dedicated channel is used for carrying large or more frequent data traffic [42] from *one* MS to the BS; whereas, the common channel is *shared* by several MSs to send short and infrequent data traffic [42] to the BS [10].

In cdma2000, there are three types of dedicated traffic channels: fundamental, supplemental code and supplemental channels [10]. There is only one supplemental code channel with variable spreading gains [43] and it is used to provide high rates. On the reverse link of cdma2000, the highest data rate can be provided at 144 kbps [44]. It can provide a higher rate than IS-95B because different modulation and coding schemes are used in cdma2000. In UMTS, there is only one type of dedicated traffic channel called dedicated physical data channel (DPDCH). Higher rates can be provided by variable processing gain and multiple DPDCHs. The highest transmission rate of each DPDCH is 960 kbps [1].

The common physical channels that can be used for data traffic transmission in cdma2000 are the reverse enhanced access channel (REACH) and the reverse common control channel (RCCCH). Similar physical common channels are used in UMTS: physical random access channel (PRACH) and physical common packet channel (PCPCH) [24]. How these channels are used for multi-rate transmission is discussed next.

In IS-95B, an active MS always has the fundamental code channel that can provide the basic rate of 9.6 kbps. When the MS requires transmitting data at a high rate, a burst admission control must be performed [45, 46]. The MS requests a transmission rate by sending a supplemental code channel request message, which contains the amount of backlog data and the requested rate, on the fundamental channel to the BS. This burst admission control responds to the MS by sending the message that specifies the number of supplemental code channels, burst length, and start time of the burst. This decision is based on the interference level at the BS [47]. This procedure of the burst admission control is also employed in cdma2000-1x [45, 48]. In IS-95B, if the request is accepted, then up to seven supplemental code channels can be allocated to achieve the assigned rate. Each supplemental code channel can support 9.6 kbps. Therefore, the peak rate that can be offered to the MS is 8×9.6 kbps = 76.8 kbps [43]. Dedicated channels in IS-95B always support power control while common channels may or may not support power control.

In cdma2000, the MS can select two access modes based on its message size and the BS's preference: basic access (BA) and reservation access (RA) [49]. The BA mode is used for sending very short bursts and the RA mode is suitable for sending extended short bursts. In BA mode, the message data is transmitted on the REACH without access control from the BS. However, the rate allowed is specified in the access parameter message from the BS. There is no closed loop power control and soft handoff when operating in the BA mode. In RA mode, the MS must send a request to the BS on the REACH before transmitting data on the RCCCH. This request specifies the required rate and the soft handoff option. The MS waits for permission from the BS. Next, the MS sends data on the RCCCH with closed loop power control and without contention. Similar physical common channels are used in UMTS:

physical random access channel (PRACH) and physical common packet channel (PCPCH) [24]. These common channels however do not support soft handoff. The open loop power control is used in this common channel packet transmission [42]. The PCPCH can transmit a message at a larger size than the PRACH; therefore, closed loop power control is required on the PCPCH. Table 2.1 summarizes the supported power control for each channel type.

In cdma2000-1x-EV-DO, the five levels of service rates offered are 9.6, 19.2, 38.4, 76.8 and 153.6 kbps. Note that 153.6 kbps is the maximum rate (R_{max}) and 9.6 kbps is the minimum rate (R_{min}). The rate control in 1x-EV-DO is different from cdma2000-1x which assigns the rate based on scheduling of data transmission. The allowed transmission rate and the duration of transmission time are negotiated during the burst admission control in cdma2000-1x. Similarly, the rate is not changed for the whole assigned burst duration. In contrast, the transmission rate in 1x-EV-DO is updated every packet transmission interval (16 times the power control update period) [50]. Accordingly, the rate control in cdma2000-1x leads to slow adaptation and under-utilization of the radio resources compared to the case of 1x-EV-DO [51]. In 1x-EV-DO, fast rate control is based on the interference levels at all sectors in the *active set* of a MS (a list of cell sectors that a MS has established the connections). When the reverse link interference level (I_o) is higher/lower than a threshold level, each sector in the active set will broadcast a bit 1/0 (called reverse activity – RA bit) to the MS. The MS then decides the data rate based on this RA bit in a probabilistic way [8]. A set of a probability pair, (p, q), is specified by a sector such that the sector can differentiate the rate assignment behavior of each MS. Probability p (q) indicates the likelihood that a MS will decrease (increase) the transmission rate one step when at least one (all) sector(s) in the active set has (have) the interference level(s) higher (lower) than the threshold value(s). The status of the interference level [50] (whether it is higher or lower than the threshold) is transmitted to MSs by the transmitters in each cell sector. In [8], the parameters are set as: $p = \max\{0, 0.5 \times (\text{current rate}/153.6) - 0.1\}$ and $q = \max\{0, 0.4 - 0.5 \times (\text{current rate}/153.6)\}$.

Next, the review of rate control in the research literature is provided. These rate control schemes can be classified into different categories based on the location of the rate controller: centralized, distributed or network assisted; the rate adaptation granularity level: burst, frame or slot; the optimization objective: throughput maximization or radio resource utilization maximization; the criterion metric: interference at a BS, SIR, or transmit power or rate; and the transmission characteristic: continuous or bursty. These classifications are shown in Figure 2.4. The literature review is organized according to the location of the rate controller.

Table 2.1 Supported power control options for each reverse link channel type of cdma2000 and UMTS

Data traffic channel type		Open loop power control	Closed loop power control
cdma2000	Dedicated channel		
	Fundamental	X	X
	Supplemental code	X	X
	Supplemental	X	X
	Common channel		
	REACH	X	
	RCCCH	X	X
UMTS	Dedicated channel		
	DPDCH	X	X
	Common channel		
	PRACH	X	
	PCPCH	X	X

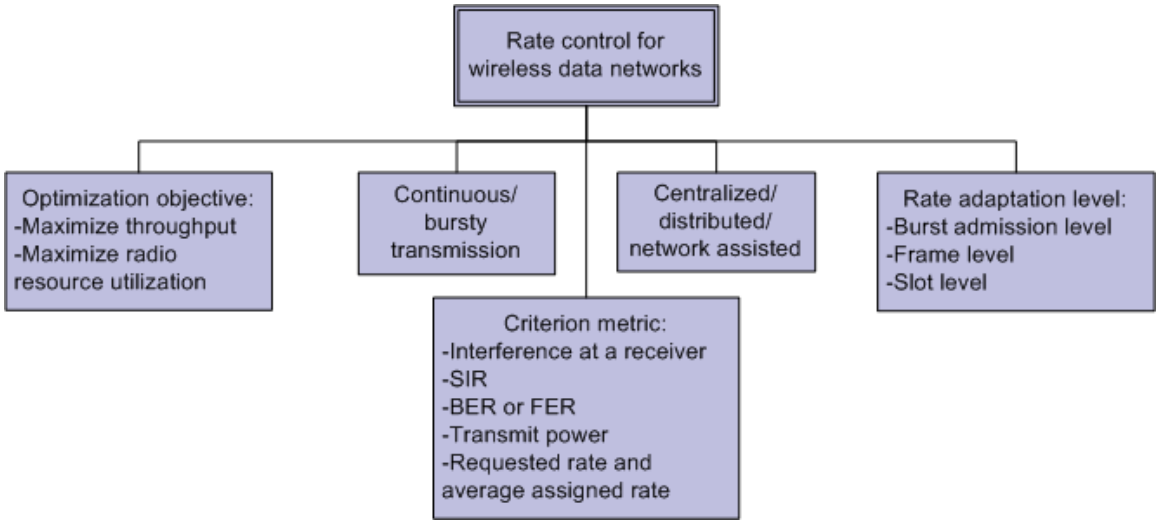

Figure 2.4 Classification of rate control

2.2.2.1. Distributed rate control

Fiorini studies two reverse link rate control schemes based on the employed channel quality metrics in WCDMA: block error rate (BLER) and mobile output power [52]. The proposed rate control is on a per frame basis. Four levels of reverse link service rates studied in [52] are 30.4, 60.8, 121.6 and 243.2 Kbps. The MS's BLER at the receiver is estimated from the rate of retransmissions. If the BLER is higher than an upper BLER threshold, then the MS reduces its rate to the lowest. On the other hand, the MS increases its rate to the next higher one if its BLER is less than a lower BLER threshold. In power based rate control, the MS decreases its rate to the next lower rate if its output power is more than an upper power threshold level. In contrast, if the MS's power level is less than a lower power threshold at least a predefined amount of time, then the MS will increase its transmission rate to the next higher level. The purpose of the dwell timer is to reduce too frequent changes of the MS's transmission rate (ping-pong effect). This work is evaluated by simulation. A multi-cell scenario and bursty traffic is employed in the simulation. Mobility is not considered in the evaluation. The simulation results show that these rate control schemes improve the performance in terms of the BLER, the interference level, the average rate, and total throughput compared with the case of no rate control. Additionally, power based rate control performs better than BLER based rate control in terms of BLER and power consumption.

2.2.2.2. Network assisted rate control

Koo *et al*. propose rate control scheme called autonomous data rate control for 1x-EV-DV by modifying the rate control scheme from 1x-EV-DO [53]. In cdma2000-1x-EV-DV, the reverse link can provide data

rate up to 1.024 Mbps on the supplemental code channel. There are eight levels of service rates offered in this system: 9.6, 19.2, 38.4, 76.8, 153.6, 307.2, 614.4 and 1024 Kbps [53]. Basically, a MS accesses the channel at the basic rate of 9.6 kbps in 1x-EV-DO. A BS periodically sends a message called congestion control bit (CCB) to the MS in order to indicate the congestion condition at the receiver of the BS. If CCB is 1 (0), then the MS will decrease (increase) its transmitted power or rate. Koo *et al*. propose that the BS periodically send an additional four-bit message to inform an available data rate (ADR) to the MS such that the initial access rate is not necessarily limited to the basic rate. In their evaluation, the update rate is 20 ms (equal to the frame size). When the initial access does not succeed, the MS waits for a time called back-off delay. This delay is selected uniformly from integer numbers between 0-9 in units of frames. Each MS is assumed to subscribe to different plans of service: gold, silver and bronze. Each plan limits the maximum data rate service. Furthermore, the allowed service rate is limited according to the MS's location. The cell coverage area is divided into three regions based on the distance from the BS. The rate assigned to the MS is limited to 1.024 Mbps, 307.2 Kbps or 76.8 kbps based on the region of its location, i.e., the MS in the closer region can transmit at a higher rate. Accordingly, the maximum rate of each MS is limited by the minimum allowed transmission rate between the service plan and the region. The simulation results show that the proposed scheme obtains higher average throughputs than the rate control scheme in 1x-EV-DO.

2.2.2.3. Centralized rate control

An efficient radio resource allocation supporting multi-rate traffic (multimedia) should assign users the resources to meet at least the minimum requirements (fairness) and when some resources are idle, the users should obtain the remaining as much as they require (efficiency).To accomplish this goal, the concept of generalized processor sharing (GPS) is proposed for the rate allocation [21]. The rate of each user is adjusted by a BS on a per slot basis. Power control based on the fixed target SIR is employed. The required components of this approach in addition to the current systems are as follows. 1) A token bucket at a mobile terminal for controlling the generated traffic 2) Every time slot, the scheduler at a BS requires the following information: each MS's buffer state information (amount of backlogged data) and the amount of arrived traffic in the previous slot (for estimation of the arrived traffic in the current slot) 3) Slot synchronization. To implement such systems is nontrivial. It might require a new design of the MAC protocol, power control, signaling protocol, transport formats, etc.

2.2.2.4. Evolving rate control in 1x-EV-DV revision D

Recently, cdma2000-1x-EV-DV revision D has been developed to enhance the reverse link capability, especially the throughput. A new approach of rate assignment for this new CDMA standard is proposed in [25] by using a new parameter defined for each MS called *priority* to provide fairness. The priority of each MS is defined as a function of the requested rate, the average allocated rate in the past and the received power at a BS. The highest priority MS is assigned with the requested rate first as long as the interference is lower than the threshold level. A lower priority MS is assigned the requested rate if the interference is lower than a predefined threshold. In this way, the number of transmitting MSs is minimized. However, the sensitivity analysis of this priority function and the evaluation of the rate assignment are not provided.

2.2.3. Joint rate and power allocation

Yao and Geraniotis addressed the problem of using power control from the voice cellular network when multimedia services are enabled [54]. The power control scheme in this work is based on the fixed target SIR and the rates of each MS are assumed to be fixed. They state that future wireless networks would provide multimedia services to multi-rate MSs which require different levels of bit error rate. The power control designed for voice-MSs is based on the equal received power at the BS because all MSs simply require the same bit error rate. When this power control is applied in voice cellular systems, it can provide not only the required bit error rate but also the maximum system capacity and the minimum total transmit power [2]. In contrast, this power control approach may not be able to provide the required bit error rate to each multimedia-MS while maximizing the system capacity and minimizing the total transmit power [54]. The system capacity is measured as the number of admitted MSs in voice cellular networks [2] and in [54]. Therefore, the study in [54] considers the optimization problem of power control in multi-rate wireless networks. The optimization objectives are to maximize the number of MSs and to minimize the total transmit power subject to the constraint of each multimedia-MS's bit error rate requirement. The problem is solved by dynamic programming. The multi-rate approach considered in [54] is based on the variable spreading factor (VSF). The assumption in [54] is that a BS knows all link path gains of the MSs in a cell and each MS always obtains the requested data rate. Additionally, a single cell is considered. The performance evaluation is compared with the equal received power approach. A snapshot analysis is employed. A system that uses the proposed optimal power control can support more number of users and requires less power consumption than the system that used the equal-received power approach. Extending this work to multi-cell scenarios and implementation issues are left for future work.

Optimal power and rate assignments with the aim of maximizing the system throughput on the reverse link of cellular systems based on the constraint of the allowable ranges of power and rate are studied in [55]. This work does not have any constraint on the minimum bit error rate. The variable processing gain approach is considered for multi-rate. The processing gain can be varied to any real number that is greater than one. In reality, the processing gains or the rates offered in the system are in a finite set of integer numbers. A multi-cell scenario is analyzed in this work. A nonlinear programming approach is used for solving for the optimal solution. The analysis shows an interesting result that only the user that has the highest channel gain (including shadow fading) can transmit data in the cell in order to maximize the system throughput. This user transmits at the maximum allowable rate and transmits at the optimal power that is the solution to the nonlinear programming problem. Similarly, the optimal solution is to operate in a time slot mode (only one user at a time) and transmit at the maximum rate at the optimal power level. Fairness is an issue for this optimal assignment because some users that never have the highest path gain may not get service at all. Further, this work investigates the performance of this time slot mode if the user transmits at the maximum power (no power control) and the maximum rate. The numerical results show that the throughput obtained by using the maximum transmit power is worse than the case of using the optimal power. Evidently, the optimum transmit power control has an impact on the system throughput. The practical limitations of this work are enumerated here. 1) The global information requirement of all users' path gains and transmit power levels. 2) The rates offered in practice are discrete. This work assumes that rates can be any positive real number. 3) The maximum bit error rate and interference requirements are not considered. 4) Fairness issue has to be addressed. Otherwise, some users may not have chance to transmit data. 5) Computational complexity of nonlinear programming. A similar approach to [55] is investigated in [56, 57]. The main difference is that the throughput of each user in [56, 57] has a different weight. This weight can represent a feature such as priority. The rate considered in this work is assumed to be a continuous variable. The authors state that their models should be extended to cover the issues of QoS requirements (no particular metric is specified), fairness and distributed algorithms.

Jafar and Goldsmith study the joint power and rate assignment to maximize the system throughput with the minimum requirement of the SIR threshold [20]. The purpose of [20] is to derive an upper bound for the achievable throughput, so the availability of path gain information is assumed and other important requirements are ignored such as the inter-cell interference and fairness constraints. The analysis of this work shows that the MSs that are closer to a BS get higher throughput than the MSs that are farther away. Accordingly, the MSs can be classified into three groups according to the radio resource assignments: the group that transmits at the maximum rate and power, the group that transmits at the maximum power but at a rate lower than the maximum, and at most one MS transmits at the rate and

power lower than the maximum level. The authors suggest (from the fairness problem shown in their evaluation) that the optimal radio resource assignment should include the fairness constraint to accomodate MSs that are not able to achieve high throughput because of bad channel conditions [20]. Another open research issue from [20] is how much interference the optimal assignment causes to other neighboring cells.

The optimal RRM based on the interference constraint is studied in [19]. The peak interference level of the non-real-time (NRT) data MSs is limited such that the quality of the real-time (RT) MSs can be guaranteed. Power and the processing gain of the NRT users are assigned such that their aggregate throughput is maximized based on two constraints of the maximum power and the RT users' interference limitation. Two important assumptions are made here. First, the processing gain, which is varied according to the rate, is assumed to be a real number. Second, the path gains used in the optimization formulation are assumed to be known (they can be derived from pilot strength measured by MSs in a cell). This pilot strength is needed for soft handoff so no additional overhead incurs. The approach used in [19] computes the optimal processing gain based on the number of NRT-MSs and the maximum power and interference constraints first. Then the optimal power allocation for maximizing the system throughput is computed based on the optimal processing gain. This optimization results in three groups of users. 1) A group of users that have better channel conditions transmit at the maximum power level. 2) At most one user transmits at the power lower than the maximum to meet the constraint of interference requirement of RT users. 3) Some users have to delay the transmission if they have higher path losses (worse channel conditions) than users in group 1) and 2). This is because the change of aggregate throughput is negative if any user in this third group is added. The users in group 3 will be able to transmit only when the system interference level decreases or they have improved channel conditions. According to these results, this optimization provides a greedy resource allocation to maximize the throughput of the NRT users in a time-sharing manner. Only one user's transmit power is less than the maximum level in order to keep the interference level less than the threshold. Most users transmit at either the maximum or zero power level depending on the channel condition. This is very similar to the scheduling on the downlink of 1x-EV-DO and HSDPA. The result of the optimal solution shows the problem of fairness. Similarly, the user that has better channel quality receives higher resource allocation than others.

Feng, Mandayam and Goodman extended their previous work of power control in [14] to joint power and rate assignment based on game theory [58]. The authors studied this problem because the joint power and rate assignment for wireless data services was a new problem at that time. Moreover, no work had studied this joint assignment by using game theory before. The authors modified the utility function

of [14] by including the length of the error detection code and also adding the constraint of the minimum required rate in addition to the maximum transmit power. This utility function still has the unit of bits per joule like the utility function in [14]. However, there is no pricing term in the utility function studied in [58]. By formulating the problem this way, each MS tries maximizing its own utility non-cooperatively. The authors prove the existence of the Nash equilibrium but they found that the equilibrium is not unique, i.e., there is more than one equilibrium solution. In order to have a unique Nash equilibrium solution, the authors suggest that the rate of all MSs in the system is set equally at the highest rate among the minimum required rates of all MSs. Only a single cell is considered in this work. This problem is formulated as a one shot game (no consequence after the MS makes a decision) and a snapshot analysis (no mobility) is employed. Information of all MSs such as path gains and minimum required rates is assumed to be known by all MSs. In addition, all MSs are assumed to have the same utility function in bpj. Using the pricing mechanism to improve the equilibrium utilities of all MSs (Pareto efficiency) is their future work.

A comparison of all these optimal power and rate assignments is presented in Table 2.2. Fairness is the most important issue that needs to be addressed for further research. Bursty transmission has not been considered in the joint power and rate assignment.

2.3. CONCLUSIONS

Radio resource management determines how the radio resources should be assigned in order to provide a MS the required signal quality and utilize the available radio resources as efficiently as possible. Traditional RRM for voice cellular networks is based on the fixed target SIR and power control plays an important role for this task. The next generation cellular networks are evolving towards multi-rate wireless data networks. Consequently, rate assignment becomes a new RRM task in addition to power control. Due to the different characteristics of data and voice traffic, a new paradigm of RRM has to be explored. Since power and rate assignments are closely related and directly affect the SIR and the interference level, the integration of these two RRM tasks should be investigated.

Table 2.2 Comparison of pptimal power and rate assignment schemes

	Optimum metric	Controller location	Criteria	Power and rate	Bursty transmission	Drawbacks
[54]	Maximize number of MSs and minimize total transmit power	Centralized	Tolerable bit error rates	Continuous transmit power and fixed multi-rate	Not considered	Fixed multi-rate assignment, global knowledge of path losses, computational complexity
[55]	System throughput (bps)	Centralized	Continuous power and rate ranges	Continuous	Not considered	Fairness, global knowledge of path losses, computational complexity
[20]	System throughput (bps)	Centralized	Minimum SIR thresholds	Continuous	Not considered	Fairness, global knowledge of path losses, computational complexity
[19]	System throughput (bps)	Centralized	Maximum allowable interference and transmit power	Continuous	Not considered	Fairness, global knowledge of path losses, computational complexity
[58]	Each MS's throughput to power (bpj)	Distributed / game theory	Maximum transmit power and minimum required rate	Continuous	Not considered	Common knowledge of path losses and computational complexity

3.0 PROBLEM FORMULATION AND SOLUTION APPROACHES

3.1. INTRODUCTION

As described in Chapter 2.0, game theoretic approaches have been used in the literature to model the power control problem on the reverse channel for mobile data networks. The basis for this approach is that the MSs will select an equilibrium set of strategies (transmit powers) such that by individually changing their transmit powers they will not be able to benefit in terms of the utility they derive from such a change. That is, no MS has any incentive to unilaterally change its transmit power from the equilibrium value. If the complete information, i.e., path gains (path losses) of all MSs, transmission rates and the range of transmitted power levels is known as common knowledge in the system, then the exact Nash equilibrium can be computed at each mobile station (MS) [13, 14], for example by using Newton's method [12]. However, some information is not common knowledge in the system or it is too costly to make this information available to everyone (for example, the path gains of all MSs). In fact, path gain information is required for computing the received power from all MSs in the system. The received power is used for computing the interference to MS *i* from other MSs in a cell (same-cell interference) and the interference from the neighboring cells (extra-cell interference). Then the signal-to-interference ratio (SIR) at the base station (BS) of MS *i* can be computed as a function of received power of MS *i*, noise at the BS, same-cell and extra-cell interference. Note that the BS is in charge of controlling the transmit power of each MS only in its own cell in the real systems. In other words, the BS cannot control the transmit power of other MSs in the neighboring cells. In practice, the received power of each MS in the cell, the SIR and the extra-cell interference can be measured at the BS. Therefore, we suggest computing the equilibrium received power of MS_i *at the BS* rather than the MS. This chapter demonstrates that computing the Nash equilibrium at the MS and at the BS can result in the same Nash equilibrium. Computing the Nash equilibrium at the BS can eliminate the problem of providing common knowledge of path loss information.

Several utility functions have been studied in the literature. Most of these utility functions are composed of two terms: an efficiency function and pricing of power. The efficiency function represents

the percentage of receiving data correctly at the BS and it is a function of the SIR. A pricing term is included in the utility function to penalize the MS that uses too high power. The objective of pricing mechanisms is to improve the efficiency of Nash equilibria, e.g., all MSs' equilibrium utility. This chapter does not focus on the selection of these utility functions (Chapter 4.0 does), but the location of computing the Nash equilibrium. Accordingly, a simple utility function that consists of the efficiency function and the pricing term is used for this study. This chapter presents the problem formulations of both approaches: computing the Nash equilibrium at the MS and the BS. The analysis shows that the same Nash equilibrium can be achieved in both approaches by selecting proper pricing coefficients.

3.2. NASH EQUILIBRIUM COMPUTATION AT MS

Suppose there are N data-MSs in a cell (assume CDMA) that are competing for resources. Assume that all MSs are rational (i.e., they all try to maximize their utilities and not behave otherwise). Denote the transmitted power of MS i by p_i and transmitted powers of *interfering MSs* by $\mathbf{p}_{-i}$. For each MS $i \in \{1,2,...N\}$, the utility function is given by: u_i: $p_1 \times \ldots \times p_N \rightarrow R$ (a mapping from the outcome space into a real number). This utility function is defined in Equation (3.1) below. Let c_i denote the pricing coefficient (bps/watt). This pricing coefficient is included here to control the equilibrium solution and make the utility function strictly concave (see Chapter 4.0). R_i is the bit rate of the MS i. The bit rate is used as a constant parameter in the efficiency function. The BER, P_e, is dependent on the employed modulation scheme, coding, and receiver architectures. In this chapter, the BER expression of non-coherent FSK modulation scheme is employed as in [14]. This BER expression is shown in Equation (3.2). The expression for the SIR (γ_i) is shown in Equation (3.3). It is a function of the transmitted power of MS i (p_i), transmitted powers of *interfering MSs* ($\mathbf{p}_{-i}$), path loss from a MS i to the BS (h_i), path loss from interfering MSs to the BS ($\mathbf{h}_{-i}$), the spread spectrum bandwidth (W), the bit rate of the MS i (R_i), and the AWGN noise at the receiver in the BS (σ^2). In a non-cooperative power control game, each user tries to maximize its own utility. The strategy space of transmitted power in this game is defined by $\{p_i : p_i \in R^+, p_i \le \overline{p}_i\}$, where $\overline{p}_i$ is the maximum power allowed for MS i.

$$u_i(p_i, \mathbf{p}_{-i}) = R_i[1 - P_e(p_i, \mathbf{p}_{-i})] - c_i p_i \tag{3.1}$$

$$P_e = \frac{1}{2} e^{-\gamma/2} \tag{3.2}$$

$$\gamma_i = \frac{W}{R_i} \frac{h_i p_i}{\sum_{j \neq i} h_j p_j + \sigma^2} \tag{3.3}$$

The objective of the game is to arrive at the equilibrium outcome. To this end, there are N maximization objectives as shown in (3.4). Every MS tries to maximize its utility that is simultaneously dependent on the actions of other MSs. The equilibrium utility of each MS is the best utility that cannot be improved by the individual change of its transmitted power.

$$\underset{p_i}{\text{maximize}} \;\; u_i(p_i, \mathbf{p}_{-i}) \qquad \text{for all } i \in N \tag{3.4}$$

$$\text{subject to} \quad \{p_i : p_i \in R^+, p_i \leq \overline{p}_i\}$$

The utilities of all MSs in the system are represented as a column vector as shown in (3.5) below. Each element of the vector is the utility of a MS and this needs to be maximized subject to the actions of the other MSs.

$$\mathbf{u}(\mathbf{p}) = \begin{bmatrix} u_i(p_i, \mathbf{p}_{-i}) \\ \vdots \\ u_N(p_N, \mathbf{p}_{-N}) \end{bmatrix} \tag{3.5}$$

As the utility function is differentiable, the equilibrium transmitted power: $\mathbf{p}^* = [p_1^* \quad p_2^* \quad \ldots \quad p_N^*]$ can be found by solving Equations (3.6) and (3.7)

$$\nabla \mathbf{u}(\mathbf{p}^*) = \mathbf{0} \tag{3.6}$$

$$\nabla \mathbf{u}(\mathbf{p}) = \begin{bmatrix} \dfrac{\partial u_i(p_i, \mathbf{p}_{-i})}{\partial p_i} \\ \vdots \\ \dfrac{\partial u_N(p_N, \mathbf{p}_{-N})}{\partial p_N} \end{bmatrix} = D\mathbf{u}(\mathbf{p}) \tag{3.7}$$

However, it is very tedious to solve for the exact solution of the above nonlinear system of equations. The expected utility studied here is twice differentiable. Therefore the equilibrium power $\mathbf{p}^*$ can be obtained numerically by Newton's method [59]. The derivative of $\nabla_{\mathbf{u}(\mathbf{p})}$ can be written as the matrix shown below.

$$D^2\mathbf{u} = \begin{bmatrix} \frac{\partial^2[\mathbf{u}(p_1,\mathbf{p}_{-1})]}{\partial p_1^2} & \frac{\partial^2[\mathbf{u}(p_1,\mathbf{p}_{-1})]}{\partial p_2 \partial p_1} & \cdots & \frac{\partial^2[\mathbf{u}(p_1,\mathbf{p}_{-1})]}{\partial p_N \partial p_1} \\ \frac{\partial^2[\mathbf{u}(p_2,\mathbf{p}_{-2})]}{\partial p_1 \partial p_2} & \frac{\partial^2[\mathbf{u}(p_2,\mathbf{p}_{-2})]}{\partial p_2^2} & \cdots & \frac{\partial^2[\mathbf{u}(p_2,\mathbf{p}_{-2})]}{\partial p_N \partial p_2} \\ \vdots & \vdots & \ddots & \vdots \\ \frac{\partial^2[\mathbf{u}(p_N,\mathbf{p}_{-N})]}{\partial p_1 \partial p_N} & \frac{\partial^2[\mathbf{u}(p_N,\mathbf{p}_{-N})]}{\partial p_2 \partial p_N} & \cdots & \frac{\partial^2[\mathbf{u}(p_N,\mathbf{p}_{-N})]}{\partial p_N^2} \end{bmatrix} \quad (3.8)$$

To use Newton's method, we need some initial guess of the solution (**p**). We plug in this initial solution into both D**u** and $D^2\mathbf{u}$. The updated vector $\Delta\mathbf{p}$ is then obtained from $-D^2\mathbf{u}/D\mathbf{u}$. In the next iteration, the solution is updated by the expression: $\mathbf{p} = \mathbf{p} - \Delta\mathbf{p}$. A number of iterations are run. At the end of each iteration, the norm of $\Delta\mathbf{p}$ is examined. If there is no change in the norm value, then the vector **p** is the solution. This solution **p** is the Nash equilibrium of the incomplete information game. At this point, if any one MS changes its transmit power, its utility will fall.

The existence and uniqueness of the Nash equilibrium of this game can be demonstrated using the results from [60]. Rosen shows that if the utility function of each player is strictly concave (i.e. if any pair of different points A and B on the graph of the utility function, the line segment AB lies entirely below the graph, except at A and B), then the equilibrium solution of the game exists and it is unique. Figure 3.1 shows the utility function for three cases of pricing coefficients when a constant interference level is assumed. A simple path loss model as in [14] without shadow fading, $h=K/d^4$, is employed, where K is equal to 0.097. $\sigma^2 = 5*10^{-15}$ watts [14]. The distance (d) of 1000 m is used for Figure 3.1. When the pricing coefficient in the utility function is not zero, a global equilibrium exists. Illustrations of the utility function and the Nash equilibrium by assuming only two MSs in the systems are shown in Figure 3.2 to Figure 3.4. The distances of MS1 and MS2 from a BS are 800 m and 900 m, respectively. The pricing coefficients of both MSs are set to 2.8747 x 10^5 bps/W. The intersection of the two lines in Figure 3.4 shows the existence of the Nash equilibrium.

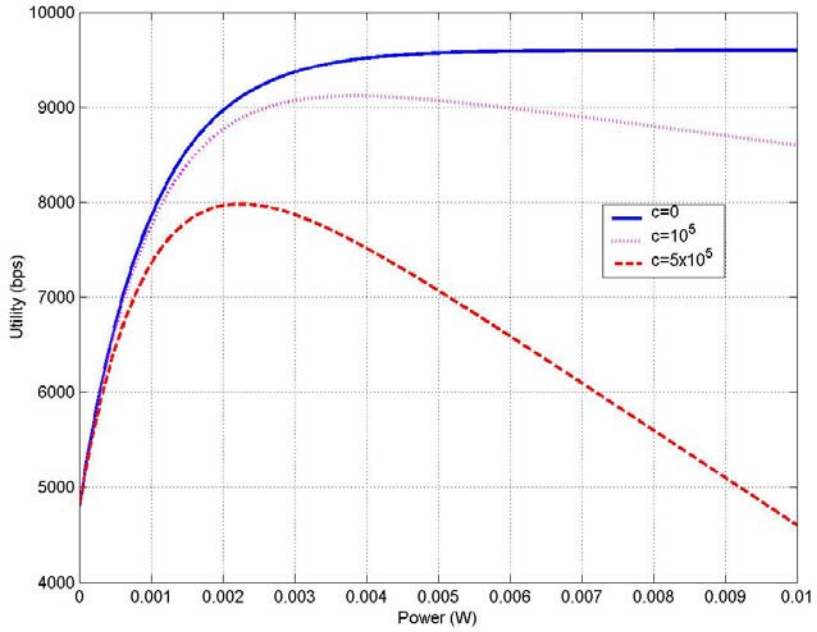

Figure 3.1 Utility function with different values of pricing coefficients

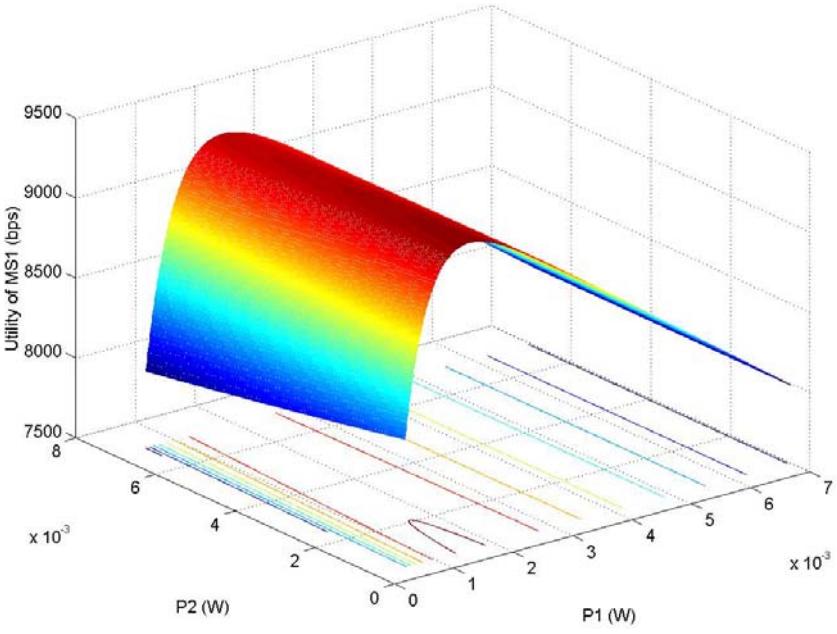

Figure 3.2 Utility of MS1

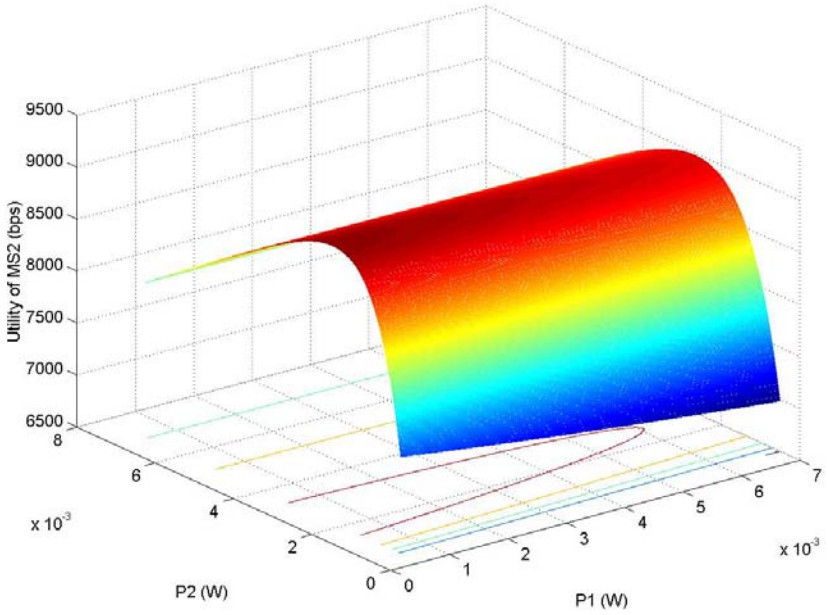

Figure 3.3 Utility of MS2

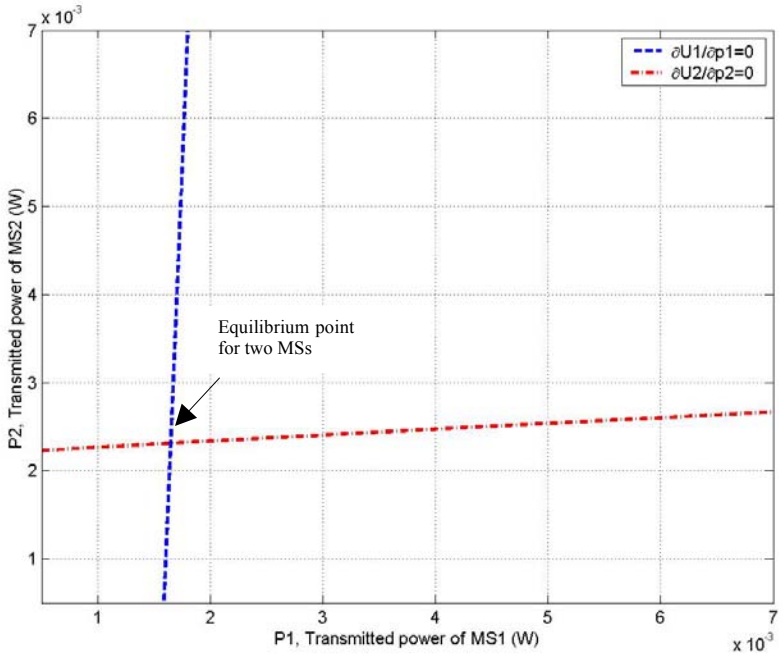

Figure 3.4 The Nash Equilibrium

To implement the solution of the power control game in practice, each MS may need a more efficient searching algorithm than the Newton's method to find the equilibrium strategy (transmitted power) that

can provide the equilibrium utility. Further, the approach of finding the equilibrium transmit power in this section requires each MS to knows other MSs' path losses and transmission rates. In practice, this information is not common knowledge for every MS. To make this information available might be too costly. The next section proposes an alternative that can eliminate this problem and still provide the same Nash equilibrium.

3.3. NASH EQUILIBRIUM COMPUTATION AT BS

Next, the problem formulation when computing the Nash equilibrium at the BS is presented. The advantages of this technique are as follows: 1) It eliminates the Nash equilibrium computation at the MS 2) It eliminates the requirements of each MS to know its own local path gain information and interference level as required for computing the equilibrium at the MS. The SIR and the utility function are redefined as shown in (3.9) and (3.10). The SIRs computed from Equations (3.3) and (3.9) are the same. The difference is the parameters in both equations. p_i^r is the received power at a BS and it is equal to $h_i p_i$. I_i is the interference experienced by MS *i* and it is equal to $\sum_{j \neq i} h_j p_j$. Both p_i^r and I_i can be measured at the BS. Note that the expressions of P_e in Equations (3.1) and (3.10) are the same as in Equation (3.2). The equilibrium *received power* of MS *i* at the BS denoted by $\hat{p}_i^r$ is the point where u_i in (3.10) is maximized. To find the equilibrium, set the derivative of the utility function in (3.10) to zero. Then $\hat{p}_i^r$ can be found as shown in (3.11).

$$\gamma_i = \frac{W}{R}\frac{p_i^r}{I_i + \sigma^2} \tag{3.9}$$

$$u_i = R_i\left(1 - P_e\right) - c_i p_i^r, \quad \text{where } P_e = 0.5e^{-\gamma_i/2} \tag{3.10}$$

$$\hat{p}_i^r = -2\frac{R_i\left(I_i + \sigma^2\right)}{W}\ln\left[4c_i\left(\frac{I_i + \sigma^2}{W}\right)\right] \tag{3.11}$$

Both utility functions in (3.1) and (3.10) have two terms: the effective rate, $R_i(1-P_e)$, and pricing. They are different because of the pricing term. The pricing term in (3.1) is a function of transmitted power; in comparison, the pricing term in (3.10) is a function of received power. Assume that there is only one MS in the systems. Similarly, there is no interference for this MS (I=0). A path loss model, $h=K/d^4$ [14], is employed, where K=0.097 [14] and d=1 km. Therefore, h=0.097/$(10^3)^4$=0.97*10^{-13}. The spectrum

bandwidth (W) of 1.228 MHz, the transmission rate (R) of 10 kbps and the noise (σ^2) of $5*10^{-15}$ watts are assumed. Figure 3.5 shows the plots of the utility functions expressed in (3.1) and (3.10) are the same when the pricing coefficients of both equations are set to zero. In contrast, when the pricing coefficient of the utility function in (3.1) is set at $5*10^5$ bps/watt, a different pricing coefficient in (3.10) is required. An important observation is that the global maxima of these two utility functions are different when the same value of the pricing coefficient is used. To have the same global maximum of utility, we have to set the pricing coefficient in (3.10) = the pricing coefficient in (3.1)/the path gain (h) = $5*10^5/0.97*10^{-13}$ $=5.15*10^{18}$. Figure 3.5 shows that the utilities of (3.1) and (3.10) are almost the same when the pricing coefficient in (3.10) is set at $5*10^{18}$ bps/watt. However, this value of path loss (h) is not required in the proposed power control algorithm in this dissertation. The reason for this is as follows. The pricing coefficient is adaptively changed by an algorithm discussed in Chapter 5.0 to assure the power control performance can satisfy certain requirements as described there.

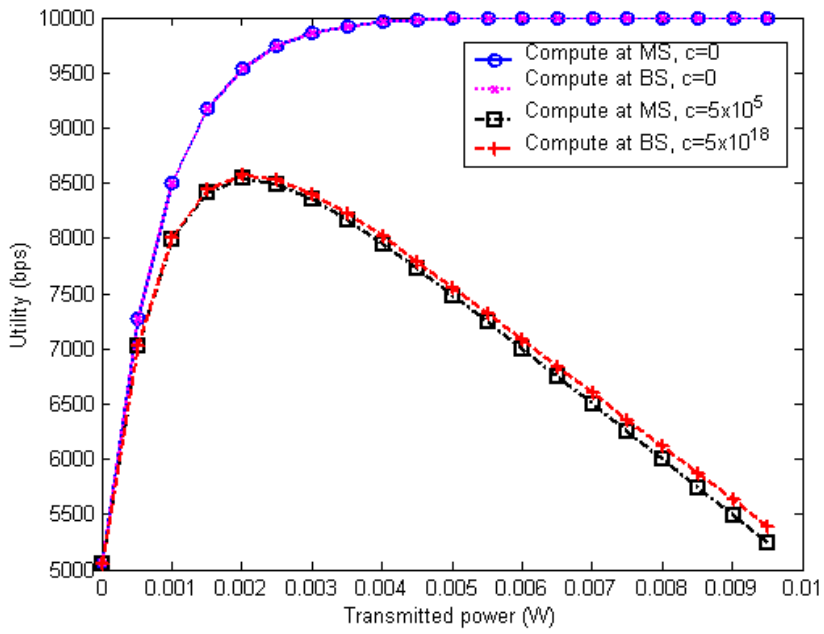

Figure 3.5 Utility when computing the equilibrium at a MS as Equation (3.1) and at a BS as Equation (3.10)

3.4. OTHER LIMITATIONS IN THE LITERATURE AND SOLUTION APPROACHES

Sections 3.2 and 3.3 show the traditional problem formulation of power control using game theory and how to reformulate this problem to eliminate the common knowledge of path gain information. However, a simple form of a utility function is used in this demonstration. Several utility functions have been proposed in the literature and no work has compared or analyzed them together before. Therefore Chapter 4.0 provides the analyses of the utility functions and selects one of them that meets our design goal of power control. Additionally, most utility functions in the literature are functions of bit error rates (BERs). Non-coherent FSK modulation scheme is assumed in most cases. Consequently, the SIR that results in a 1% frame error rate is not close to 6-7 dB like in the real systems. Accordingly, a more realistic bit error rate expression is proposed for the utility functions in Chapter 4.0.

A limitation in the literature that has not been addressed elsewhere is the interference caused by power control. Since each MS tries to maximize its own utility by using power control based on game theory, the interference at the BS can be higher than the allowable level. The power control game formulated in [14] is used for illustration here.

The basic idea in [14] is that every MS in a cell tries to maximize its own utility, by adjusting its transmitted power. The utility in [14] is defined as the number of information bits received successfully per joule of energy expended. It is a function of transmitted power (**p**), packet length: L information bits in an M bit-frame, bit rate (R), SIR (γ) and bit error rate (BER) that depends on the modulation scheme. This utility expression is shown in Equation (3.12). In a non-cooperative power control game, each user tries to maximize its own utility as shown in Equation (3.13). The strategy space of transmitted power in this game ranges from 0 to p_{max}.

$$u_j\left(p_j, \mathbf{p}_{-j}\right) = \frac{RL}{M}\frac{f\left(\gamma_j\right)}{p_j} \tag{3.12}$$

where $f(\gamma) = \left(1 - 2BER\left(\gamma_j\right)\right)^M$ is a function of BER.

$$\max_{p_j \in P_j} u_j(\mathbf{p}) = u_j\left(p_j, \mathbf{p}_{-j}\right) = \frac{RL}{M}\frac{f\left(\gamma_j\right)}{p_j} \text{ for all } j \in N \tag{3.13}$$

The convergence of the utility maximization process by all MSs is to the Nash equilibrium where no single MS can improve its utility by changing its strategy. To find the Nash equilibrium of the

noncooperative power control game, the derivative of the utility function in (3.12) is set to zero. The equilibrium SIR then can be found by solving $f'(\gamma_j)\gamma_j - f(\gamma_j) = 0$. A noncoherent FSK modulation scheme is assumed in [14]. The equilibrium utility is achieved at a certain value of the SIR, which is evaluated to be 12.4 (10.9 dB) for certain parameters (W=10^6 Hz, R=10 kbps, L=64 bits per frame, M=80 bits per frame and thermal noise =$5*10^{-15}$ watts). All MSs must try to adjust their power to achieve this SIR at the BS.

To demonstrate the cause and effect of the interference, the extra-cell interference from neighboring cells in a multi-cell scenario is considered. Assume there is only one MS in a center cell that is surrounded by six neighboring cells. This MS is stationary and its distance is 500 m away from the BS. The MS is assumed to have unlimited maximum transmit power (only for this demonstration). Assume the extra-cell interference is increasing from -140 to -130 dBm. The required transmit power is increased with the extra-cell interference to attain the equilibrium SIR as shown in Figure 3.6. Additionally, this demonstration includes the results of the traditional power control that maintains the target SIR at 7 dB. The required transmit power for attaining the 7 dB is also increased with the amount of extra-cell interference as shown in Figure 3.6. Since the transmit power of the MS is increased in both cases, the intra-cell interference levels are also increased as shown in Figure 3.7. In turn this increases the extra-cell interference to neighboring cells. MSs in these cells can increase their transmit powers leading to an unstable situation. These results indicate that the power control based on game theory using the formulation discussed previously and the traditional power control based on the fixed target SIR can cause high interference levels.

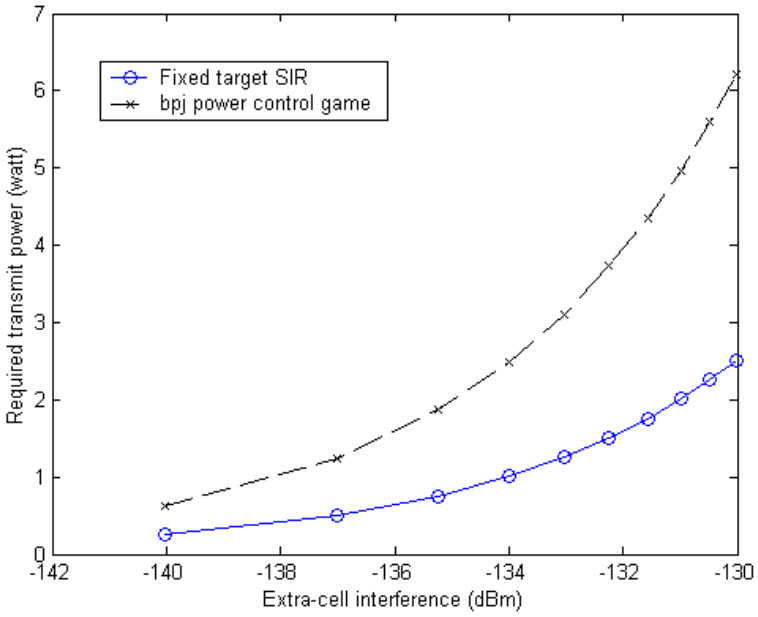

Figure 3.6 Required transmit power for different levels of extra-cell interference when a single MS is in a cell at 500 m from a BS

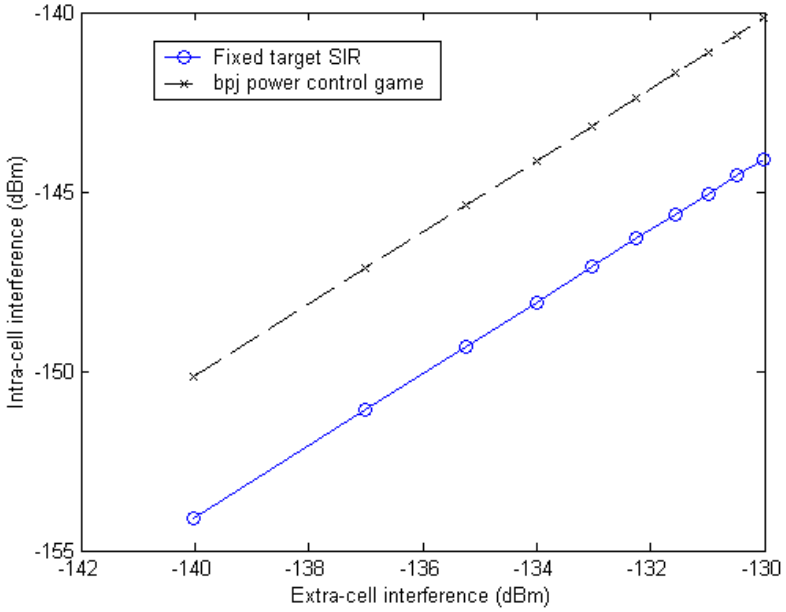

Figure 3.7 Intra-cell interference results from a single MS in a cell at 500 m from a BS for different extra-cell interference levels

In the next demonstration, the MS has a limited maximum transmit power at 1 mW. Assume the MS is moving farther away from the BS. The extra-cell interference from the neighboring cells is -167 dBm. Both power control approaches are examined again. The SIR results are shown in Figure 3.8. The power

control based on game theory cannot reach the equilibrium SIR after 400 m. The traditional power control based on the fixed target SIR cannot maintain the target SIR after 500 m. These results indicate that the extra-cell interference can cause undesirable performance to the power limited systems.

In view of that, power control based on game theory for data-MSs should include interference in its consideration as described in Chapter 5.0.

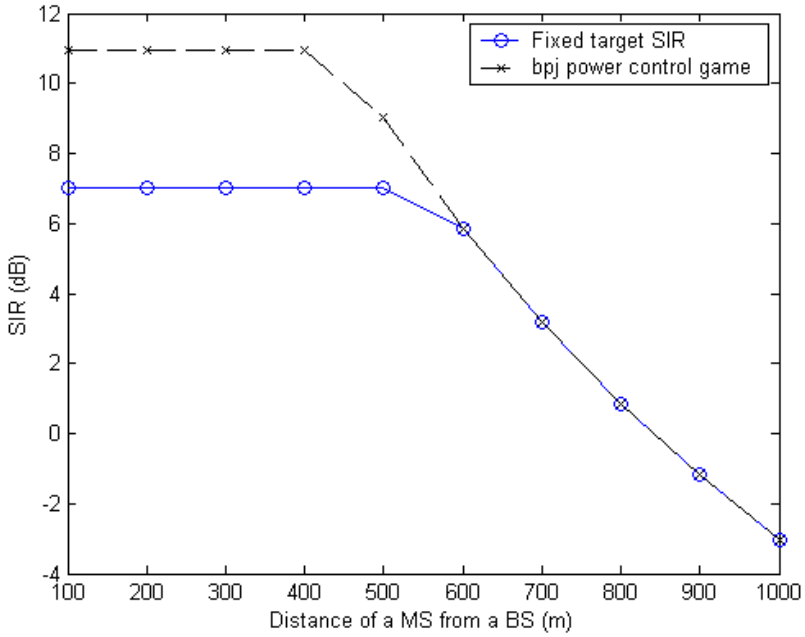

Figure 3.8 SIR results from a single MS in a cell moving farther away from a BS when the extra-cell interference is -167 dBm and the maximum allowable transmit power is 1 mW.

Another important characteristic of data traffic is its bursty transmission. Bursty traffic can result in more radio resource availability in the systems than continuous traffic. Accordingly, radio resource management requires efficient algorithms that can utilize the radio resource as completely as possible. Moreover, the discontinuous transmissions of bursty traffic can cause worse performance of power control due to the problem of convergence to the equilibrium point starting from an initial value at the beginning of every burst. No work on power control based on game theory in the literature has considered this bursty transmission issue before. Chapter 5.0 addresses this issue as well.

The other missing knowledge gap in the literature of power control based on game theory is how it performs in multi-rate systems. Chapter 6.0 discusses this issue. Further, there are some limitations of optimal rate and power assignments in the literature and rate control in the current systems as discussed

comprehensively in Chapter 2.0. Therefore, joint rate and power control algorithms are proposed in Chapter 6.0.

3.5. ASSUMPTIONS AND LIMITATIONS OF THIS WORK

Some research assumptions/limitations in this work are listed as follows. All MSs in a system are non-real time data-MSs. Handoff and admission control are not considered in this work. Both variable rate transmission approaches of variable processing factor (VSF) [61] and multi-code (MC) [62] are considered. In the case of MC, we assume no self-interference from the aggregated codes of the same MSs (since multi-path delay spread effects are not considered). The maximum allowable interference (I_{max}) determines the amount of radio resources that all data-MSs in a cell can consume and it is determined from the quantity *Rise over Thermal* (ROT) in this work. ROT indicates how much load is present on the reverse link and it is defined as the ratio of the interference level at a BS (I_{BS}) to the thermal noise (σ^2) [63]. This work uses I_{max} as the interference threshold in the evaluation of the proposed schemes. Therefore, the term interference threshold and I_{max} are used interchangeably in this work. Game theory applied in this work is not totally non-cooperative because the Nash equilibrium is controlled by a mechanism called a pricing mechanism to improve the system performance. The proposed power and rate control algorithms are decentralized [4] but not fully distributed. Energy consumption at MSs is not considered in this work. The bit error rate expression used in this work may not be completely representative of the actual bit error rate in real systems. We also ignore the changes to the bit error rate expression with time due to the changing environment (MS velocity, intervening objects, etc.).

3.6. CONCLUSIONS

Power control modeled by using game theory in the literature requires common knowledge of all MSs's path gains to compute the Nash equilibrium at each MS. This chapter presents a reformulation of the problem to eliminate this requirement. To do so, we propose to move the computation of Nash equilibrium from the MS to the BS. The analysis shows that computing the Nash equilibrium at either the MS or the BS can provide the same Nash equilibrium. The limitations of work in the literature and this dissertation are addressed.

4.0 ANALYSIS OF UTILITY FUNCTION FOR POWER CONTROL

4.1. INTRODUCTION

Game theoretic approaches for power control in mobile data networks have been investigated in recent years. In this approach, each mobile station (MS) tries to maximize its *utility* in competition with other MSs. The properties and selection of a proper utility function have not been studied in the literature. In most cases, the utility functions have been picked intuitively.

In this chapter we compare the utility functions used in the literature and also investigate issues such as pricing and the range of equilibrium signal to interference ratios for providing dynamic power control. We find that a strictly concave property and the sensitivity of the equilibrium with pricing should be considered in selecting the utility function. We selected examples that represent concave and quasi-concave functions with units that are both in bits per second and in bits per joule. The range of the equilibrium SIRs and the sensitivity of these utility functions to the pricing coefficient are analyzed. The equilibrium SIR of each utility function is illustrated graphically and by numerical analysis. The results show that the concave utility function in bits per second can provide a wide range of equilibrium SIRs, and is more sensitive to the pricing coefficient than the utility in bits per joule. It also requires less computational complexity than the quasi-concave utility function because a local maximum of the concave function is also a global maximum but this is not necessarily true in the case of the quasi-concave functions [64]. Additionally, this chapter studies modifications to the pricing term to improve the range and the granularity of the equilibrium SIRs.

The organization of this chapter is as follows. Section 4.2 describes the utility functions developed in the literature and the utility functions used in the analyses of this chapter. Section 4.3 analyzes the Nash equilibria of each utility function and Section 4.4 provides the conclusion.

4.2. UTILITY FUNCTION EXPRESSIONS

Non-cooperative game theory has been applied to model a distributed power control in wireless data networks. The basic idea is that every mobile station (MS) in a cell tries to maximize its own satisfaction, which is called the *utility*, by adjusting its transmitted power. The desired utility function should be able to provide a good range of equilibrium signal to interference ratios (SIRs) [13, 39, 55, 65] without increasing the computational complexity of the power control algorithm. In this research we investigate the properties of utility functions for such game theoretical approaches for power control in wireless data networks.

Several expressions of utility functions have been developed in the literature for power control. The meaning (or units) of these utility functions are different. They mostly focus on throughput (bits per second) [13, 65-67] and throughput per unit consumed power (bits per second per watt or bits per joule) [14, 16]. The utility functions are composed of two main components: the *amount of assigned radio resources* and the *percentage of correctly received information* at the BS. In the literature, the amount of assigned radio resource is either the assigned transmission rate (R) for the utility in bits per second or the ratio of the assigned rate to the transmit power (R/p) for the utility in bits per joule. Several functions are used in the literature to represent the percentage of information correctly received at the base station (BS). Such functions are called *efficiency functions* in [14]. The bit error rate expression for non-coherent FSK is used in [66]. A modified frame and bit error rate expressions with non-coherent FSK are used in [14, 16] and [65, 67, 68], respectively. A sigmoid function is used in [69] that does not depend on the bit error rate or frame error rate. Information theory is used to derive a bound to the efficiency function and this bound is used in the power control based on game theory in [13] without requiring the knowledge of the modulation and coding. These efficiency functions impact the shape of the utility functions. The shapes of utility functions can be described as concave or quasi-concave [14]. A function f is concave/convex if and only if the line joining between any two points on the curve of f (assume it is a function of one variable) is not below/above the curve f. Specifically, if this joining line segment is always below the curve f, then the function f is a strictly concave function. The curve of the quasi-concave function is composed of both convex and concave shapes. The formal definition of these functions can be found in [64]. The shape of the utility function has an effect on the range of the Nash equilibrium and the computational complexity. No work in prior literature has addressed or examined the effect of the shape of utility function for power control.

We select utility functions for study from [13, 14, 16, 65, 66, 69]. The efficiency functions of these utility functions determine the concavity property. The first group of efficiency function makes use

of the bit error rate expression of non-coherent FSK. The efficiency function in Equation (4.1) is the probability that a transmitted bit is received correctly [66]. The efficiency function in Equation. (4.2) is the probability that a transmit frame is received correctly. The number of bits in a frame is denoted by *M*. The bit error rate expression of non-coherent FSK in the efficiency function of [14] is modified as shown in Equation (4.3). This is done to prevent the utility function from going to infinity (the utility function in [14] is $(R/p)*f_3$) when the transmit power is equal to zero. The efficiency function in Equation (4.4) is another possible function that can be used in the utility function.

$$f_1 = \left(1 - 0.5e^{-\gamma/2}\right) \tag{4.1}$$

$$f_2 = \left(1 - 0.5e^{-\gamma/2}\right)^M \tag{4.2}$$

$$f_3 = \left(1 - e^{-\gamma/2}\right)^M \tag{4.3}$$

$$f_4 = \left(1 - e^{-\gamma/2}\right) \tag{4.4}$$

In [65], the bit error rate expression of non-coherent FSK modulation is modified to a general form such that it reflects a more realistic BER. The general form of the efficiency function used in [65] is shown in Equation(4.5).

$$f_5 = (1 - \alpha^{-1} e^{-\gamma/\beta}) \tag{4.5}$$

A similar BER expression has also been employed in [70] for other purposes. If α=2, γ_{th} = 7 dB for 1 % FER and *M* = 256 bits for 9.6 kbps, then β = 0.5304 [65]. The details of this BER expression are provided in Appendix A. Another possible efficiency function that can be used in the utility function is represented in the equation shown below.

$$f_5 = (1 - \alpha^{-1} e^{-\gamma/\beta})^M \tag{4.6}$$

The efficiency function in [69] is a Sigmoid function as shown in Equation (4.7). Let *a* and *b* denote the tuning parameters that can be used for defining different qualities of service requirements of each user [69]. Examples of parameters *a* and *b* used for illustration in [69] are 1 and 10, respectively.

$$f_{sigmoid} = \frac{\left(1 + \exp(-a(\gamma - b)\right)^{-1} - \left(1 + \exp(ab)\right)^{-1}}{1 - \left(1 + \exp(ab)\right)^{-1}} \tag{4.7}$$

In [13], the efficiency function is derived from an information theoretic approach. If we assume a binary symmetric channel, the efficiency function can be expressed as shown in Equation (4.8), where $q(\gamma)=0.5\text{erfc}(\sqrt{\gamma})$. This efficiency function does not assume any modulation or coding schemes.

$$f_{BSC} = 1 + q(\gamma)\log_2 q(\gamma) + (1 - q(\gamma))\log_2 (1 - q(\gamma)) \tag{4.8}$$

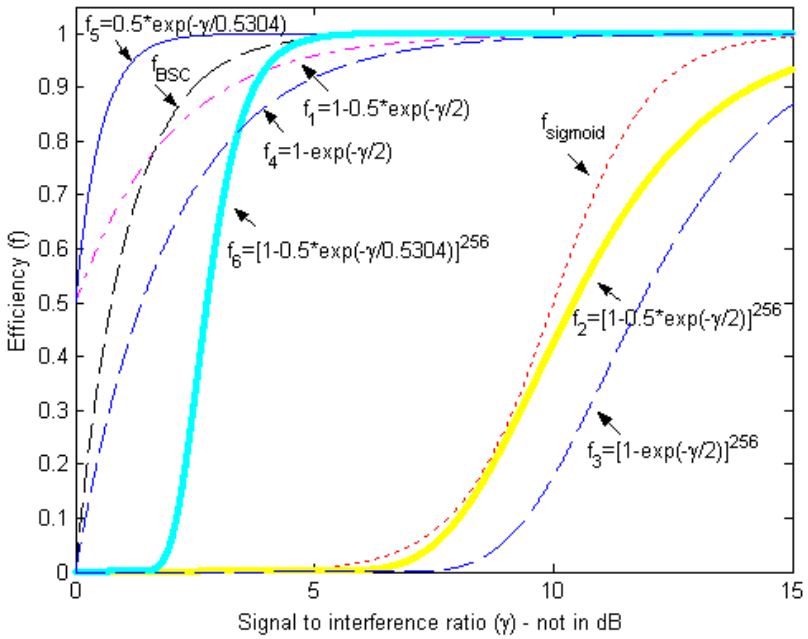

Figure 4.1 Concavity illustrations

All functions in Equations (4.1) to (4.8) are plotted in Figure 4.1. We assume M=256 bits for this plot. We see that the efficiency function can be quite different as a function of the SIR. As discussed previously, the utility itself can have different meaning depending on these efficiency functions.

The shapes of these efficiency functions can be classified into two groups: concave and quasi-concave functions [14]. Equations (4.1), (4.4), (4.5) and (4.8) are concave and the remaining are quasi-concave. The efficiency functions in the same group can provide similar characteristics of Nash equilibrium according to the concavity property. Therefore, only some of these efficiency functions are selected for further analyses.

The utility in [65, 66] is defined as the effective rate in bits per second (bps). The original utility is shown in Equation (4.9) and its modified version is shown in Equation (4.10).

$$u_i = R \times f_1 \tag{4.9}$$

$$u_i = R \times f_2 \tag{4.10}$$

The utility in [14, 16] is defined as the number of information bits received successfully per joule of energy expended (bpj). It is a function of transmitted power (p), packet length: L information bits in an M bit-frame, bit rate (R), SIR (γ) and the efficiency function (f) described previously. Two utility expressions used in this study are those modified from [14, 16] as shown in Equations (4.11) and (4.12). The ratio of actual amount of information to the transmitted bits (L/M) is neglected here.

$$u_i = (R / p_i) \times f_3 \tag{4.11}$$

$$u_i = (R / p_i) \times f_4 \tag{4.12}$$

Suppose there is only one MS in the system implying that there is no interference for this MS. If the spread bandwidth (W) is 1.228 MHz, the transmission rate (R) is 9.6 kbps, the noise (σ^2) PSD is 5×10^{-15} watts [14] and the packet length (M) is 256 bits, the SIR (γ_i) = $W/R \times (h_i p_i/\sigma^2)$. Using $h_i = K/d^4$ where K=0.097 [14], we can plot the utility functions in bpj and bps as shown in Figure 4.2 and Figure 4.3, respectively. In all of the examples in this chapter, we use the numbers for the maximum point with only one user in the system. The actual equilibrium value will be different depending on the number of users and their locations [14, 39, 66]. The equilibrium can be computed as described in Chapter 3.0. However, the equilibrium value shows a trend that is similar to this maximum value of the utility function for one user when the utility function is concave.

The plots in Figure 4.2 and Figure 4.3 illustrate that a global maximum exists in the case of Equation (4.11) only. In this case, the best SIR (equilibrium) from Equation (4.11) is around 15. At this SIR level (γ_i), $p_i = (W/R)^{-1}(\gamma_i \sigma^2/h_i)$. If the MS is at 100 m from the BS, then p_i= 0.6 μW. If the SIR is increased to be higher than 15, the effective rate still keeps increasing. If this utility function is employed, the users will transmit at the equilibrium SIR of around 15 but improvement of throughput is still possible. Therefore, the utility function in (4.11) is not suitable if the MS wants to maximize its own throughput. The other utility functions in Equations (4.12) to (4.10) do not have the global maximum points. Note that this does not include the points where p_i is equal to the minimum or maximum power. To create a maximum point, these utility functions employ *pricing*. They are however more flexible in moving this maximum point as discussed later.

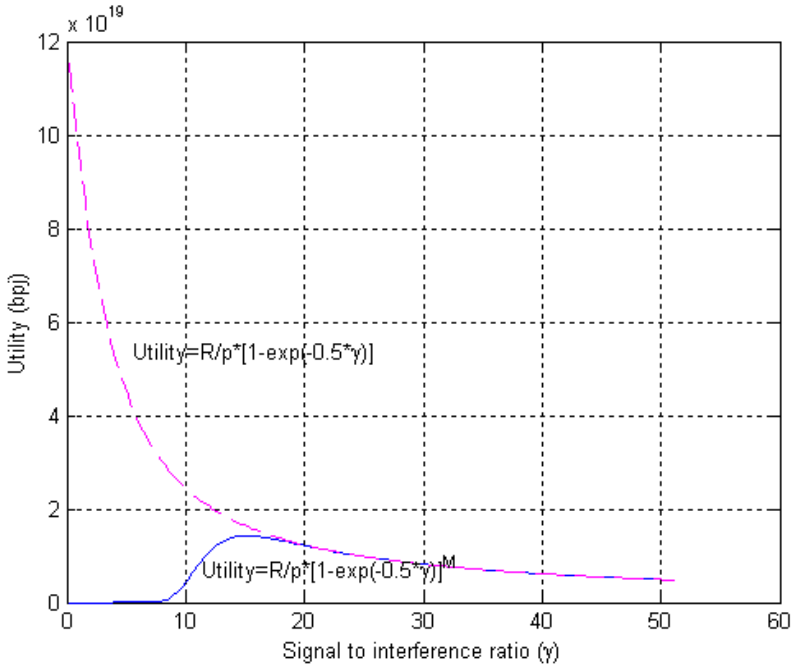

Figure 4.2 Utility in bits per joule (bpj)

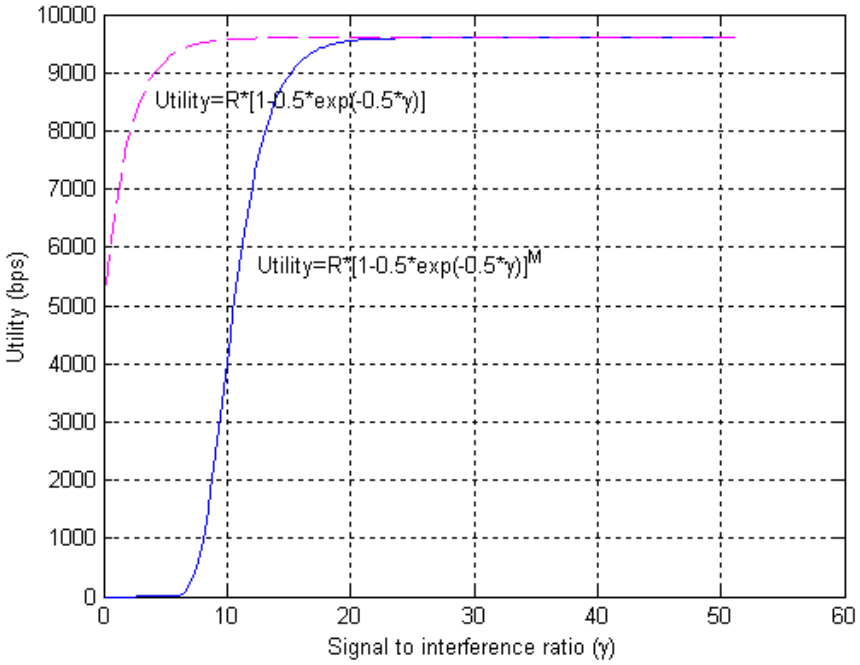

Figure 4.3 Utility in bits per second (bps)

It is well known that a totally non-cooperative game may result in a Nash equilibrium that causes poor system performance. Pricing mechanisms are often used in the literature for improving the efficiency of

the Nash equilibrium by adding the pricing term in the utility function. In the literature of power control based on game theory, the utility function with pricing term is defined as $u_i^c = u_i - c_i p_i$, where u_i, c_i and p_i denote the original utility, the pricing coefficient and the transmit power of MS i, respectively. In this case, the pricing term is just a function of an additional parameter c_i and the transmit power. When the pricing coefficient is changed to a different value, the utility is also changed. Accordingly, the maximum utility can be changed depending on this pricing coefficient. The meaning of *pricing* can be either based on economics (monetary) or control signaling. In wireless networks, pricing has been shown to improve the efficiency of the Nash equilibrium in if power control is implemented as a non-cooperative game [14]. The purpose of using this pricing strategy in this research is to control the Nash equilibrium to meet the desirable system performance. However, no work has studied how sensitive the utility functions employed in the literature are, to the pricing component. In addition, utility functions can be modified to be functions of the received power and interference at a BS instead of the transmit power at MSs. This eliminates the global information requirement by all MSs and depending on scaling parameters, can represent the same utility as before. This approach is taken in [65] and discussed in Chapter 3.0.

Pricing can be applied to move MSs from the equilibrium towards a more efficient set of strategies. The utility function in Equation (4.11), for example, can be reformulated by including a pricing coefficient (c_i) as shown in Equation (4.13). (The utility function in Equation (4.12) is not further considered since it is a convex function as shown in Figure 4.2.) The unit of this pricing coefficient is in b/J/watt = bps. Similarly, the utilities in bps from Equations (4.9) and (4.10) with the pricing term can be expressed as shown in Equations (4.14) and (4.15). The unit of the pricing coefficient here is in bps/watt.

$$u_i = \left(R / p_i\right) \times f_3 - c_i p_i \tag{4.13}$$

$$u_i = R \times f_1 - c_i p_i \tag{4.14}$$

$$u_i = R \times f_2 - c_i p_i \tag{4.15}$$

Solving for the equilibrium transmitted power locally using the above utility functions is not likely to be practical because of the need for common knowledge of MS parameters and the associated computational complexity. An approach to overcome this problem is to compute the Nash equilibrium at the BS instead [65, 66]. In this case, these utility functions can be redefined as shown in Equations (4.16) to (4.18) by using the received power at the BS denoted by p_i^r.

$$u_i = \left(R / p_i^r\right) \times f_3 - c_i p_i^r \tag{4.16}$$

$$u_i = R \times f_1 - c_i p_i^r \tag{4.17}$$

$$u_i = R \times f_2 - c_i p_i^r \tag{4.18}$$

4.3. UTILITY FUNCTION ANALYSES

The utility functions in Equations (4.16) to (4.18) are evaluated next by varying the pricing coefficients. Global maxima exist for all utility functions when the pricing coefficients are not zero as shown in Figure 4.4 to Figure 4.6. When the pricing coefficients are varied at three levels: 1, 10^{18} and 5×10^{18}, the maximum points in the case of Equations (4.17) and (4.18) change more significantly than Equation (4.16) whose maximum points *are nearly the same*. If the pricing coefficients increase to 5×10^{33} and 10^{34}, then the global maxima of Equation (4.16) also changes significantly as shown in Figure 4.4. However, using a too high value of the pricing coefficient may face a number representation limitation in the central processing unit of the equipment at a BS.

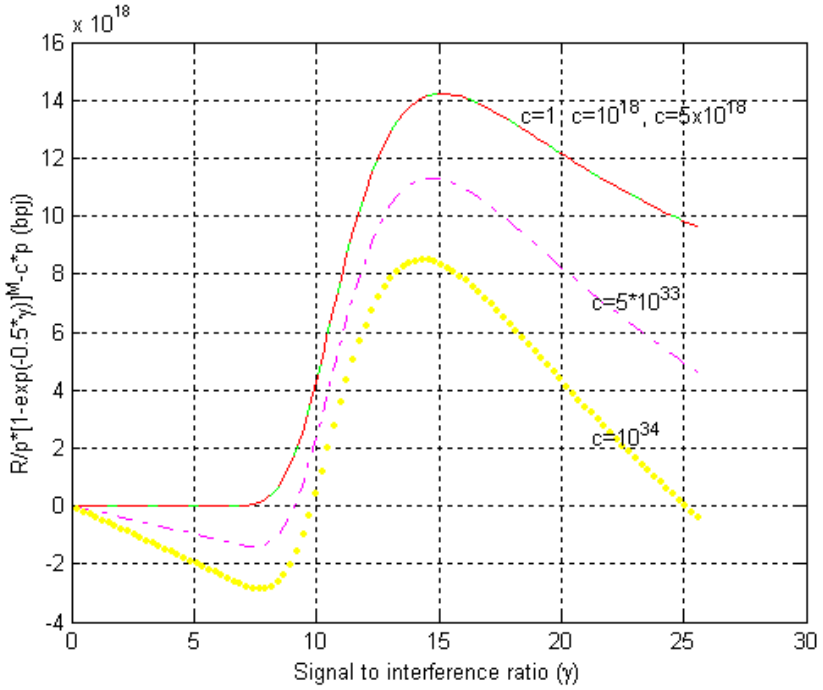

Figure 4.4 Sensitivity of the utility function in Equation (4.16) with the pricing coefficient

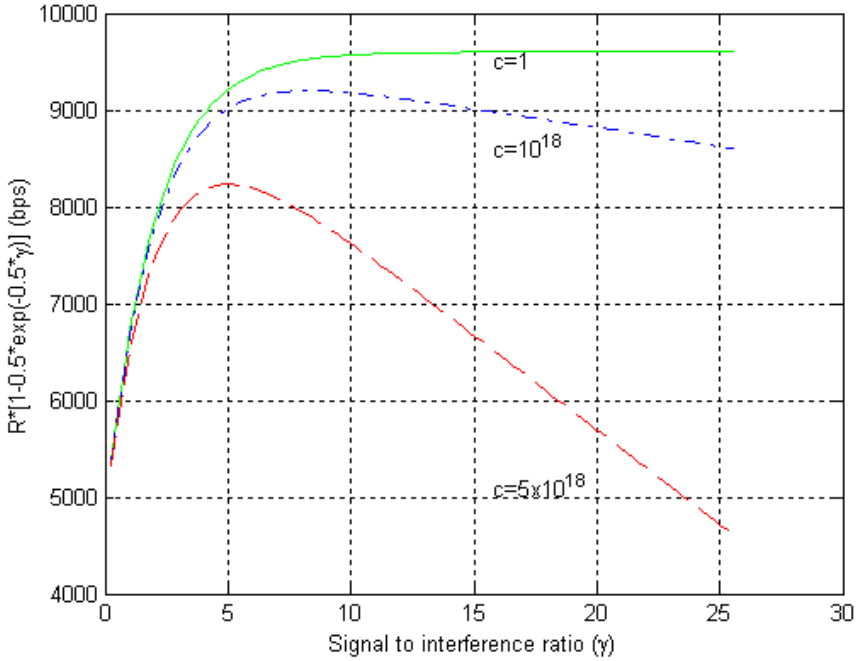

Figure 4.5 Sensitivity of the utility function in Equation (4.17) with the pricing coefficient

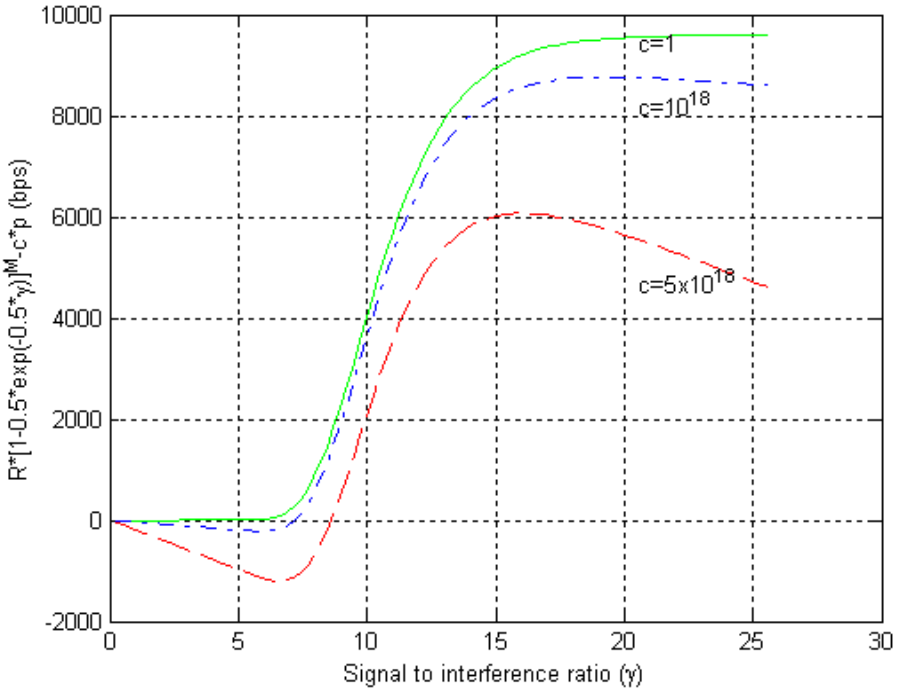

Figure 4.6 Sensitivity of the utility function in Equation (4.18) with the pricing coefficient

We can use numerical analysis based on the Newton's method [12] to compute the SIRs for maximum utility from the utility functions for different pricing coefficients. These values are shown in Table 4.1 for Equations. (4.16) to (4.18). We can clearly see that the SIR for maximum utility is nearly constant in the case of Equation (4.16). In contrast, the utility functions of Equations (4.17) and (4.18) are more sensitive to the pricing coefficient variation than Equation (4.16) as shown in Table 4.1. Consequently they allow for more flexibility in implementation. Additionally, only the utility function defined in Equation (4.17) is strictly concave as graphically illustrated in Figure 4.4 to Figure 4.6 and the closed form solution of Equation (4.17) found in [66].

In conclusion, the utility in bits per joule with the pricing coefficient, which is a quasi-concave function, has much lower sensitivity to the pricing coefficient than the utility functions in bits per second. The utility function in bits per second can be both concave and quasi-concave functions depend on the efficiency function. Both have a similar sensitivity to the pricing coefficient.

Accordingly, we select the utility function defined in Equation (4.17) as the most suitable for a controllable Nash equilibrium approach because it has the following properties. First, it has a wide range of the equilibrium SIRs that can be controlled by the pricing coefficient. The utility function in b/J does not have this property because it has a very narrow range of the equilibrium SIRs. Second, it is strictly concave. In comparison, the utility function defined in (4.18) is not concave, so it is less appropriate than Equation (4.17). In Chapters 5.0 and 6.0, we use the modified efficiency function f_5 in Equation (4.5) instead of f_1 in Equation (4.1). However, it displays characteristics similar to (4.1).

Next, the sensitivity of this utility function to increases in the exponent of the power in the pricing term in Equation (4.17) is studied. The pricing term is modified as shown in Equation (4.19) by adding another parameter called a pricing index (n).

$$u_i = R \times f_1 - c_i\left(p_i^r\right)^n \tag{4.19}$$

The sensitivity of the utility function to the pricing index n as expressed in Equation (4.19) is examined. Three levels of the pricing coefficients are evaluated again: 1, 10^{18} and 5×10^{18} bps/W. Four levels of n are examined: 0.95, 0.98, 1 and 1.2. The plots of the utility functions are shown in Figure 4.7 to Figure 4.9.

For the pricing coefficient of 1 bit/sec/watt, the plots of the utility functions are close together as shown in Figure 4.7. When the pricing coefficients are 10^{18} and 5×10^{18} bps/W, the utility has a global maximum. This maximum point changes when n changes as shown in Figure 4.8 and Figure 4.9. The equilibrium SIRs (solved by the Newton's method) are shown in Table 4.2. Comparing the numerical results in Table 4.1 and Table 4.2, we see that Equation (4.19) can extend the granularity and range of the

Nash equilibrium compared to (4.17). For example, the numerical result for the equilibrium SIR in Table 4.1 is 91.130 when the pricing coefficient is 1 bit/sec/watt for the utility in (4.17). The results in Table 4.2 at the pricing coefficient of 1 bit/sec/watt show a wide range of the equilibrium SIR from 87.901 to 104.019. Consequently, the pricing index and the pricing coefficient in the utility function defined in (4.19) can potentially be used for controlling the range and granularity of the Nash equilibriums to meet the desired performance in power sensitive systems.

Table 4.1 The equilibrium SIR (not in dB) for different pricing coefficients for different utility functions

Utility function	Pricing coefficient (c)				
	1	1e18	5e18	5e33	1e34
bpj in Equation (4.16)	15.140	15.140	15.140	14.714	14.364
bps in Equation (4.17)	91.130	8.236	5.017	0	0
bps in Equation (4.18)	102.220	19.310	16.023	0	0

Table 4.2 The equilibrium SIR for different pricing coefficients and a pricing index for the utility in bps in Equation (4.19)

Pricing coefficient (c)	Pricing index (n)			
	0.95	0.98	1	1.2
1	87.901	89.838	91.130	104.019
1e18	4.716	6.8422	8.236	21.572
5e18	1.373	3.598	5.017	18.596

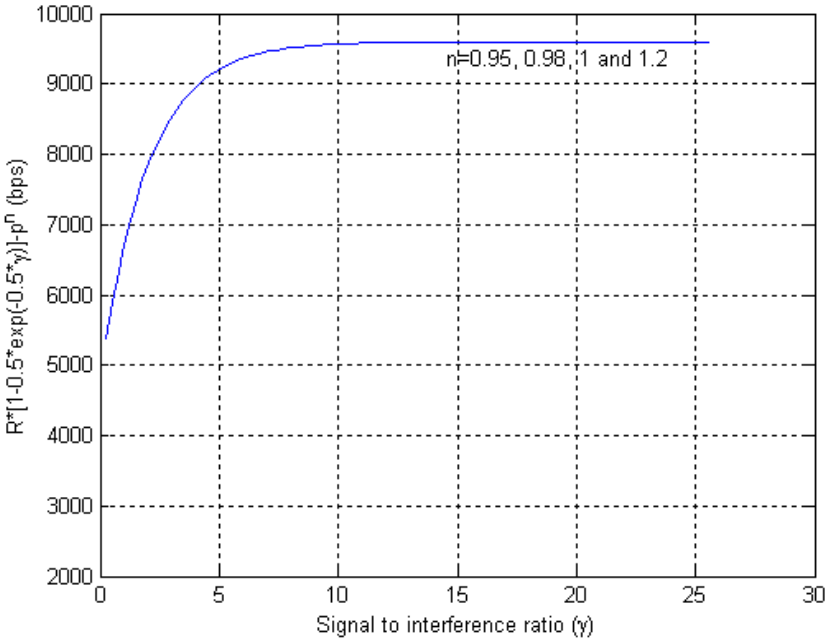

Figure 4.7 Effect of the pricing index (*n*) on the utility function in Equation (4.19) when *c*=1

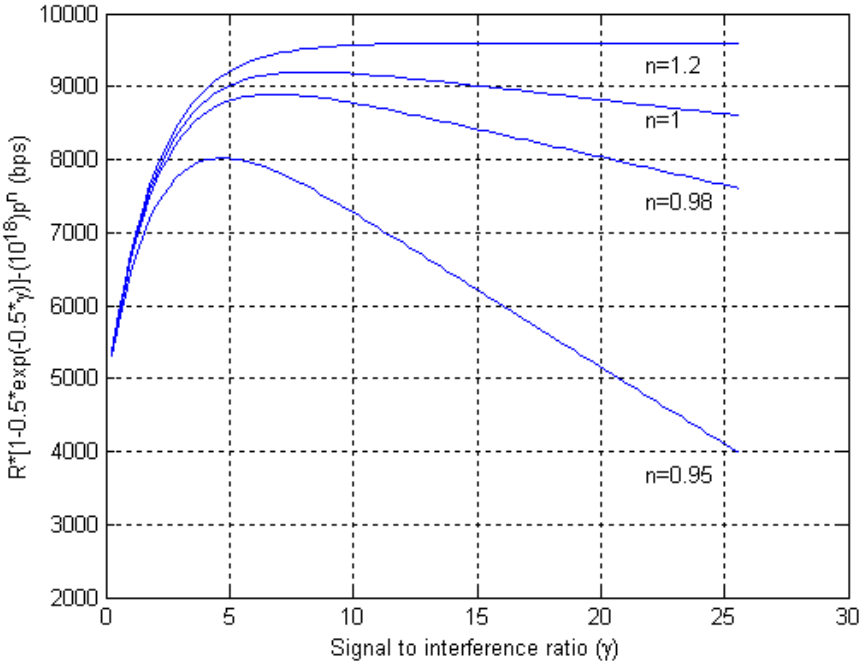

Figure 4.8 Effect of the pricing index (*n*) on the utility function in Equation (4.19) when c=10^8

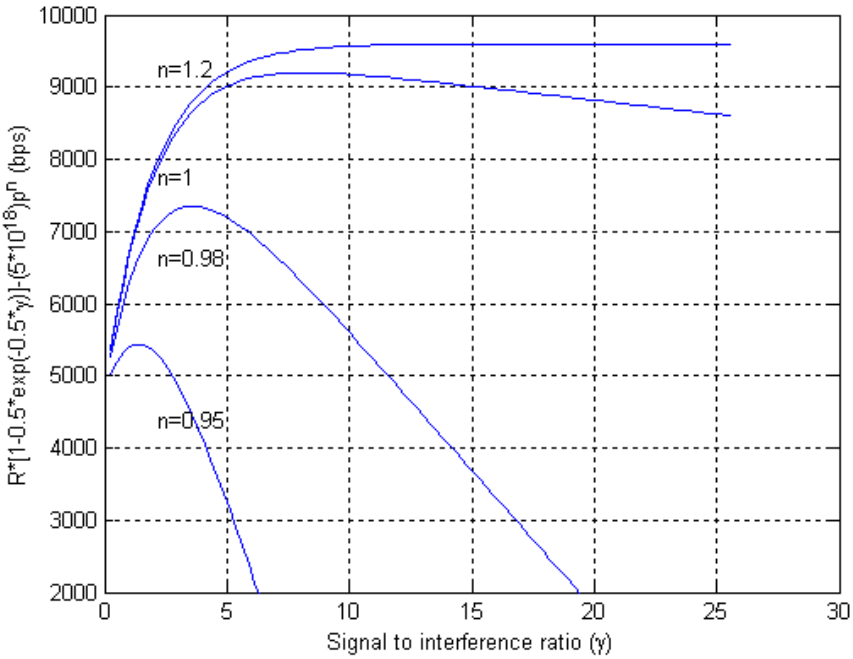

Figure 4.9 Effect of the pricing index (*n*) on the utility function in Equation (4.19) when $c=5\times10^8$

4.4. CONCLUSIONS

Utility functions for game theoretic approach to power control in mobile data networks were studied. The shapes and units of various utility functions used in the literature were discussed. To have a wide range of Nash equilibria, the utility function and the pricing coefficient have to be selected carefully. A utility function based on bps seems appropriate for this purpose as it provides flexibility in picking the equilibrium point by changing the pricing coefficient. Further, we find that the range and granularity of the controllable Nash equilibrium can be improved by varying the power index of the transmit power in the pricing term of the utility function. A closed form solution to the equilibrium point using these utility functions needs to be further investigated.

5.0 POWER CONTROL ALGORITHMS

5.1. INTRODUCTION

A totally non-cooperative game may result in Nash equilibrium with poor system performance. Pricing mechanisms are often used in the literature for improving the efficiency of the Nash equilibrium. The meaning of pricing can be either based on economics (monetary) or control signaling. For wireless networks, pricing has been shown to improve the efficiency of the Nash equilibrium if the power control problem is modeled as a one shot game [14]. A one shot game or simultaneous move game is the case where each participant chooses its action without knowing the decisions of the other participants. Thus, there is only one chance for each participant to choose a strategy. The power control problem can also be modeled as a repeated game. In this case, punishment is employed to control a misbehaving user. If a user transmits at a power level higher than the value suggested by the equilibrium, other users will punish that user by increasing their power levels in the next frame [16]. The research area of algorithmic mechanism design or implementation theory studies methodologies to ensure desirable behavior in selfish users. The goal of mechanism design is to inspire users to reveal their data or strategy truthfully. Payment from a user to an authorized entity is a common technique to achieve this goal [71]. For example, consider the problem of shortest path routing in a communication network that is modeled by a directed graph [72]. A node in this network might not want to forward data because of the transmission cost. It is necessary to ensure that each node in the network broadcasts its true routing cost to others in order to obtain the "lowest-cost" routing path. Algorithmic mechanism design for this problem provides for payment to a node if it becomes a part of the route and that route is the shortest path [72]. A Leader-Followers or Stackelberg strategy is another approach used in controlling the users' behavior to achieve a preferable system performance [73]. Here, one of the participants is selected as a leader and the remaining are grouped as followers. This strategy can be applied in sequential move games where each participant knows the previous actions of others before it chooses its own action. Accordingly, the leader selects its action and followers will choose actions that result in the desired performance. The routing problem studied in [74] employs this strategy by assuming that a leader is a central entity that knows the behavior

of all other users in real time. The leader chooses its own route and sends some signaling or traffic into the network. The transmission delay of each route is changed because of the traffic generated by the leader. Followers have to adjust their routing accordingly. The new equilibrium is what the leader plans in advance in order to achieve the desirable network performance. In this dissertation, the pricing mechanism is applied in the proposed power control algorithms to control the Nash equilibrium to meet the desired level of throughput performance.

Section 5.2 presents the development of power allocation to MSs for achieving the best SIR while maximizing the throughput of each user and considering both the maximum transmit power level and the maximum allowable interference. This power control algorithm is applied with the existing closed loop power control mechanism where *only a one-bit* power command feedback from a BS periodically informs a MS whether to increase or decrease the transmit power by a predefined step size. The pricing mechanism is applied in an algorithm called *adaptive pricing*. This adaptive pricing algorithm is used in the closed loop power control to determine the required level of received power at a BS. The running time of the algorithm is discussed in Section 5.3.The performance of this closed loop power control algorithm with the one-bit power command feedback is close to the power control algorithm with the exact feedback information as discussed in Section 5.4. When bursty traffic is considered in Section 5.5, the proposed power control results in a dynamic target SIR approach based on the number of simultaneous burst transmissions in the cell. The proposed algorithms control the incurred interference at a BS such that it converges to the maximum allowable interference. The performance of the proposed power control algorithms is examined under bursty transmissions and unpredictable interference from the neighboring cells. The performance is compared with the traditional power control based on the fixed target SIR. The simulation results show that the proposed power control scheme can provide higher SIR allocations than the traditional power control when the radio resources are under-utilized.

5.2. PROPOSED POWER CONTROL ALGORITHM

Radio resource utilization is determined by the SIR requirement, the maximum allowed transmitted power, and received interference level. The maximum allowable interference (I_{max}), which corresponds to the highest level of resource consumption on the radio access part, needs to be defined. The concept of *rise over thermal* (ROT) is used for determining the value of I_{max}. The ROT indicates how much load is present on the reverse link (MS to BS) and it is defined as the ratio of the interference level at a BS (I_{BS}) to the variance of the thermal noise (σ^2): ROT = I_{BS}/σ^2 [63]. If the level of thermal noise is 5×10^{-15} watts

[11] and the maximum ROT allowed is 6 dB (in 1x-EV-DO systems) [8], the maximum allowable interference (I_{max}) is equal to 1.99×10^{-14} watts. This value of I_{max} is used in our numerical analysis. Also, the uplink interference at a BS can occur from MSs in both the same cell and other cells (extra-cell). The ratio of extra-cell to intra-cell interference is defined by the neighboring cell interference factor (f). Typically, a value of $f = 0.55$ is used for back of the envelope calculations [75]. The value of f in reality, is changing dynamically.

To illustrate how this maximum interference threshold impacts power control, an example of equal radio resource allocation for single rate data traffic (i.e. the received power from all N MSs is the same and it equals $I_{max}/N/(1+f)$) is given here. Assume that the number of active MSs (N) is known and all of them transmit at 9.6 kbps. If the maximum allowable interference is given as 1.99e-14 W (from the previous example) and there is only a single cell in the system, i.e., f =0, the maximum received SIR can be determined as shown in Figure 5.1. N_j denotes the number of MSs in cell j. The second SIR plot assumes that there is extra-cell interference which is quantified by $f = 0.55$.

In Figure 5.1, the maximum number of MSs that can be supported is around 20 under the constraints of a required 7-dB SIR and allowable interference of 1.99×10^{-14} W. Under-utilization of radio resources can occur when the number of data-MSs in a cell per carrier is less than 20 MSs (or 13 MSs in a multi-cell scenario) when such a fixed target SIR power control is employed. Consequently, a data-MS may not achieve higher throughput although there are unused radio resources. For example, if the number of MSs is five, the SIR should equal 14 dB (or about 12 dB in a multi-cell scenario) as shown in Figure 5.1 instead of 7 dB. If however they all try to get a SIR far higher than 14 dB (or about 12 dB in a multi-cell case), the interference level can exceed the maximum allowed. Thus, to prevent under or over utilization of radio resources, an interference threshold (I_{th}) should be included in power control. This interference threshold is a function of the maximum allowable interference (I_{max}) and should be dynamically changed according to the environment. However, this threshold is set to I_{max} for simplicity in this work. In traditional radio resource management, the number of MSs is limited such that the interference is not greater than this threshold and all MSs still obtain the minimum requirements of signal quality. Since a data-MSs can tolerate some delay and allow retransmissions, an additional number of data-MSs can also be admitted. For example, if 25 MSs want to transmit at the same time in a single cell scenario, traditional radio resource management can admit only 20 voice-MSs. This is not efficient if these 25 MSs are data-MSs. All of them should perhaps be allowed to transmit data because they can tolerate some delay if there are packet losses.

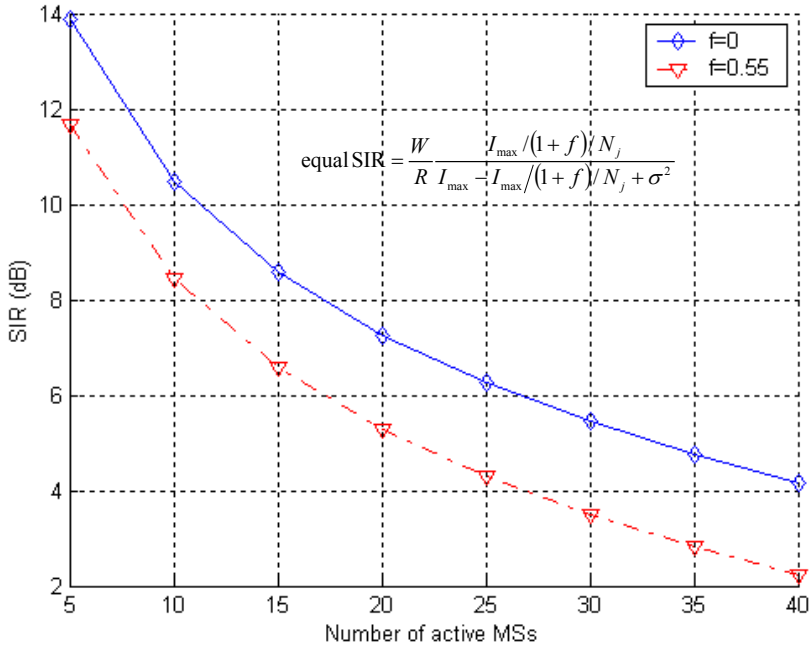

Figure 5.1 Equal received SIR allocation for 9.6 kbps given the maximum allowed interference level

The purpose of this work is to design a new power control algorithm that can consider *the criteria of the maximum allowable interference level while providing flexibility in allocating radio resources*. Note that this work does not focus on finding the suitable level of FER that a data-MS could tolerate based on the acceptable delay from data retransmission. In this work, we still look at continuous transmissions and single rates, but this work can be extended to account for bursty [65] traffic and multi-rate transmission [67] as well and is described later in this chapter and Chapter 6.0.

Basically, the SIR of MS i at BS j (γ_{ij}) is the function of MS i's received power $\left(p_{ij}^{r}\right)$ and interference level (I_{ij}) at BS j as shown in Equation (5.1). W, R, and σ^2 denote the spreading bandwidth, the transmission rate and the noise at the BS. By using the equal received power strategy, the SIR obtained by each MS is equally assigned and can be expressed as shown in Equation (5.2). N_j is the number of active MSs transmitting data to BS j. I_{max} is the maximum allowable interference at the BS. f is the ratio of the extra-cell interference from neighboring cells to the intra-cell interference. In practice, f is not known [10].

$$\gamma_{ij} = \frac{W}{R_{ij}} \frac{p_{ij}^{r}}{I_{ij} + \sigma^2} \tag{5.1}$$

$$\text{equal SIR} = \frac{W}{R}\frac{I_{\max}/(1+f)/N_j}{I_{\max} - I_{\max}/(1+f)/N_j + \sigma^2} \tag{5.2}$$

From the fact that the interference can be divided into intra-cell and extra-cell interference and the latter is difficult to predict [10], the proposed algorithms cannot work perfectly. The same-cell interference is controllable by using our approach but the extra-cell interference is hard to control and predict. Therefore, the proposed power control algorithms are designed to be partially adaptive to the dynamic interference level. Nonetheless, the evaluation in the next sections using simulations includes the effect of the unpredictable interference from neighboring cells to show how well the proposed algorithms perform.

The proposed power control algorithm can be implemented in the existing power control schemes with some modification as shown in Figure 5.2. The open loop power control algorithm is required initially during the access of each MS's burst transmission when the feedback from the BS is not available. In the open loop power control algorithm, the MS transmits data at the power level determined by Equation (5.3) [28]. p_{ij}^{r-BS} denotes the received power at the MS *i* on a reference channel (usually the pilot channel) from the BS *j*. $P_{control}$ is a parameter specified by a BS. This work assumes $P_{control}$ = 0 dB [28].

$$p_{ij}(\text{dBm}) = -p_{ij}^{r-BS}\ (\text{dBm}) - 73 + P_{control}(\text{dB}) \tag{5.3}$$

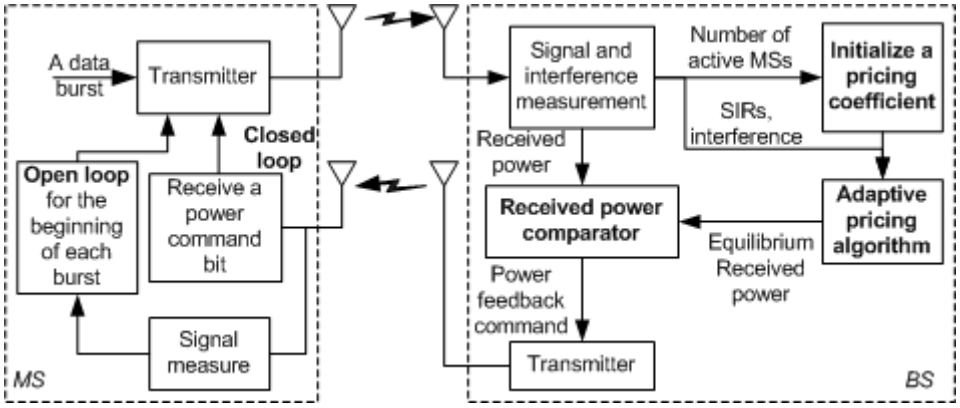

Figure 5.2 Block diagram of power control for bursty transmission

The BS measures the received power from the MS and the interference level for further computing the suitable power level. This power level is defined by the Nash equilibrium from game theory. It is best that each MS does not deviate from its equilibrium power level because its satisfaction defined by a utility function is reduced otherwise. In this research, the utility function is defined as the effective rate as shown

in Equation (5.4). Its unit is in bits per second (bps). P_e is the bit error rate (probability of error transmissions) which is a function of SIR as explained in Appendix A. The second term (pricing term) consists of the pricing coefficient (c_{ij}) in bits per second per watt and the received power level in watt. The equilibrium received power level that can maximize this utility function can be found by setting the derivative of the utility in (5.4) with p_{ij}^r to zero. The closed form solution of this equilibrium received power is shown in Equation (5.5). α and β are the parameters defined in Appendix A for the bit error rate expression.

$$u_{ij} = R_{ij}\left(1 - P_e\right) - c_{ij}\, p_{ij}^r \tag{5.4}$$

$$\hat{p}_{ij}^r = -\beta \frac{R_{ij}\left(I_{ij} + \sigma^2\right)}{W} \ln\left[\alpha\beta c_{ij}\left(\frac{I_{ij} + \sigma^2}{W}\right)\right] \tag{5.5}$$

From the strategy space of the transmit power $\{p_{ij}: p_{ij} \in R^+, p_{ij} \leq \overline{p}\}$, the range of the Nash equilibrium power determines the feasible range of the pricing coefficient as shown in Equation (5.6) (see Appendix B).

$$\frac{W}{\alpha\beta\left(I_{ij} + \sigma^2\right)} \exp\left[-\frac{\overline{p}W}{\beta R_{ij}\left(I_{ij} + \sigma^2\right)}\right] \leq c_i < \frac{W}{\alpha\beta\left(I_{ij} + \sigma^2\right)} \tag{5.6}$$

Note that this approach is still decentralized [4] as the BS does not exercise control/make decisions using global information, nor is the BS capable of controlling MSs in other cells. Moreover, this approach is still based on game theory as the BS in each cell will only assist the MS to reach a suitable equilibrium state, in the process maximizing the throughput of the MS under the constraint of the maximum allowable interference level as described next.

5.2.1. Adaptive pricing algorithm

In our work, the pricing coefficients are not required to be the same for all MSs. We investigate an algorithm that can change the pricing coefficient at the BS according to the cellular environment to control the Nash equilibrium. *By doing so, it is possible to achieve an SIR that is closest to the equal SIR allocation* (Figure 5.1) *and the interference is not higher than the threshold level* (I_{th}). We call this procedure as "*adaptive pricing*". The implementation of this algorithm can be done in a manner that is similar to the outer loop power control in IS-95, but it performs at a faster rate (equal to the update rate of closed loop power control).

In the case of bursty data transmissions, the number of active MSs is changed more frequently than the case of voice transmission. The frequent change in the number of MSs can cause a rapid change of the interference level. Consequently, the BS that uses the adaptive pricing algorithm to control the equilibrium may not be able to lead other MSs to change transmit powers to the desirable level quickly. Similarly, the convergence of the Nash equilibrium to the desirable level can be slow. Accordingly, the initial pricing coefficient should be changed to a value that can provide the Nash equilibrium closest to the desired value every time there is a new arrival or a departure of a data burst.

The pricing algorithms are operated iteratively and separately among all active radio channels and so a closed form solution to the initial pricing coefficient cannot be easily obtained. To approximate the initial pricing coefficient, a simplified scenario of power control is used below.

Assume N_j-1 MSs in the cell are transmitting data continuously and an additional MS denoted by MS i wants to transmit data in that cell also. The amount of load that each MS can equally share is specified by the equally received power as shown in Equation (5.7). Denote f as the neighbor cell interference factor [75]. As a result, MS i experiences the interference shown in Equation (5.8).

$$\hat{p}_{ij}^{r} = \left[I_{\max} / (1+f) \right] / N_j \tag{5.7}$$

$$I_{ij} = I_{\max} - p_{ij}^{r} \tag{5.8}$$

Plugging these equations into Equation (5.5), we get the initial pricing coefficient in Equation (5.9).

$$c_{ij}^{0} = \frac{W}{\alpha\beta\left(I_{ij} + \sigma^2\right)} \exp\left(- \frac{I_{\max} W / (1+f)}{\beta N_j R_{ij} \left(I_{ij} + \sigma^2\right)} \right) \tag{5.9}$$

The transmit power level is indirectly controlled by changing the pricing coefficient in Equation (5.5). The pricing coefficient can be defined as a function of *an initial pricing coefficient* and *a pricing delta* (Δ). The BS determines which MS needs to adjust the pricing coefficient in each power control update interval. Then the BS either increases or decreases the MS's pricing coefficient $\left(c_{ij}^{n+1}\right)$ in the update interval n+1 from the previous interval n by Δ as explained in Figure 5.3.

The initial pricing coefficient and the pricing delta (Δ) play an important role in determining the convergence rate of the Nash equilibrium to the required operating point. The factor f is hard to predetermine in multi-cell wireless environments. As a result, if the initial pricing coefficient is not chosen correctly, a solution very far from the desired equilibrium may result. The parameter Δ is therefore required in the algorithm to deal with this situation.

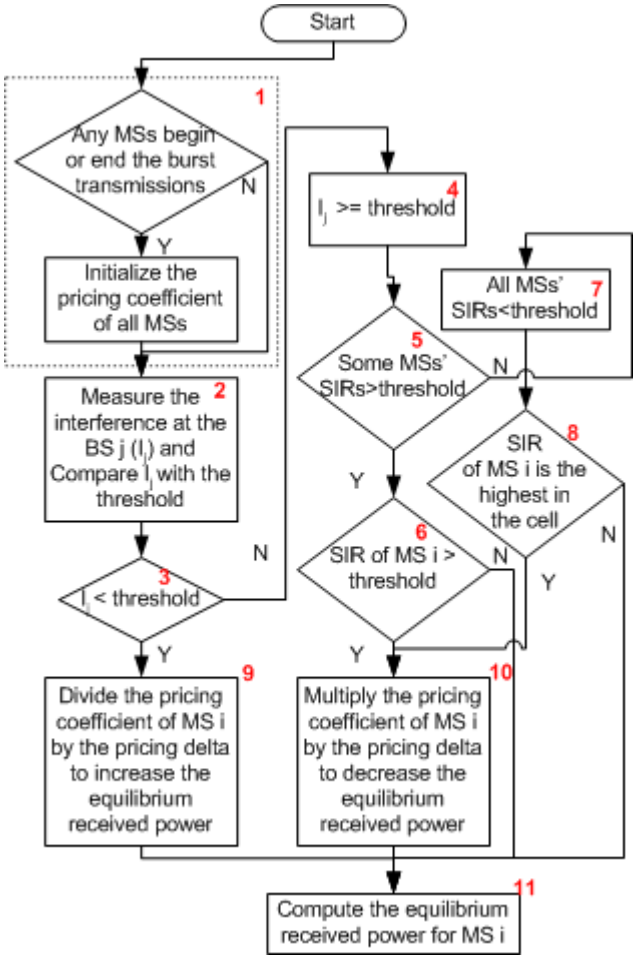

Figure 5.3 Adaptive pricing algorithm

Each process in Figure 5.3 is marked by a number used for reference in the following explanation. The process marked by number 1 performs the initialization of the pricing coefficient when the number of active MSs is changed in order to quickly converge to the equilibrium. The process number 2 checks the status of radio resource utilization. If the actual interference is lower than the threshold as in the decision process number 3, the radio channel is under-utilized. A MS can transmit at a higher power level to get a higher SIR as shown in the process number 9. If the actual interference is higher than the threshold as indicated in process number 4, the radio resources are over-utilized. Additionally, if some SIRs are higher and some are lower than the threshold (the SIR level that can provide 1% FER, e.g. the SIR threshold = 7 dB for 9.6 kbps), i.e., some MSs over-utilize the radio resources as indicated in the decision process number 5, then the transmit powers of all MSs should be adjusted in order to move the radio resources to the MSs that are not getting sufficient SIR as shown in process numbers 6 and 10. On the other hand, if the measured interference is higher than or equal to the threshold and all MSs' SIRs are lower than the threshold as indicated in the process number 7, the networks cannot provide all MSs the required

threshold SIR in this over-utilization case. Consequently, the radio resources have to be equally shared among all active MSs as in the decision process number 8. This adaptive pricing algorithm ends by computing the equilibrium received power in Equation (5.5) according to the adjusted pricing coefficient as shown in process number 11.

Next, the algorithm compares the equilibrium received power (that is computed by the adaptive pricing algorithm) with the measured received power. The BS sends a one bit power command to order the MS i to either increase or decrease its power level by a predefined step size (δ). The proposed power control algorithms periodically updates the transmit power by employing all of these processes.

5.3. RUNNING TIME OF THE ALGORITHM

The running time of the algorithm can be considered in terms of two aspects: the computational complexity and the convergence rate. The computational complexity of the power control algorithm in each update interval is very simple and it can be represented by $O(N_j)$, where N_j is the number of MSs in a cell. The convergence to a fixed point can not be guaranteed [76] for our proposed power control algorithms because the algorithms do not use perfect feedback information. The proposed power control algorithm employs a 1-bit feedback power control as used in the current CDMA standards. The SIR convergence of the 1-bit-fixed-step power control algorithms has been shown in [76] to be in a certain range of the threshold SIR ± (power feedback step size)^2. A similar approach of the analysis in [76] is applied to our proposed algorithm by using the threshold of interference instead of the SIR. The derivation of the *convergence range* in the case of our proposed power control algorithms is described next.

Let $p_{ij}(n)$, h_{ij}, $\gamma_{ij}(n)$ and γ_o denote the transmit power of MS i to BS j at time n, the path gain of MS i to BS j, the SIR of MS i to BS j and the threshold SIR, respectively. The interference at the BS j denoted by $I_j(n)$, at each update interval when the interference is less than or greater the maximum level (I_{max}) can be found in Equations (5.10) to (5.12).

If $I_j(n)<I_{max}$, all MSs can increase their transmit powers by an amount equal to the power step size according to process numbers 3 and 9 in Figure 5.3. Therefore the highest interference in the next update interval (n+1) can be expressed by Equation (5.10). This interference is however, less than $\delta^2 I_{\max}$.

$$I_j(n+1) = \sum_{\forall i} h_{ij} p_{ij}(n)\delta + \sigma^2 \le \delta^2 I_{\max} \tag{5.10}$$

If $I_j(n)>I_{max}$ and some $\gamma_{ij}(n)>\gamma_o$, the MSs that have SIRs higher than the threshold decrease their transmit power levels in the next update interval according to process numbers 4, 5, 6, and 10 in Figure 5.3. $G1_n$ and $G2_n$ denote the groups of MSs at the update interval n that have the SIR higher and lower than the threshold level at the update interval n when the interference is higher than I_{max} , respectively. Only the MSs in $G1_n$ reduce their transmit power by δ. The interference at the update interval n+1 is shown in Equation (5.11).

$$I_j(n+1) = \sum_{G1_n} h_{ij} p_{ij}(n)\delta^{-1} + \sum_{G2_n} h_{ij} p_{ij}(n) + \sigma^2 \geq \delta^{-2} I_{\max} \tag{5.11}$$

If $I_j(n)>I_{max}$ and all $\gamma_{ij}(n)<\gamma_o$, the MS that has the highest SIR level decreases its transmit power at the update interval n+1 according to the process numbers 7, 8 and 10 in Figure 5.3. Let k be the identification of MS that has the highest SIR in the cell. The interference can be found as shown in Equation (5.12). This interference level is bounded by $\delta^{-2}I_{\max}$.

$$I_j(n+1) = h_{kj} p_{kj}(n)\delta^{-1} + \sum_{i\neq k} h_{ij} p_{ij}(n) + \sigma^2 \geq \delta^{-1} I_{\max} \geq \delta^{-2} I_{\max} \tag{5.12}$$

Accordingly the range of the converged interference can be represented in Equation (5.13).

$$\delta^{-2} I_{\max} \leq I_j \leq \delta^2 I_{\max} \tag{5.13}$$

5.4. NUMERICAL ANALYSIS FOR CONTINUOUS TRANSMISSIONS

5.4.1. Experimental design

The objective of this analysis is to examine the performance of the closed loop power control algorithm in both under and over utilization cases. Two sets of experiments are conducted. Firstly, a comparison between the 1-bit feedback command and perfect feedback information is presented in Subsection 5.4.2. Secondly, the effects of the number of cells and the shadow fading on the performance of the proposed power control scheme are evaluated in Subsection 5.4.3.

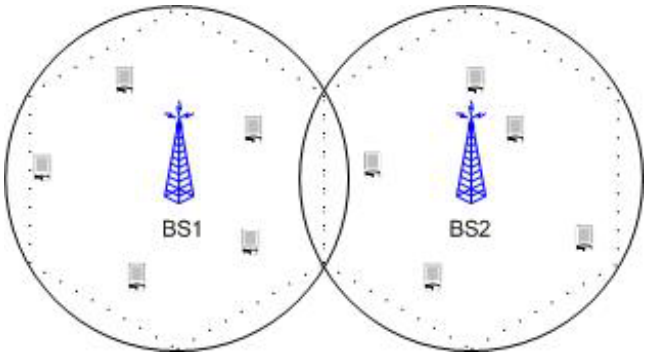

Figure 5.4 A two-cell scenario

In the first experiment, the factor considered is the number of MSs. Two cells are considered in this case as shown in Figure 5.4. Each cell is assumed to have an equal number of MSs. Six levels of the number of MSs in each cell are used in this study: 5, 10, 15, 20, 25 and 30 MSs. We assume all MSs are stationary and transmit continuously at 9.6 kbps. The locations of stationary MSs are uniformly distributed in both cells. A number of replications with different seeds are run such that MSs are randomly located in each replication. The average results of all response variables are then plotted (the number of experiments satisfy a 95% confidence interval). In this dissertation, the number of runs is varied in each experiment from 3 to 15 runs to achieve the 95% confidence interval. The response variables examined in this study are as follows: the average transmitted power, the average SIR and the average uplink interference in each frame, and the average frame error rate. Assume the radius of each cell is 1 km. A simple path loss model is used in this study. The path loss as a function of distance from MS i to BS j (d_{ij}) is given by $h_{ij} = K/d_{ij}^{n}$. The constant K is equal to 0.097 and the path loss exponent $n = 4$ is assumed as in [14]. The variation of K with distance or location can occur because of shadow fading. The practical implementation of the power control algorithm does not require the exact value of K. In the first experiment where the comparison of the perfect feedback information and the one bit feedback command is conducted, the shadow fading is not considered.

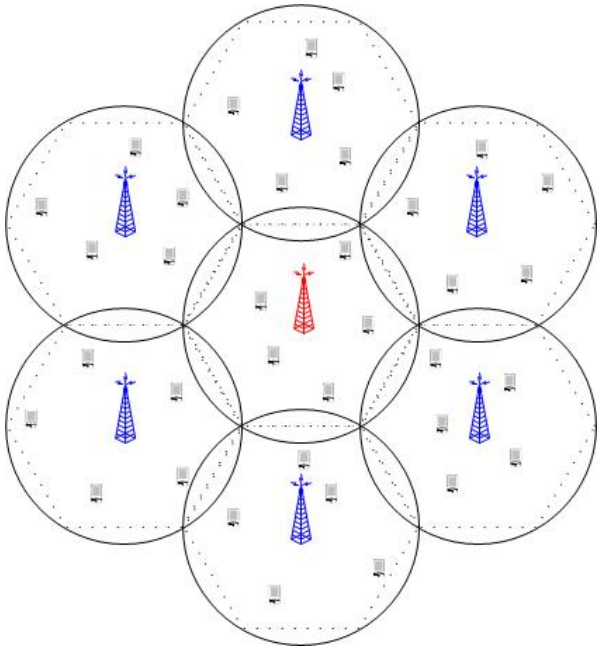

Figure 5.5 A seven-cell scenario

In the second experiment, two levels of the number of cells are considered: 2 and 7 cells. The 7-cell scenario is shown in Figure 5.5. The effect of shadow fading on the performance is considered. Therefore both cases of simulation with and without shadow fading are examined. The shadow fading component is updated every transmission slot in our simulation. In [77], it has been shown that there is a spatial correlation between the sample values of shadow fading with a different distance. This dissertation uses the correlated shadow fading model from [78, 79] in Equation (5.14).

$$p_{ij}^{r}(n) = \rho \; p_{ij}^{r}(n-1) + \sigma_s \sqrt{1-\rho^2}\, N(0,1) \tag{5.14}$$

$p_{ij}^{r}(n)$ denotes the received power at the update interval n. ρ is the correlation factor. In this dissertation, ρ=0.82 [77, 78] is used. $N(0,1)$ represents the Gaussian random variable. σ_s is the standard deviation of the shadow fading. The correlated shadow fading with a mean of 0 dB and standard deviation of 7.5 dB is used in this dissertation.

Eight levels of the number of MSs in each cell are used in this study: 5, 10, 15, 20, 25, 30, 35 and 40 MSs. Mobility is also considered in this second experiment. The initial locations and the moving directions of the MSs are randomly selected from a uniform distribution. All MSs are moving at a constant speed of 50 km/h and they are allowed to move only in their own cell. The average results of all response variables are then plotted (the number of experiments satisfy a 95% confidence interval). The

response variables considered here are the average error rate, the average SIR, the average uplink interference and the average effective rate in each frame.

In this work, the transmit power is updated every 1.667 ms as in cdma2000 1XEV-DO [8]. One update interval is equal to the period of one transmission slot. One frame consists of 16 slots. The transmission rate is 9.6 kbps, so each bit is transmitted every 0.1 ms and each update interval consists of 16 bits. These 16 bits are transmitted at the same transmit power level. If a MS is moving, then the received power is changed according to the distance from the BS. Even if a MS is stationary, if received power levels of other MSs at a BS are changed, then the SIR can change dynamically. Accordingly, the transmit power, SIR, and interference levels in the analysis are updated every bit and the average of these parameters are computed every frame (e.g., every 256 bits for 9.6 kbps).

5.4.2. Numerical results for the effect of feedback information

Perfect feedback information and one-bit feedback command are compared with the proposed power control scheme to examine how close they are in performance. The results of all response variables (in the case of 2-cell scenario) are selected from one of the cells**.** The results are shown in Figure 5.6 to Figure 5.9.

Figure 5.6 shows the interference level incurred from the transmissions. In the case of a 7-dB target SIR, the number of MSs that can be serviced in a cell per carrier is about 20 when the extra-cell interference is small (close to zero) and given that the maximum allowable interference (I_{th}) is 1.99 × 1e-14 watts (or -167 dBm) as illustrated in Figure 5.1. If the number of MSs is higher than 20, this can cause an interference greater than I_{th} which is not desirable. In contrast, the proposed power control based on game theory can support a larger number of MSs while keeping the incurred interference around I_{th}. The closed loop power control algorithm maintains the interference at less than I_{th} when the number of MSs is less than or equal to 15 MSs. Because of the inaccuracy of the one bit feedback command in the closed loop algorithm, the interference is slightly higher than I_{th} when the number of MSs is higher than or equal to 20 as shown in Figure 5.6. In comparison, the perfect feedback information power control based on game theory can control the interference and maintain it to be less than I_{th} since a MS is assumed to have the exact information of the required equilibrium received power.

The plots of each MS's average transmit power and SIR of the power control algorithms are given in Figure 5.7 and Figure 5.8. The closed loop algorithm in the case of 1-bit feedback performs close to the case with perfect feedback information. When the number of MSs is increased, each MS transmits at a lower power level in order to maintain the interference level at less than I_{th}. Consequently, the SIR is

reduced with the number of MSs. Our power control algorithm performs as well as the equal SIR allocation because all SIRs in the power control schemes based on game theory in Figure 5.8 are close to the equal SIR allocation when $f = 0$ as illustrated in Figure 5.1. If the number of cells in the system is higher, the result will be close to the plot of equal SIR allocation when f=0.55 in Figure 5.1.

The power control algorithms perform well in both under and over utilization cases. The under utilization case is when the number of MSs is less than 20 and the over utilization case is when the number of MSs is greater than that. The SIRs in the case of under-utilization is higher than 7 dB (which is the fixed target SIR scheme) as shown in Figure 5.8. As a result, these power control algorithms provide a very low FER in this case – much lower than 1 % (as in the fixed target SIR scheme) as shown in Figure 5.9. This lower FER can provide higher throughput to data-MSs. In the over-utilization case, the power control algorithms can provide an equilibrium SIR close to the equal SIR allocation in Figure 5.1. However, the FER is increased and is higher than 1 % as the number of MSs is increased. This flexibility is provided by the proposed power control algorithms for data-MSs that can allow data retransmissions due to higher FER when a large number of MSs want to transmit at the same time. The economics of the network operator can decide the appropriate admission control strategy to limit the FER. Note that the FER of the 1-bit feedback case is slightly higher than the perfect feedback case as shown in Figure 5.9 because the precise amount of power that needs to be adjusted is not known in practice.

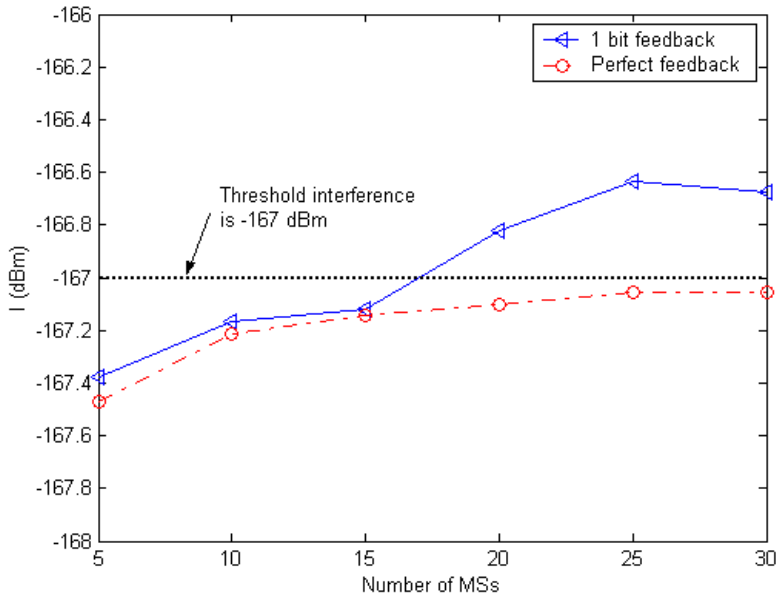

Figure 5.6 Interference level for 2-cell case

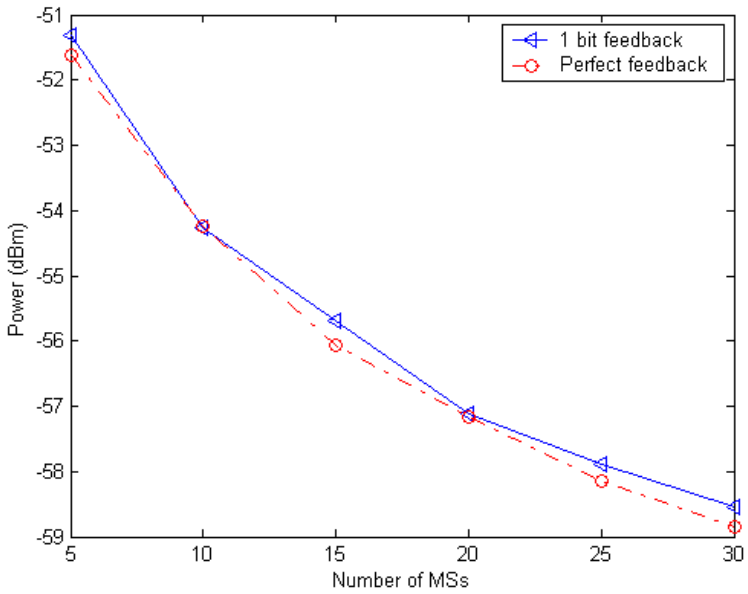

Figure 5.7 Average transmit power of each MS for 2-cell case

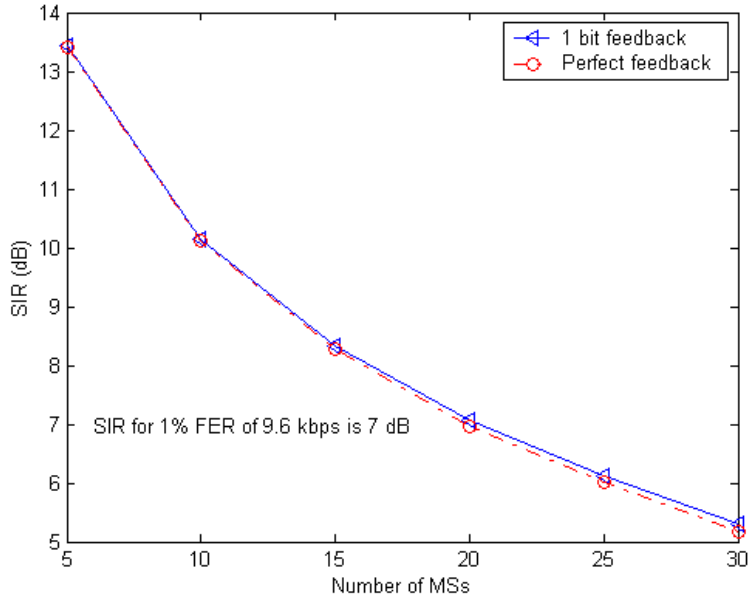

Figure 5.8 SIR for 2-cell case

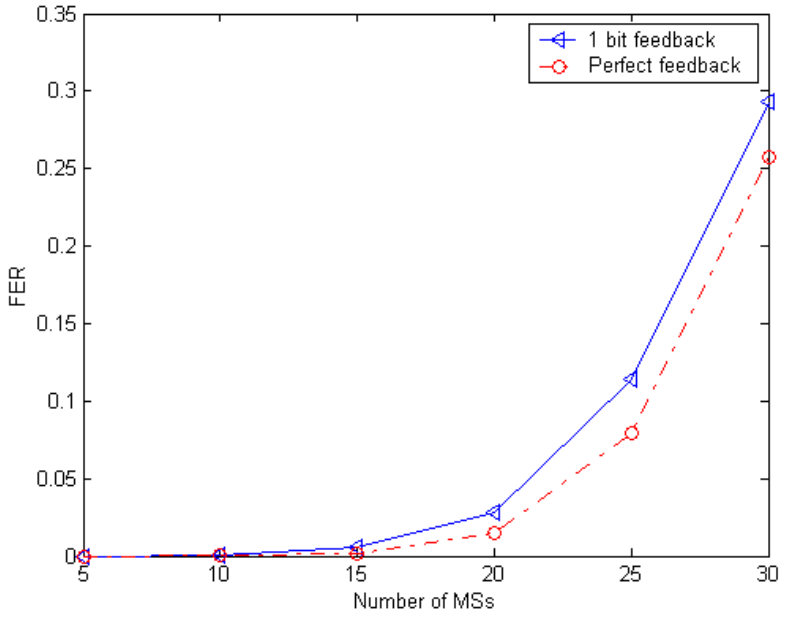

Figure 5.9 FER for a 2-cell case

5.4.3. Numerical results for the effect of the number of cells and shadow fading

The response variables in the case of 2-cell scenario are selected from one cell and in the case of the 7-cell scenario are selected from the center cell that receives the most severe interference from the neighbors.

The average interference results shown in Figure 5.10 indicate that shadow fading affects the performance of the proposed power control algorithm by causing the interference to be higher than the threshold. Additionally, with 7-cells, the interference is obviously higher as shown in the figure.

The average SIR results in Figure 5.11 indicate no major differences compared to the 2-cell case, except in the case of the 7-cell-with-fading scenario. The SIR results are close to the analytical result in Figure 5.1 when f=0. The 7-cell-with-fading scenario is close to the case of f=0.55 in Figure 5.1.

When considering the average FER and effective rate in Figure 5.12 and Figure 5.13, the FER/effective rate increases/decreases when the number of MSs increases, the number of cells increases and the shadow fading is considered. Shadow fading has more impact to the performance of power control when the number of MSs is increased because the proposed power control requires a higher number of iterations to converge to the required equilibrium. This issue is discussed in Section 5.5.2. Also, the result of the 2-cell case with fading is slightly worse than the 7-cell case without fading, this

implies that *shadow fading has more impact* on the performance of power control than the number of cells.

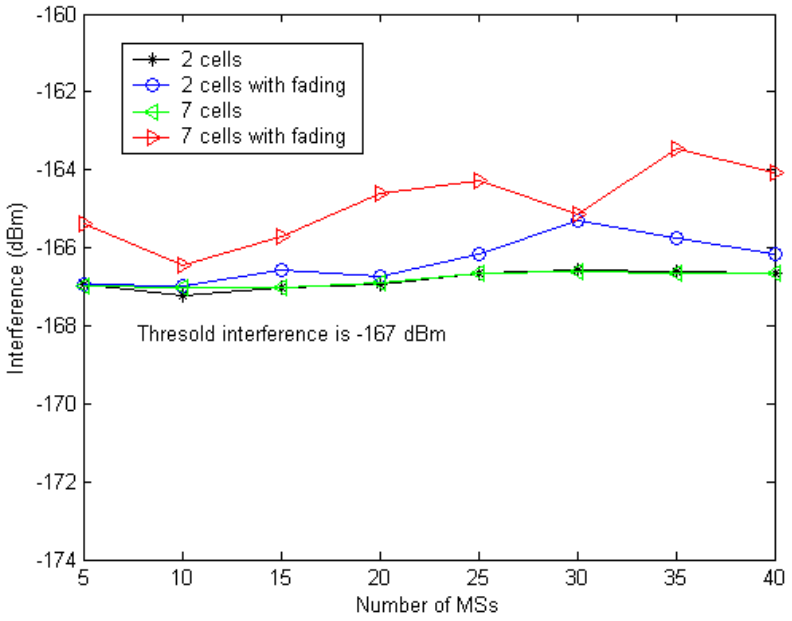

Figure 5.10 Interference for 2 and 7 cells with/without shadow fading

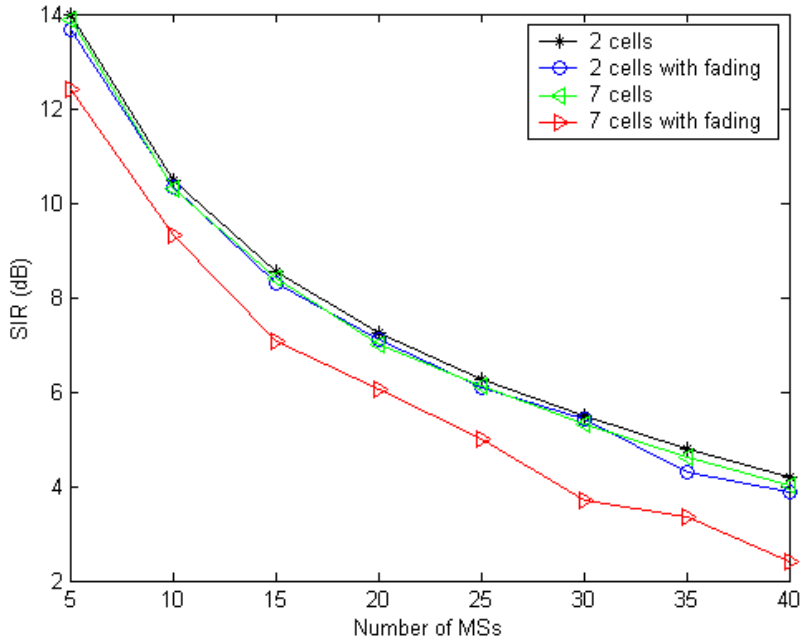

Figure 5.11 SIR for 2 and 7 cells with/without shadow fading

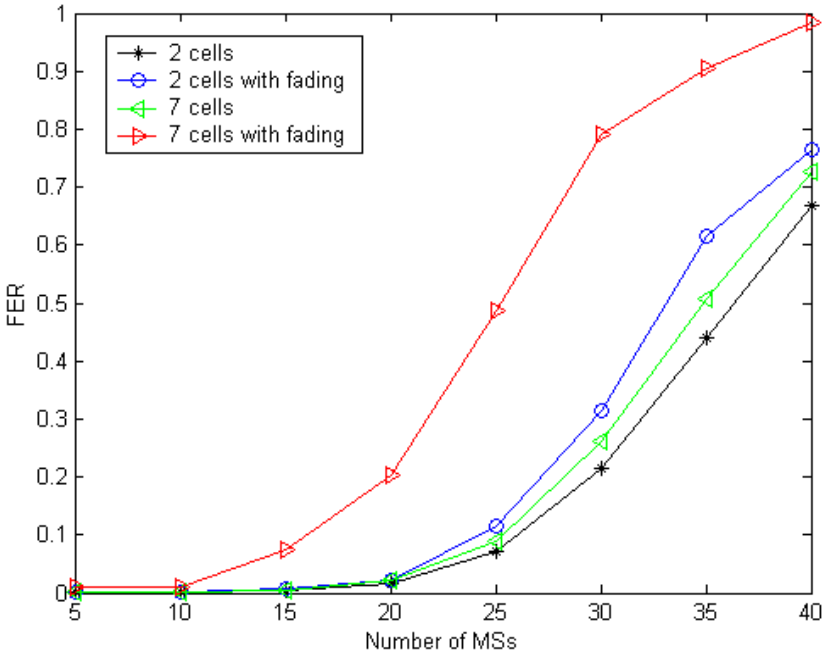

Figure 5.12 FER for 2 and 7 cells with/without shadow fading

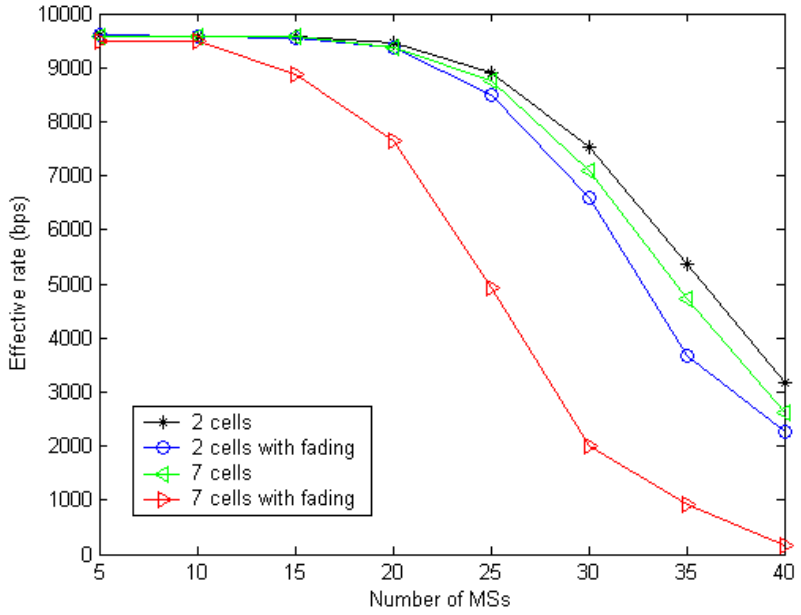

Figure 5.13 Effective rates for 2 and 7 cells with/without shadow fading

5.4.4. Conclusions of power control for continuous transmissions

A novel closed loop power control algorithm that can fully utilize the radio resources and equally assign transmit power to any numbers of MSs is proposed for multi-cell wireless data networks based on a game

theoretic framework. This power control algorithm can assign transmit powers close to the equal SIR allocation in both under and over utilization cases.

5.5. NUMERICAL ANALYSIS FOR BURSTY TRANSMISSIONS

5.5.1. Experimental design

An on-off traffic model as shown in Figure 5.14 is employed to model the bursty data traffic source of each MS. In Figure 5.14, *a* denotes the on period of data transmission, *b* denotes the off period of data transmission, and λ denotes the packet arrival rate. The power control scheme is investigated with this on-off traffic model. As in the case of [80-83], the durations *a* and *b* with exponential distributions and the packet arrival rate λ with a Poisson process are typically employed to study bursty traffic. In this evaluation, we use an on-off traffic model with exponentially distributed on and off durations. The durations *a* and *b* are exponentially distributed with means 1 and 10 [82] seconds, respectively. The packet arrival rate (λ) according to the Poisson process is 2 packets/second [82]. The packet length is exponentially distributed with a mean of 2.25 Kbytes [83].

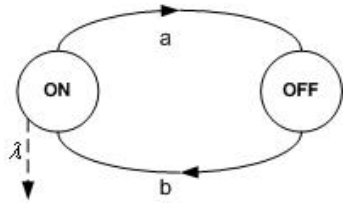

Figure 5.14 On-off traffic source model

In all of the studies in this chapter, the initial locations and the moving directions of the MSs are randomly selected from a uniform distribution. All MSs are moving at a constant speed of 50 km/h. Handoff (a mechanism of transferring an ongoing connection from one cell to another that can provide better signal quality) is not considered in this work; therefore, all MSs are allowed to move only in their own cell. In all of these studies, a seven-cell scenario as shown in Figure 5.5 is used. In this work, the transmit power is updated every 1.667 ms as in cdma2000 1XEV-DO [8]. Note that one update interval is equal to the period of one transmission slot and 16 transmission slots form one frame of transmission.

We assume the radius of each cell is 1 km. A simple path loss model is used in this study. The path loss as a function of distance from MS *i* to BS *j* (d_{ij}) is given $h_{ij} = K / d_{ij}^{n}$. The constant *K* is equal to

0.097 and the path loss exponent $n = 4$ is assumed as in [11]. The signal fluctuation does not only occur due to the bursty transmissions but also due to shadow fading. The numerical analysis includes the effect of shadow fading also to examine how it affects the performance of the power control algorithms. The correlated shadow fading described previously is used here for the convergence analysis. The correlated shadow fading [77] with a mean of 0 dB and standard deviation of 7.5 dB is updated every transmission slot in our simulation. In the performance evaluation of the power control algorithm, shadow fading is not considered. Only the bursty transmission effect is examined in this chapter. The effect of correlated shadow fading on the algorithm is considered in the next chapter.

The initial pricing coefficient determines how fast the convergence is to the equilibrium solution. Due to the lack of knowledge of the extra-cell interference from a neighbor, an approximation to the suitable pricing coefficient for quick convergence is difficult to determine. Accordingly, the pricing coefficient has to be adaptively changed based on the environment. The pricing delta (Δ) is used for this purpose. Δ is set to 1 dB based on preliminary convergence analyses in Subsection 5.5.2. When there is interference from a nearby cell, the result of power assignment in one cell can influence the interference to the other cell also. We study how the proposed closed loop power control based on game theory is affected by the unknown interference from a neighbor cell (convergence analysis) in Subsection 5.5.2 and the consequence of the controlled interference level (caused by the power assignment based on game theory) on the performance of the proposed power control algorithms in Subsection 5.5.3.

5.5.2. Convergence analysis

The objective of this analysis is to show how the initial pricing coefficient and the adaptive pricing algorithm affect the convergence of the power control algorithms. Eight MSs are examined in a seven-cell scenario. All of them are randomly located and moved around their own cell. Shadow fading is not included in this evaluation. The average number of update iterations required to converge to the range in Equation (5.13) are examined. Six levels of Δ are examined: 0.125, 0.25, 0.5, 1, 5 and 10 dB. The simulation results show that the convergence to the threshold level of 1.99e-14 watts (or -167 dBm) is very fast for all levels of Δ when shadow fading is not included as shown in Figure 5.15. In comparison, the convergence rates are decreased (number of iterations increase) when the shadow fading is included. Figure 5.16. The convergence rates in the case of $\Delta = 5$ and 10 dBs are higher than 20 update intervals and in the other cases of Δ are around 12 to 13 update intervals. (The update interval is one slot or 1.667 ms) From these preliminary convergence analyses, shadow fading affects the convergence rate.

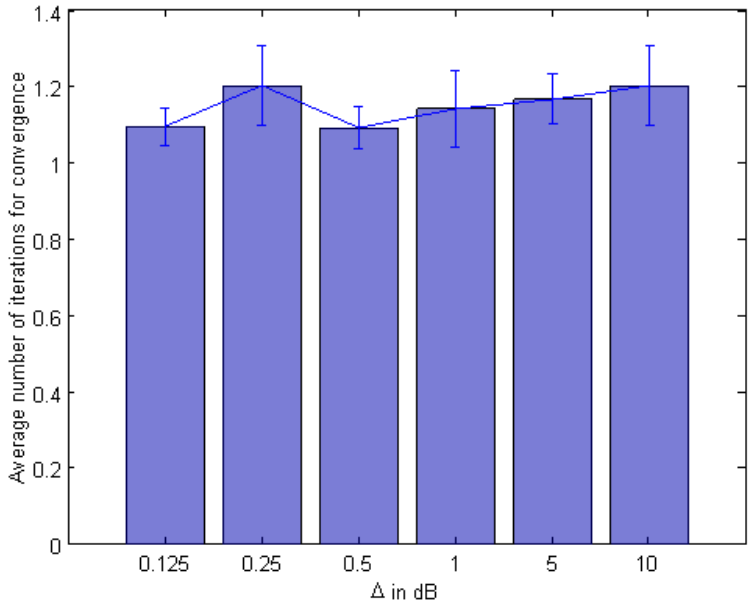

Figure 5.15 Average convergence rates in the case of 8 MSs in each cell for a 7-cell scenario without shadow fading

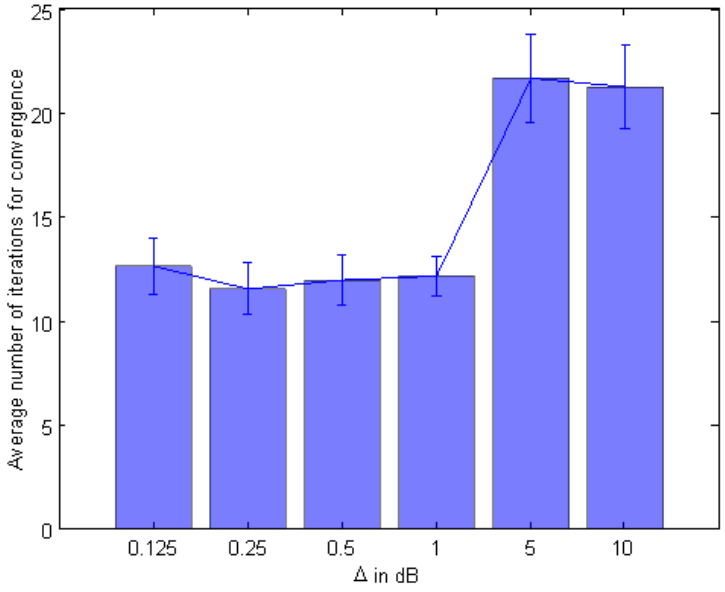

Figure 5.16 Convergence rates in the case of 8 MSs in each cell for a 7-cell scenario with shadow fading

Next, the convergence rate is further analyzed in the cases of different number of MSs in the cells. Five levels of numbers of MSs are studied: 8, 16, 24, 32 and 40 MSs. The results are illustrated in Figure 5.17.

These results show that Δ=0.25, 0.5 and 1 dBs have convergence rates closely to each other but they have quicker convergence rates than Δ=5 and 10 dBs. Consequently, Δ=1 dB is selected for further evaluation.

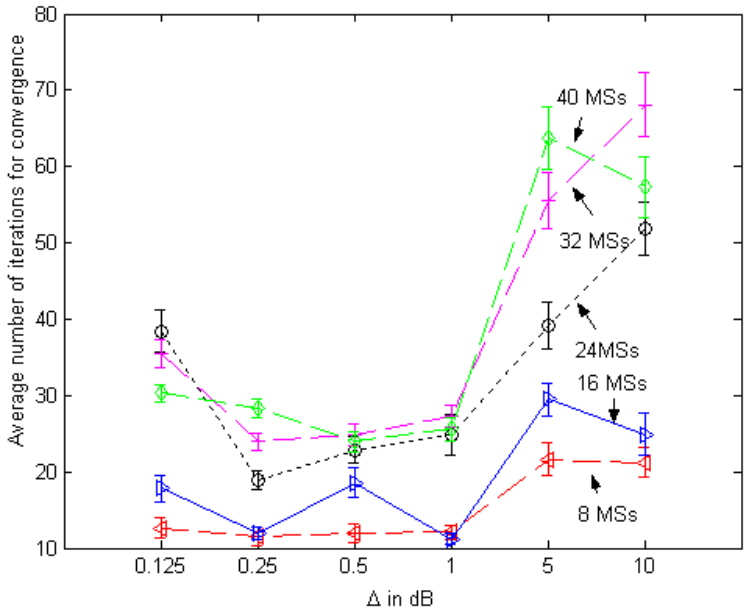

Figure 5.17 Convergence rates for different numbers of MSs when shadow fading is considered

5.5.3. Performance evaluation

The objective of this analysis is to examine the performance of the closed loop power control algorithm for bursty transmissions. The numerical results of the proposed power control algorithms are compared with the results of the traditional power control based on the fixed target SIR at 7 dB. Assume all MSs transmit data at the same rate of 9.6 kbps. Two experiments are considered in this section. First, we assume 8 MSs in each cell want to transmit bursty traffic. The performance is evaluated from the number of MSs that has bursty traffic to transmit (active MSs). Therefore, the number of active MSs in this case can be varied from 0 to 8 active MSs. In this evaluation, the simulation is done when all MSs transmit 1 million bits. Secondly, four levels of number of MSs are examined: 4, 8, 12 and 16 MSs. In this experiment, the average result for each MS level is examined. Similarly, the second experiment shows the average result for all active MSs in the first experiment. Only one level of number of MSs (8 MSs) is considered in the first experiment but four levels of MSs (4, 8, 12, and 16) are considered in the second experiment.

Three response variables are considered here in the first experiment: the average SIR, interference at a BS and the effective rate. Note that the layout of the seven cells in Figure 5.5 has an overlapping region and a MS can be randomly located or moved to this area. Since handoff is not considered in this

work, a MS may connect to one cell whereas it is closer to another cell. All the results presented here do not include this scenario. In practice, handoff mechanisms will take place in this situation.

The average results of the SIR and the interference at a BS in the first experiment are provided in Figure 5.18 and Figure 5.19, respectively. The locations of MSs are uniformly distributed in a cell. The MSs are allowed to move only in their own cell. A number of replications with different seeds are run such that MSs are randomly located and their moving directions are different in each replication. The average results of all response variables are then given (the number of experiments satisfy a 95% confidence interval). The SIR results of the proposed power control scheme as shown in Figure 5.18 are close to the analytical results of the equal SIR allocation in Equation (5.2) as computed in Table 5.1. The SIR results of the proposed scheme are better than the SIR results of the power control based on the fixed target SIR. The average interference levels of the proposed scheme are around the maximum threshold level of 167 -dBm watts as shown in Figure 5.19. In contrast, the interference in the case of the fixed target SIR power control is lower than the maximum allowable level of -167 dBm. This result indicates that the fixed target SIR power control can provide all MSs the SIR close to 7 dB but does not completely utilize the radio resources. In contrast, the proposed scheme can provide SIRs higher than 7 dB because it completely utilizes the radio resources. When considering the effective rate results in the first experiment as shown in Figure 5.20, the effective rates of the proposed power control are higher than the case of the traditional power control based on the fixed target SIR.

Table 5.1 Average SIR results (dB)

	Number of active MSs (bursts) in each cell					
	3	4	5	6	7	8
Equal SIR allocation	16.67	15.04	13.86	12.94	12.17	11.52
Simulated results	16.29	14.75	13.44	12.58	11.78	11.12

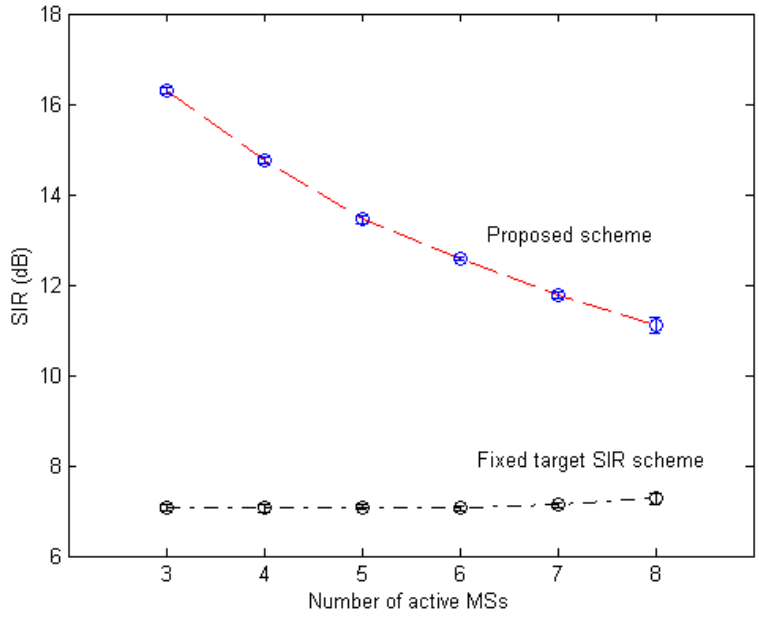

Figure 5.18 Average SIR for each number of active MSs (bursts)

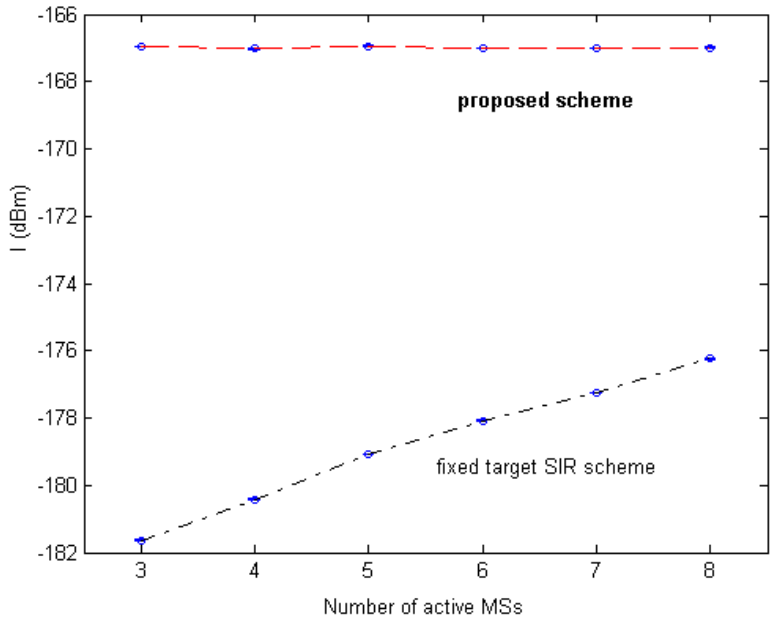

Figure 5.19 Average interference for each number of active MSs (bursts)

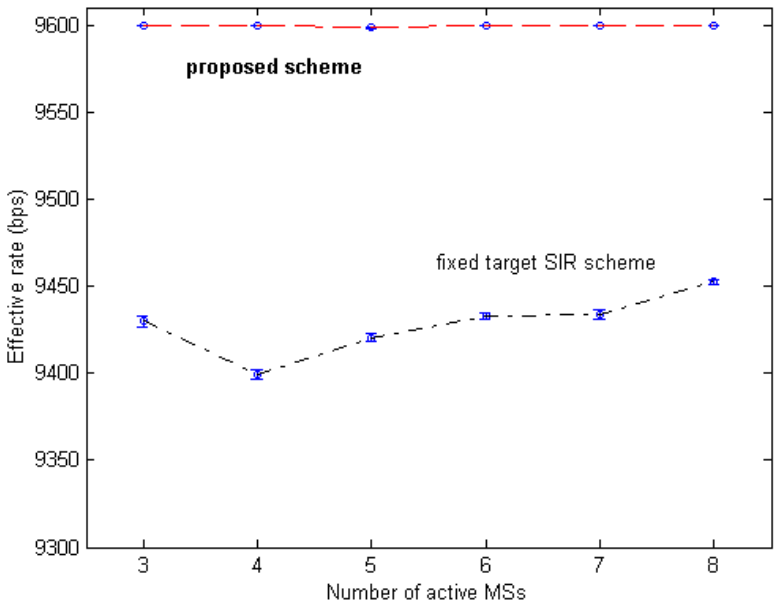

Figure 5.20 Average effective rate for each number of active MSs (bursts)

In the second experiment, all MS are moving at the speed of 50 km/h. The initial location of each MS is randomly placed in a cell and the initial moving direction is uniformly distributed between 0 to 2π. The simulation is run until each MSs transmits 800 million bits. Three replications are run in this experiment. The results with the 95% confidence intervals are shown in Figure 5.21 to Figure 5.27. The average effective rate (rate after error) results are compared between the proposed scheme and the traditional power control based on the fixed target SIR (7 dB for 9.6 kbps). The average effective rates of the proposed scheme are better than the traditional power control scheme by about 1%. This different amount is due to the fact that the traditional power control tries achieving the 1% FER and the proposed scheme tries to maximize each MS's throughput. Figure 5.21 to Figure 5.27 show the same results because the extra-cell interference in each cell is small (compared to the interference threshold of -167 dBm) and does not affect the performance in each cell.

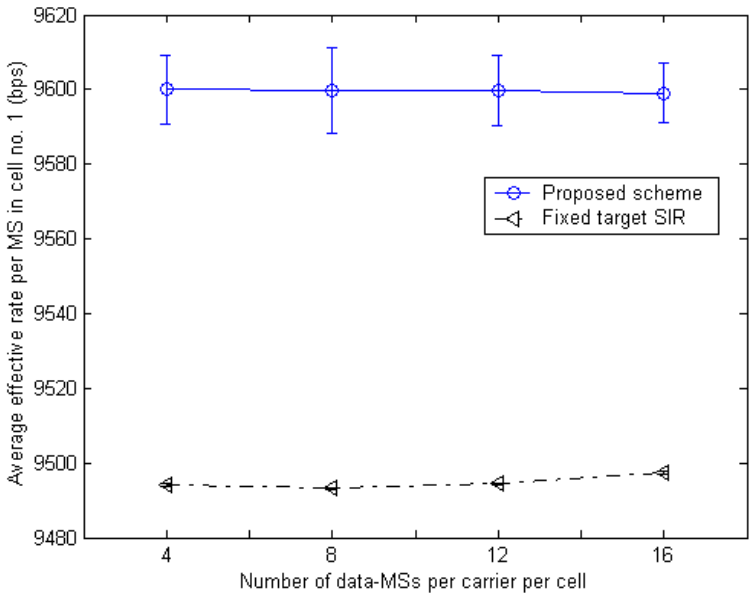

Figure 5.21 Average effective rate in cell no. 1 (the center cell)

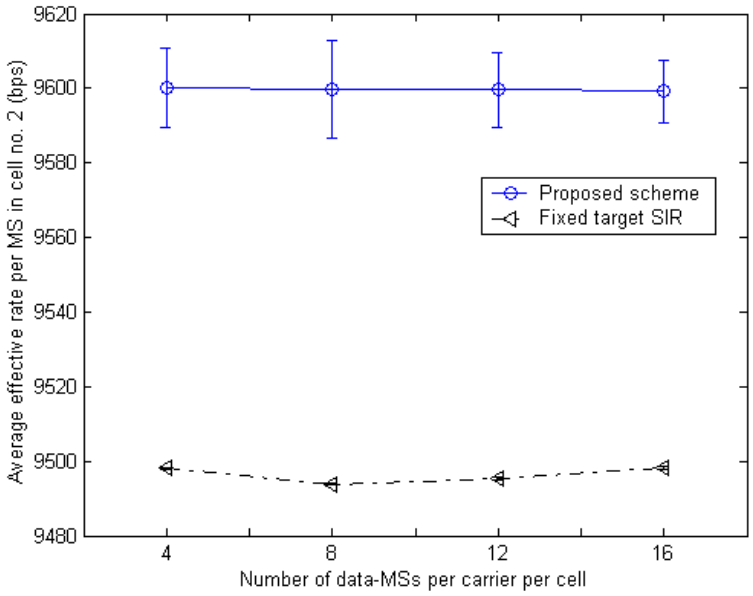

Figure 5.22 Average effective rate in cell no. 2

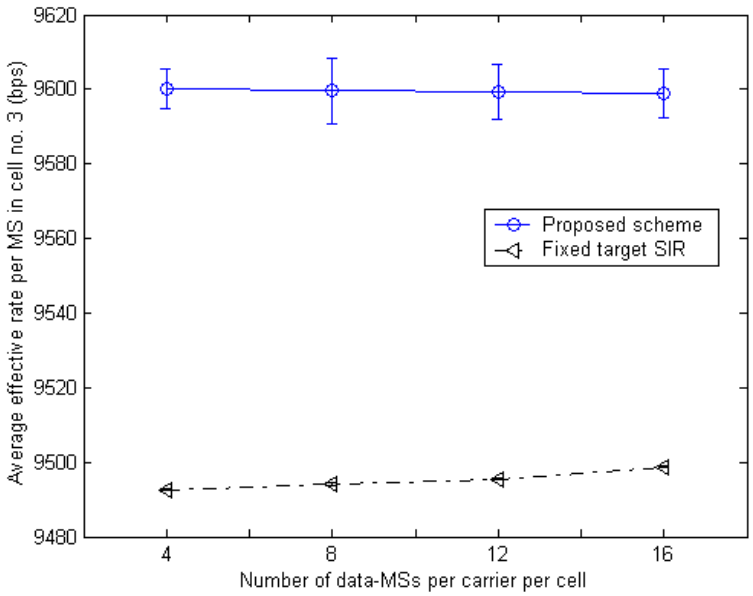

Figure 5.23 Average effective rate in cell no. 3

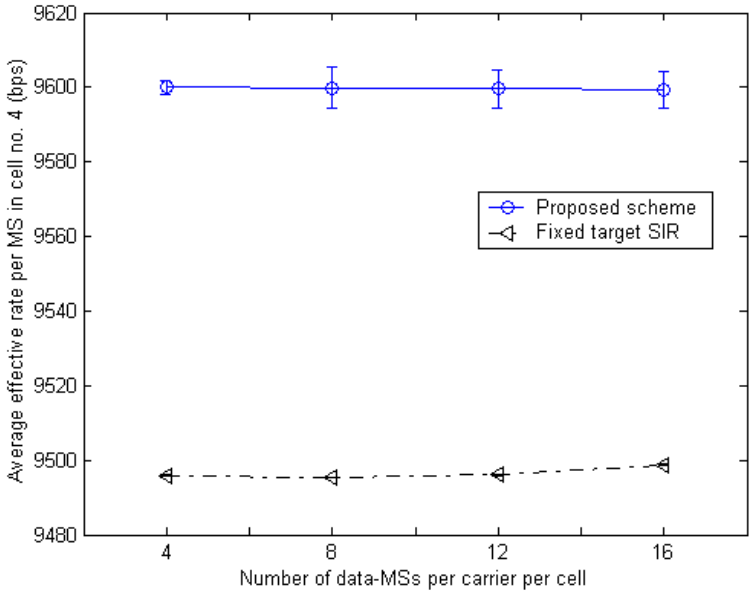

Figure 5.24 Average effective rate in cell no. 4

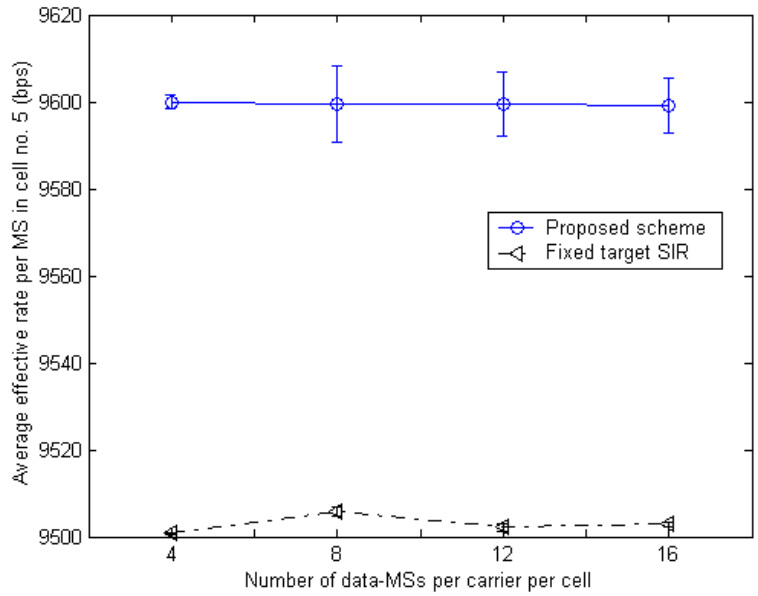

Figure 5.25 Average effective rate in cell no. 5

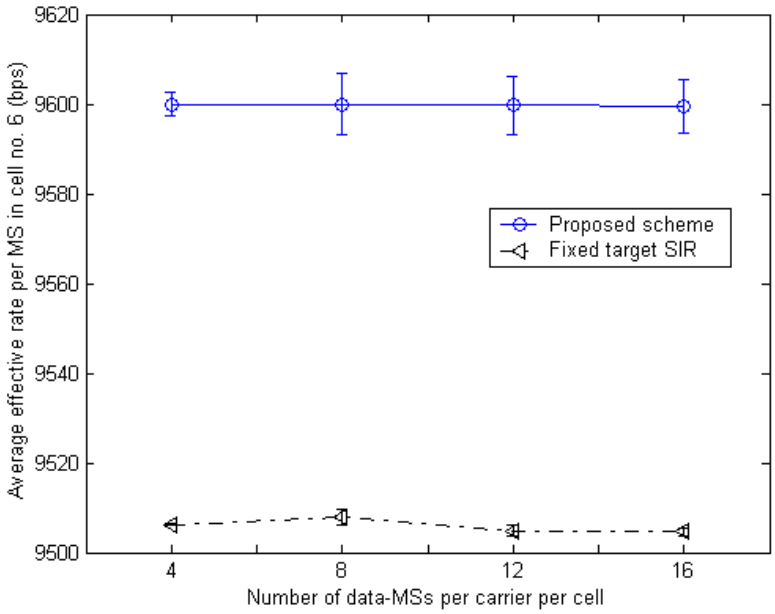

Figure 5.26 Average effective rate in cell no. 6

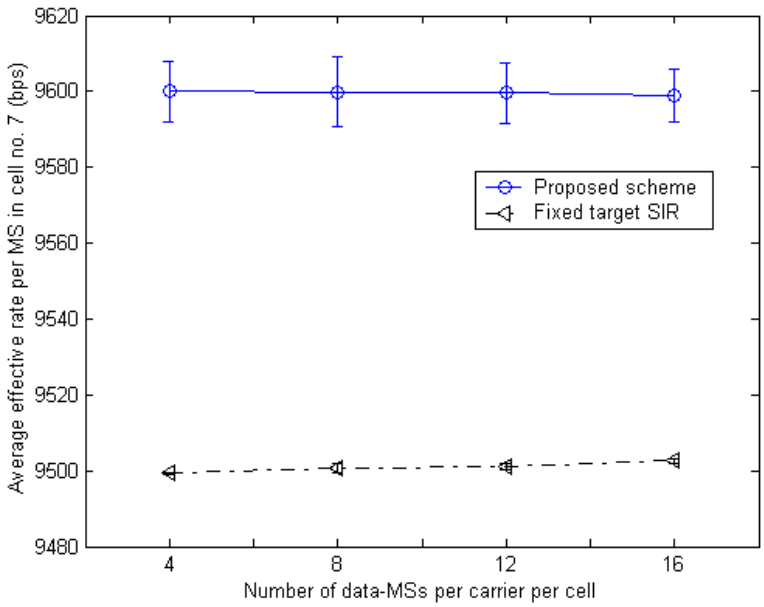

Figure 5.27 Average effective rate in cell no. 7

5.6. CONCLUSIONS

A novel closed loop power control algorithm that can equally assign transmit power to any numbers of MSs is proposed for bursty transmissions over multi-cell wireless data networks based on a game theoretic framework. The running time analyses of the computational complexity and the convergence rate shows that the algorithms are simple and converge quickly. This power control algorithm can assign transmit powers closest to the equal SIR allocation. Further investigation of this power control algorithm with multi-rate transmission is considered in the next chapter.

6.0 RATE AND POWER CONTROL ALGORITHMS

We investigate new approaches of *rate and power control* that can provide high throughput by completely utilizing and equally allocating radio resources to all mobile stations in a cell without causing high interference to neighboring cells. Existing solutions in the literature and standards attempt to maximize the system throughput and most radio resources are provided to a few MSs that have better channel conditions than others. In contrast, the proposed schemes maximize the throughput of each mobile station based on the maximum allowable interference and provide all MSs the radio resources equally. A game theoretical basis is applied in developing the proposed algorithms for dealing with the unknown extra-cell interference in multi-cell wireless networks. Practical implementation of the proposed algorithms is considered as well. The proposed schemes are evaluated by simulation. They show results close to analyses of the concept of equal allocation and full utilization of radio resources and they can provide higher throughput than the existing schemes of 1x-EV-DO when the radio resources are not over-utilized.

6.1. INTRODUCTION

This research work proposes a new approach of power and rate assignment by assigning equal radio resources to all MSs and trying to completely utilize the radio resources as much as possible. The essence of the proposed solution is that equal received power and equal transmission rates for all transmitting MS are the goal with the constraint that the interference should be less than the maximum tolerable value in each cell. With the motivation of decentralized RRM, game theory is applied to this research. To solve the requirement of global information of all MSs in a cell, *a network assisted approach* is employed in the proposed algorithms. The results show that the proposed power and rate control algorithms can provide equal rate and power to each MS and completely utilize the radio resources. The performance evaluation is compared with the power and rate control schemes in 1x-EV-DO systems.

Some assumptions/limitations in this research are listed as follows. All MSs in a system are non-real time data-MSs. Handoff and admission control are not considered in this work. Both variable rate transmission approaches of variable spreading factor (VSF) [61] and multi-code (MC) [62] are

considered. In MC, we also assume no self-interference from the aggregated codes of the same MSs (since multi-path delay spread effects are not considered). The maximum allowable interference (I_{max}) determines the amount of radio resources that all data-MSs in a cell can consume and it is determined from the quantity *Rise over Thermal* (ROT) in this research. ROT indicates how much load is present on the reverse link and it is defined as the ratio of the interference level at a BS (I_{BS}) to the thermal noise (σ^2) [63]. This work uses I_{max} as the interference threshold in the evaluation of the proposed schemes. Therefore, the term interference threshold and I_{max} are used interchangeably in this work. However, an interference margin lower than I_{max} can be applied for better system wide performance.

6.2. PROPOSED RATE AND POWER CONTROL SCHEMES

6.2.1. Overall design

Since we desire to have equal allocation of radio resources for each MS, each MS *must have the same rate and received power*. Correspondingly, the power and rate assignments should result in equally received SIRs at the BS. To provide complete utilization of the radio resources by power and rate control, the maximum allowable interference (I_{max}) is considered since I_{max} limits the amount of allocated radio resources in a cell. The uplink interference at a BS can occur from MSs in both the same cell and other cells (extra-cell). The ratio of extra-cell to intra-cell interference is defined by the neighboring cell interference factor (f). Without the extra-cell interference, accurate amounts of rate and received power can be equally assigned according to the number of active MSs, the interference constraint and the minimum SIR requirement (SIR threshold). In practice, extra-cell interference exists and it reduces the amount of allowable interference budgeted in a cell. Since the amount of extra-cell interference is very difficult to predict [10], the exact amounts of the highest equal SIR and rate allocation are not known. Game theory is used in this work to model this problem and determine an equilibrium SIR (the best allocation of radio resources) for a given scenario. The problem formulation is given in Subsection 6.2.2. Note that if each MS maximizes its own satisfaction in a totally non-cooperative way, the outcome can be unacceptable, i.e., the radio resources can be either under or over utilized. The mechanisms that can control the MS's behavior in order to obtain the proper equilibrium SIR are investigated. As a result, a mechanism called adaptive pricing and equal rate control is devised for this purpose. The details of these mechanisms are given in Subsections 6.2.3 and 6.2.4.

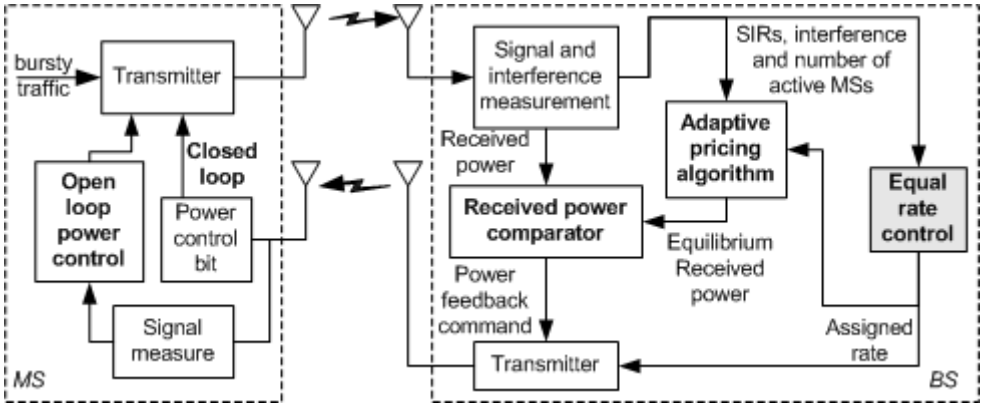

Figure 6.1 Block diagram of the proposed rate and power control schemes

Figure 6.1 illustrates the block diagram of the proposed power and rate control schemes. The equal rate control and the adaptive pricing algorithms are located at the BS. Equal rate control assigns a rate to a MS based on inputs from the SIR and interference measurement components to provide equal resource allocation under the constraint of having interference less than I_{max}. The rate controller then informs the MS of its assigned rate on the forward link. The adaptive pricing algorithm requires this assigned rate information for deciding how much power the MS should transmit in order to obtain a high effective rate while maintaining equal allocation and full utilization of radio resources. The equilibrium received power, which is expected to provide the equilibrium SIR at the BS, is computed periodically by this adaptive pricing algorithm. A MS will adjust it's transmit power to achieve this equilibrium received power.

The equilibrium received power is used as the required target power at the BS and the idea of closed loop power control is applied to adjust the transmit power for this power control algorithm. The closed loop power control operation is simple and as follows. If the actual received power is lower/higher than the equilibrium received power, the BS sends an increased/decreased power command bit on the forward link to the MS. Then the MS increases/decreases its power equal to a predefined step size. The step size used in the evaluation of the closed loop power control algorithm is 1 dB like in CDMA2000.

To use this closed loop power control algorithm, open loop power control is required initially during access of each MS's burst transmission when the feedback from the BS is not available. The MS measures the received power of a reference channel, usually the pilot channel, from the BS $\left(p_{ij}^{r-BS}\right)$and computes the transmitted power as in Equation (6.1) [28].

$$p_{ij}(\text{dBm}) = -p_{ij}^{r-BS}\ (\text{dBm}) - 73 + P_{control}(\text{dB}) \tag{6.1}$$

$P_{control}$ is specified in the access parameter message sent from the BS. This work assumes $P_{control}$ is 0 dB and the transmit power on the pilot channel from the BS is 10 watts. After the MS initially accesses the

system at the power level determined from (6.1), the proposed closed loop power control and equal rate control can be employed in the next power and rate update intervals**.** In the same way as the update intervals in 1x-EV-DO, the proposed power control scheme updates the power every transmission slot while the rate is updated every transmission frame (16 transmission slots).

6.2.2. Problem formulation based on game theory

This problem formulation takes into account both power and rate assignments. Similarly, multi-rate transmissions are considered in this formulation. Two approaches of multi-rate transmissions considered here are the variable spreading factor approach and the multi-code approach. Suppose we have N data-MSs that are competing for resources in a system. We assume that all MSs try to maximize their utilitie. For each MS, $i \in \{1, 2, \ldots, N\}$, the *utility function* with respect to the assigned BS, $j \in \{1, 2, \ldots, K_{BS}\}$ is given by: u_{ij}. We denote the transmitted power of MS i (communicating with BS j) by p_{ij}. This utility function is defined in Equation (6.2).

$$u_{ij} = R_{ij}\left(1 - P_e\right) - c_{ij}\, p_{ij} \tag{6.2}$$

The utility function consists of two terms: an effective rate term and a pricing term. The first term of the utility function represents the *effective rate* (after bit errors) of MS i, where R_{ij} is the bit rate (bps) and P_e is the bit error rate (BER). In the case of the multi-code approach, $R_{ij} = m_{ij}R_{basic}$, where m_{ij} is the number of codes assigned to MS_i that is connected to BS_j and R_{basic} is the basic rate which is the same for all codes. We use $P_e = \alpha^{-1}e^{-\gamma/\beta}$, where α =2 and β =0.5304 (see Appendix A). The quantity P_e is a function of the SIR or energy per bit to interference density ratio of MS i at BS j (γ_{ij}). The SIR γ_{ij} can be determined from the transmit power of MS i (p_{ij}), the path loss from the MS i to BS j (h_{ij}), the spread spectrum bandwidth (W), the transmission bit rate (R_{ij}) and the variance of the AWGN noise at the receiver of the BS (σ^2). The SIR expressions are given by (6.3) and (6.4) for the cases of VSF and MC, respectively. However, the expressions of (6.3) and (6.4) are essentially the same.

$$\gamma_{ij} = \frac{W}{R_{ij}} \frac{h_{ij}\, p_{ij}}{\sum_{k=1,k\neq i}^{N} h_{kj}\, p_{kj} + \sigma^2} \tag{6.3}$$

$$\gamma_{ij} = \frac{W}{R_{ij}/m_{ij}} \frac{h_{ij}\, p_{ij}/m_{ij}}{\sum_{k=1,k\neq i}^{N} h_{kj}\, p_{kj} + \sigma^2} \tag{6.4}$$

In the pricing term of Equation (6.2), c_{ij} denotes a pricing coefficient (bps/watt) for MS i assigned to BS j. We include the pricing coefficient here in order to control the equilibrium solution [68] as explained in Chapter 5.0.

In order to eliminate the requirement of global information that needs to be known by all MSs, the utility function is redefined as shown in (6.5) [68]. Here, $p_{ij}^r = h_{ij}p_{ij}$. The SIR expression that used for finding the solution of Equation (6.5) is given in (6.6). I_{ij} is the interference experienced by MS i that can be measured at the BS j. This I_{ij} is equal to $\sum_{k \neq i}^{N} h_{kj} p_{kj}$ in (6.3) and (6.4).

$$u_{ij} = R_{ij}\left(1 - P_e\right) - c_{ij} p_{ij}^r \tag{6.5}$$

$$\gamma_{ij} = \frac{W}{R_{ij}} \frac{p_{ij}^r}{I_{ij} + \sigma^2} \tag{6.6}$$

The equilibrium received power of MS i at the BS j denoted by $\hat{p}_{ij}^r$ is the point where u_{ij} in (6.5) is maximized. To find the equilibrium, we set the derivative of the utility function in (6.5) to zero. Then $\hat{p}_{ij}^r$ can be found as shown in (6.7).

$$\hat{p}_{ij}^r = -\beta \frac{R_{ij}\left(I_{ij} + \sigma^2\right)}{W} \ln\left[\alpha\beta c_i \left(\frac{I_{ij} + \sigma^2}{W}\right)\right] \tag{6.7}$$

6.2.3. A controllable Nash equilibrium using the adaptive pricing algorithm

We propose an algorithm that is run at the BS to adjust the pricing coefficient in the utility function according to the cellular environment for the purpose of controlling the Nash equilibrium. By doing so, it is possible to achieve an SIR that is closest to the desired equal SIR allocation at a given rate and maintains the interference near I_{max}. We call this procedure as "adaptive pricing". This adaptive pricing algorithm has been explained in Figure 5.3 of Chapter 5.0.

6.2.4. Equal rate control

Assume that the number of active MSs in cell j (N_j) is known and all of them are assigned the same data rate by either the MC or the VSF approach. The offered rates of the VSF approach considered in this study are based on the 1x-EV-DO standard. The five levels of rates are 9.6, 19.2, 38.4, 76.8 and 153.6

kbps. The MC approach used in this work is based on the architecture proposed in [62]. Eight levels of rates based on the basic rate of 19.2 kbps studied in [84] are used in this work. These eight rates are 19.2, 38.4, 57.6, 76.8, 96.0, 115.2, 134.4 and 153.6 kbps.

The equal SIR allocation (γ_{eq}) at a given rate can be expressed as shown in Equation (6.8). If σ^2 is 5×10^{-15} watts [14] and the allowed ROT is 6 dB (in 1x-EV-DO systems) [8], I_{max}=ROT/σ^2 =1.99 × 10^{-14} watts (or -167 dBm). This I_{max} is used in our numerical analysis. If there is only a single cell in the system, i.e. f = 0, the value of the equal SIR allocation for each transmission rate can be found from Equation (6.8) and the corresponding plots are shown in Figure 6.2 and Figure 6.3 for the cases of MC and VSF, respectively. The SIR of each transmission rate is plotted with the number of active MSs. For example, a MS with a rate of 153.6 kbps can obtain the equal SIRs about 15 dB, 7 dB and 4.5 dB when the number of active MSs is 1, 2 and 3, respectively.

$$\gamma_{eq} = \frac{W}{R}\frac{I_{\max}/(1+f)/N_j}{I_{\max} - I_{\max}/(1+f)/N_j + \sigma^2} \tag{6.8}$$

The actual SIR requirements for multi-rate transmissions can be found from [29, 51]. In this work, a different SIR threshold level is used as shown in Table 6.1. The derivation of this SIR threshold is explained here. If the required FER is at least 1 % (which is not absolutely necessary for data transmission), the minimum SIR or the SIR threshold (γ_{th}) that has to be achieved for each transmission rate is shown in Table 6.1 (the BER expression employed in this analysis is given in Appendix A). The same principle can be applied either using the SIR thresholds in Table 6.1 or the thresholds used in [29, 51].

According to Table 6.1, the highest rate that can be supported for the 1% FER requirement can be found for a given number of MSs. For example, if the number of MSs is two, the equally allocated SIRs for rates of 153.6 and 76.8 kbps in the case of VSF are about 7 and 10.5 dB, respectively. The highest equal rate that can be allocated for the two MS case is 76.8 kbps since the equally allocated SIR of this rate is higher than the required target SIR (7.85 dB approximately).

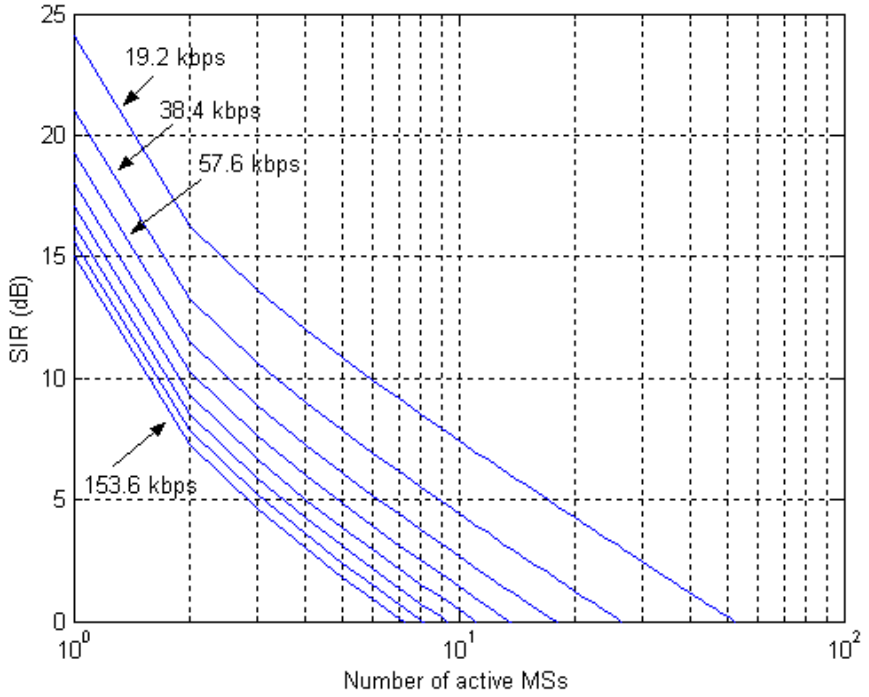

Figure 6.2 Equal SIR allocations when the rate adaptation is based on the MC approach

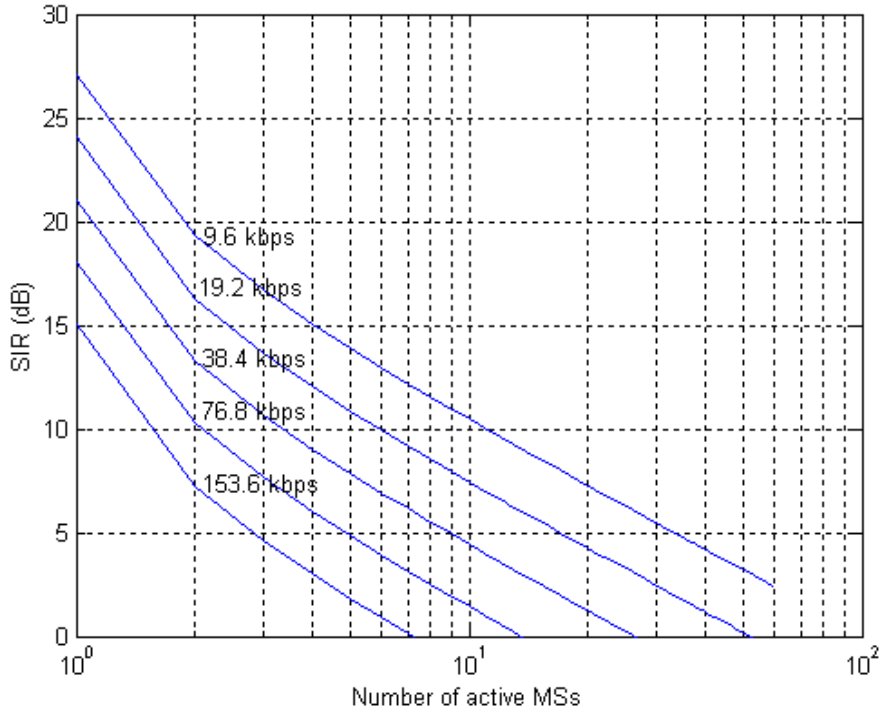

Figure 6.3 Equal SIR allocations when the rate adaptation is based on the VSF approach

Table 6.1 SIR threshold (γ_{th}) in dB for each data rate (R in kbps)

R	153.6	134.4	115.2	96.0	76.8	57.6	38.4	19.2	9.6
γ_{th}	8.12	8.07	8.02	7.95	7.87	7.76	7.60	7.31	7.0

The rate is updated every transmission frame (16 transmission slots) by the rate control scheme shown in the flowchart in Figure 6.4. First, the rate is set at the maximum possible level. Then we compute the equally allocated SIR of the assigned rate and compare it with the minimum required SIR (or threshold SIR) at the given rate. If this "equal SIR" is greater than the threshold SIR, the rate assignment of this frame is acceptable and completed. Otherwise, the rate must be decreased by one level. We recompute and compare the equal SIR with the threshold SIR at the new rate again. This procedure is repeated until the equal SIR is greater than the threshold SIR. However, this rate assignment is based on $f = 0$ which may be wrong. Therefore, the result of actual SIRs may be lower than the SIR threshold at the assigned rate from the approximation that assumes $f = 0$. If the actual interference is higher than or equal to I_{max} and all MSs' SIRs are lower than the threshold, then the radio resources are over-utilized and the assigned rate must be reduced by one step.

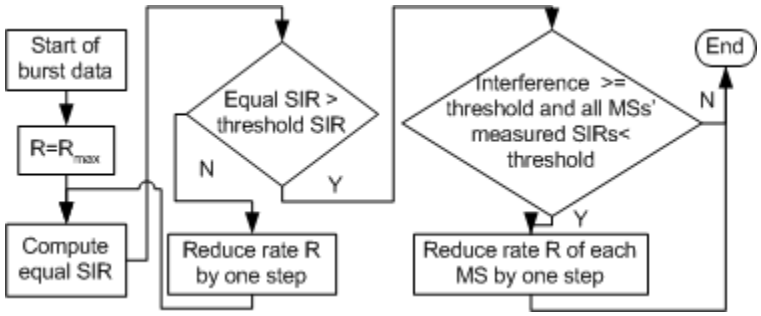

Figure 6.4 Flowchart of the equal rate control algorithm

6.2.5. Complexity analysis

The proposed rate and power control schemes are mainly based on the adaptive pricing algorithm and the equal rate control algorithm. Both algorithms are run independently at a BS although they require inputs from the outputs of each other. The computations of both algorithms in each update interval are very simple and their complexities can be represented by $O(N_j)$, where N_j is the number of MSs in a cell.

6.3. NUMERICAL ANALYSIS

6.3.1. Experimental design

The objective of this analysis is to examine the performance of the proposed schemes for both cases of MC and VSF. First, a single-cell scenario is employed to study the equal rate allocation of the proposed rate control and the effect of the pricing delta (Δ) on the convergence of the proposed rate and power control schemes. Then, a seven-cell scenario that produces the unknown extra-cell interference to the networks is considered in the performance analysis. In the seven-cell scenario, we assume that there is one center cell that is surrounded by six cells along its circumference.

A performance comparison with the traditional rate and power control schemes of 1x-EV-DO is also undertaken here. In 1x-EV-DO, rate control is performed based on the interference levels. When the reverse link interference level (I_o) is higher/lower than a threshold level, each BS will broadcast a bit 1/0 (called reverse activity – RA bit) to the MS. The RA bit is updated at intervals of four-frames and the rate is updated every frame. The MS then decides the data rate based on this RA bit in a probabilistic way [8]. A set of a probability pair, (p, q), is specified by the BS. Probability p (q) indicates the likelihood that a MS will decrease (increase) the transmission rate by one step when at least one (all) sector(s) in the active set has (have) the interference level(s) higher (lower) than the threshold value(s). The status of the interference level [50] whether it is higher or lower than a threshold is transmitted to MSs by the BS. In [8], the parameters are set as: $p = \max\{0, 0.5 \times (\text{current rate}/153.6)-0.1\}$ and $q = \max\{0, 0.4 -0.5 \times (\text{current rate}/153.6)\}$.

The response variables considered in this work are the effective rate, the interference level and the SIR. Only the results of the response variables associated with MSs in the center cell, which receive the most severe interference from all neighboring cells, are examined. The factor f that is required in approximating the initial pricing coefficient and the equal SIR is set to zero because this factor is not known in practice.

An on-off traffic model is employed to model the bursty data traffic source of each MS. In the literature, on-off durations with exponential distributions and a packet arrival rate of λ with a Poisson process are typically employed. The following traffic parameters are employed in this work. The on and off durations are exponentially distributed with means 1 and 10 seconds [82], respectively. The packet arrival rate (λ) according to the Poisson process is 2 packets/second [82]. The packet length is exponentially distributed with a mean of 2.25 Kbytes [83].

In this work, the maximum allowable transmit power is 1 watt. We assume the radius of each cell is 1 km. A simple path loss model is used in this study. The path loss as a function of distance from MS i to BS j (d_{ij}) is given by $h_{ij} = K/d_{ij}^{n}$. The constant K is equal to 0.097 and a path loss exponent n = 4 is assumed as in [14]. In this work, we consider the variation of K with distance or location that can occur because of shadow fading although the practical implementation of the proposed rate and power control algorithms does not require the exact value of K. The correlated shadow fading [77] with a mean of 0 dB and standard deviation of 7.5 dB is updated every transmission slot in our simulation.

The simulations presented below are performed using C-SIM. The initial locations and the moving directions of the MSs are randomly selected from a uniform distribution. All MSs are moving at a constant speed of 50 km/h. All MSs are allowed to move only in their own cell. In the simulation, the transmit power of each MS is updated every transmission slot (1.667 ms) and the rate is adjusted every transmission frame (26.67 ms). The iterative operations of the proposed rate control scheme are simulated as described in the flowchart of Figure 6.4. The proposed power control scheme, which is composed of the open loop and the closed loop power control, is periodically performed as described in Figure 6.1and Figure 5.3.

6.3.2. Rate allocation comparisons

This subsection examines rate allocation by assuming that two MSs are transmitting bursty data traffic in a single cell system. The sample simulations of rate control are shown in Figure 6.5 to Figure 6.7. Since the considered traffic is bursty, there is no data transmission for certain time intervals. The highest rate is assigned in our scheme for both cases of MC and VSF when there is only one active MS. In contrast, the highest rate is not always assigned even there is only one active MS in the case of 1x-EV-DO. When both MSs are active, the assigned rates are not equal in 1x-EV-DO but they are equal in our proposed scheme. The rates assigned to both active MSs in the case of MC are 115.2 kbps; whereas, they are 76.8 kbps in the case of VSF. This is because the MC approach can provide higher granularity of variable rate transmission than the VSF. Consequently, the throughput in the MC case can be higher than the VSF case.

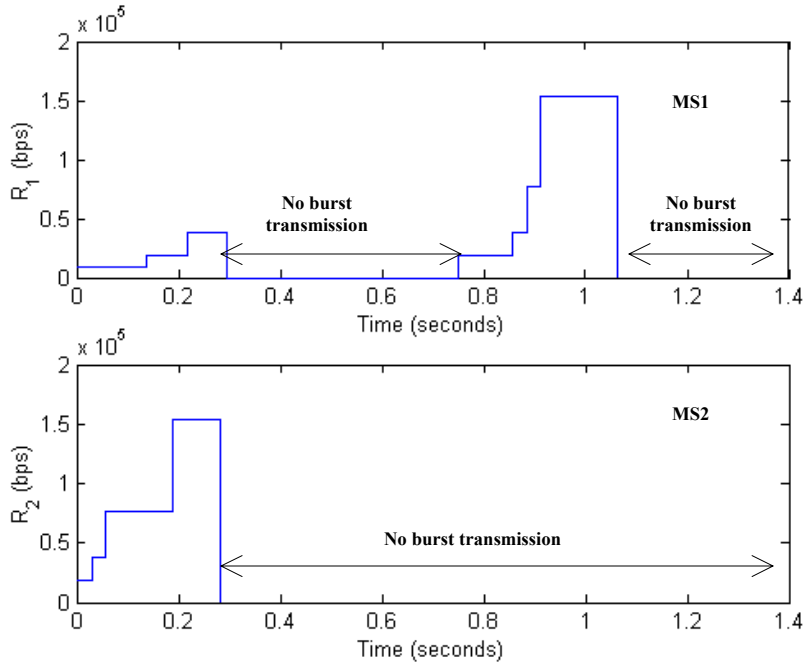

Figure 6.5 Sample simulation results of assigned rates in 1x-EV-DO

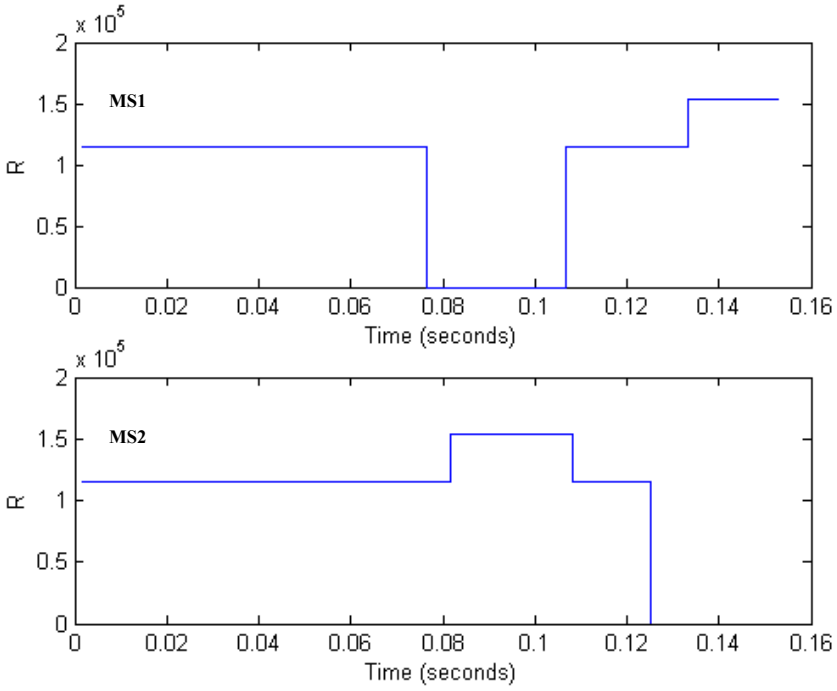

Figure 6.6 Sample simulation results of equal rate assignments (bps) based on MC in the proposed scheme

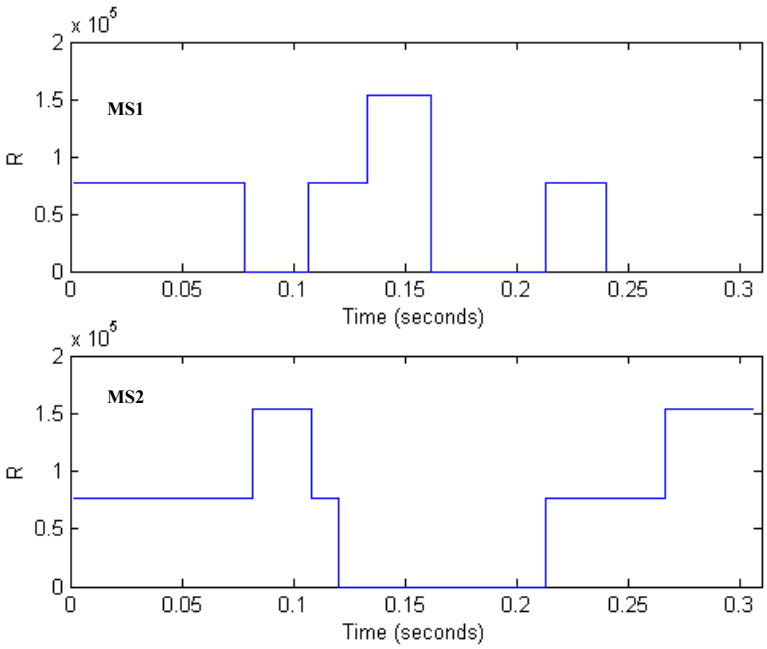

Figure 6.7 Sample simulation results of equal rate assignment (bps) based on VSF in the proposed scheme

6.3.3. Analysis of the sensitivity of the convergence of the proposed schemes to Δ

The Δ in power control determines the amount of change in the equilibrium received power in each update interval. Therefore, an appropriate value of Δ can provide fast convergence to the desirable SIR and threshold interference. Assume two MSs are transmitting bursty data in a cell. The assigned rates at each time are shown in Figure 6.6 and Figure 6.7. Three levels of Δ are examined: 1, 10 and 20 dB. When the interference converges to the threshold level, the SIR is close to the desired level (it can be less than the SIR in the equal allocation case of Figure 6.2 and Figure 6.3 because of the extra-cell interference).

Figure 6.8 to Figure 6.10 show the sample interference levels for MS1 and MS2 at each update interval in the MC case. The convergence of the interference to the threshold, which is about -167 dBm, can be determined by the number of update steps. The convergence rates of Δ = 1, 10 and 20 dB are not significantly different. The VSF case gives very similar results. Since the granularity of the rates in the case of MC is higher than the case of the VSF, the difference in the interference levels associated with the assigned rate in the case of the MC is lower than the case of VSF. Therefore, VSF requires more number of update intervals to reach the threshold interference than MC.

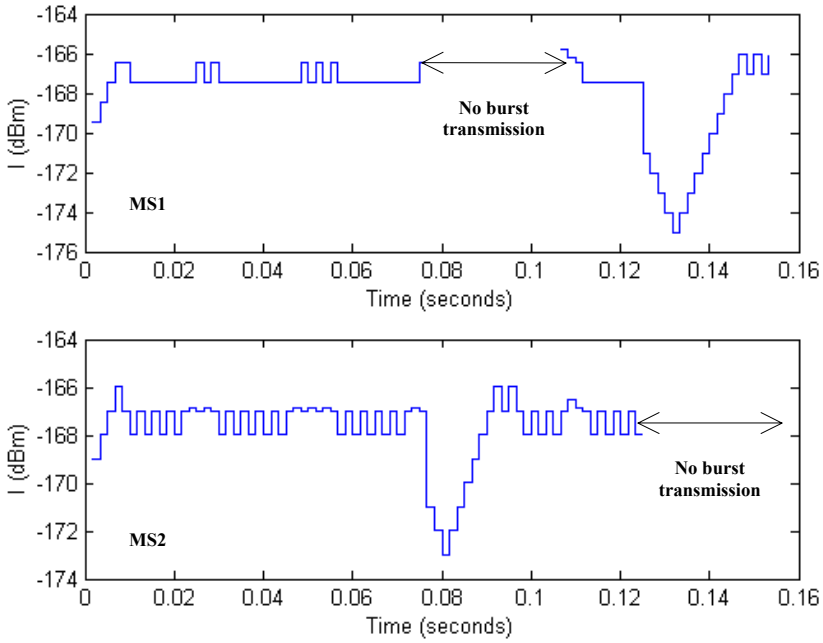

Figure 6.8 Sample simulation results for observing the convergence of interference to the threshold (-167 dBm) in the MC case when Δ=1dB

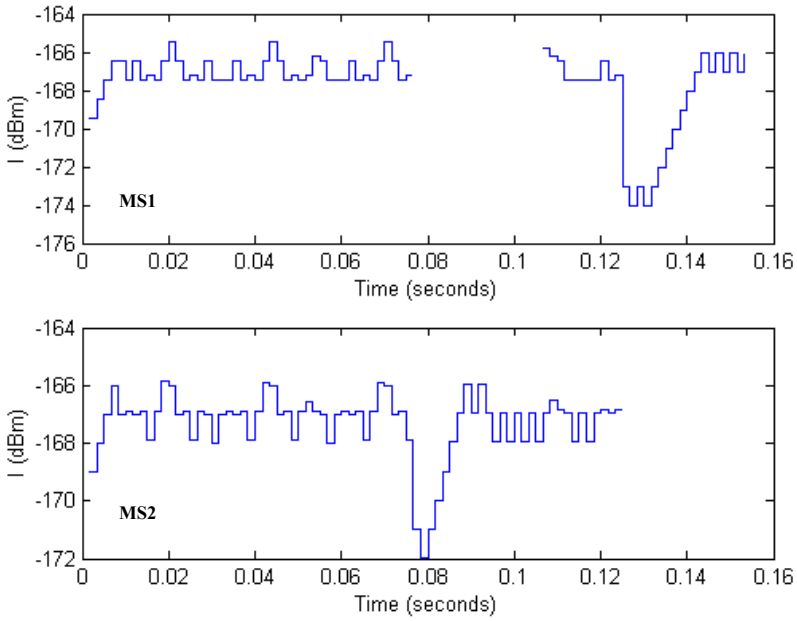

Figure 6.9 Sample simulation results for observing the convergence of interference to the threshold (-167 dBm) in the MC case when Δ=10dB

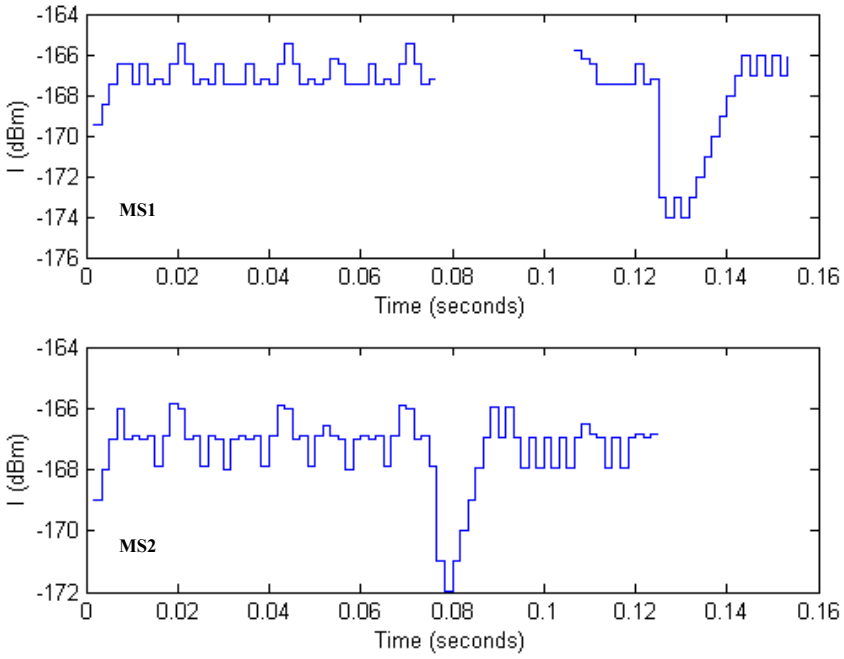

Figure 6.10 Sample simulation results for observing the convergence of interference to the threshold (-167 dBm) in the MC case when Δ=20dB

6.3.4. Simulation analysis of bursty and multi-rate transmissions

In the case of bursty transmission, the number of active MSs that transmit data at the same time is changed frequently because of the discontinuous transmission of the bursty traffic. In the first part of this section, eight MSs are simulated to examine the performance of the proposed schemes in the under-utilization case. The performance between the analyses in Figure 6.2 and Figure 6.3 and the traditional schemes in 1x-EV-DO is compared. The second part of this section studies the performance of the proposed schemes in the over-utilization case by simulating a large number of 22 MSs and it is compared with the 1x-EV-DO case. The simulation results in the case of eight moving MSs are given in Table 6.2 to Table 6.3 and Figure 6.11 to Figure 6.14. The simulation results in the case of 22 MSs are given in Figure 6.15 and Figure 6.16.

Table 6.2 and Table 6.3 show the rate assignment and *average* resulting SIR in the case of MC and VSF, respectively. In the tables, the average SIR from the simulation is compared with the equal SIR allocation (γ_{eq}) from Figure 6.2 and Figure 6.3. The average SIR from simulation when shadow fading is not included is closed to γ_{eq} from Figure 6.2 and Figure 6.3. Shadow fading deteriorates the average SIRs; however, they are still close to γ_{eq}.

Figure 6.11 and Figure 6.12 show the simulation results of the average effective rates and the average interference as a function of different numbers of active MSs when the proposed rate and power control schemes are employed. Shadow fading is not considered in these figures. These results are plotted with a 95% confidence interval. Figure 6.11 is comparable to the analysis results in Figure 6.2 and Figure 6.3. When there is only one active MS, the highest rate at 153.6 kbps can be assigned since the equal allocated SIR is 15 dB, which is higher than the required SIR at 8.12 dB (as shown in Table 6.2 to Table 6.3). When there are two active MSs, a rate of 153.6 kbps cannot be assigned since γ_{eq} in Figure 6.2 and Figure 6.3 is 7 dB which is lower than the required SIR of 8.12 dB in Table 6.1. Therefore, the next lower rate is examined. In the case of the VSF, the rate at 76.8 kbps is assigned. γ_{eq} in Table 6.3 at this rate is about 10.27 dB which is higher than the required SIR of this rate (7.87 dB as shown in Table 6.1). In contrast, a higher rate of 115.2 kbps in MC is assigned for the case of two active MSs. Although, the effective rate is lower than the assigned rate because of the bit errors, it is still higher than the VSF case. Similarly, the MC rate assigned in the case of three active MSs is 57.6 kbps which is higher than 38.4 kbps in the case of VSF. However, the assigned rates in both approaches are the same when the numbers of active MSs increases from 4 to 8 MSs because the available rates offered in both approaches are the same: 38.4 and 19.2 kbps. These results show that the MC approach, which has more granularity than VSF can potentially provide higher throughput. All the simulation results based on the proposed algorithm are close to the analytical analysis results of the equal SIR (γ_{eq}) and rate allocations as shown in Figure 6.11, Table 6.2 to Table 6.3. Correspondingly, the proposed rate and power control schemes can provide equal radio resource allocations to all MSs in a cell.

The simulation results of the probabilistic rate control scheme and the fixed target SIR power control in 1x-EV-DO are also plotted in Figure 6.11 and Figure 6.12. The effective rates of the proposed schemes are better than 1x-EV-DO when the number of MSs is less than 4. When the number of MSs is greater than or equal to 4, the effective rate of both the proposed and the traditional schemes are close to each other but the traditional schemes cause higher interference than the proposed schemes crossing the interference threshold level; on the contrary, the interference results of the proposed schemes are closed to the threshold (-167 dBm) as shown in Figure 6.12. Similarly, the traditional power and rate control schemes in 1x-EV-DO under-utilize the radio resources when the number of active MSs is less than 4 and over-utilize the radio resources when the number of active MSs is greater than or equal to 4.

Correlated shadow fading with a mean of 0 dB and the standard deviation of 7.5 dB as discussed in Equation (5.14) is included in the next results shown in Figure 6.13 and Figure 6.14. Shadow fading causes more channel variation and a higher probability of error. The difference in the performances of MC and VSF approaches becomes small as shown in Figure 6.13 and Figure 6.14. However, the proposed

schemes can provide higher rates and more completely utilize the radio resources (the interference is close to the threshold level) than 1X-EV-DO especially when the number of active MSs is small. As the number of active MSs increases, the proposed schemes do not cause interference higher than the threshold unlike 1x-EV-DO.

The next experiment simulates 22 MSs moving in each cell (the over-utilization case). All MSs use VSF in this case. The performance comparison between the proposed schemes and the traditional schemes in 1x-EV-DO are given in Figure 6.15 and Figure 6.16. Three plots are shown in each figure: two plots of the proposed schemes with and without shadow fading and one plot of the 1x-EV-DO schemes with shadow fading. When shadow fading is not included, the average effective rates of the proposed schemes shown in Figure 6.15 are close to the transmission rate of 9.6 kbps until the number of MSs exceeds 20. When the number of active MSs in a cell is 21 or 22, the effective rate in Figure 6.15 is reduced but the interference in Figure 6.16 remains near the threshold level. Including shadow fading in the simulation deteriorates the performance of the proposed schemes, i.e. the average effective rate is lower and the interference is higher than the case with no shadow fading. However, the interference in 1x-EV-DO is higher than the proposed scheme by around 20 to 30 dB (thus it supports higher effective rates than the proposed schemes). This will usually not occur and instead MSs will be rejected by admission control.

Table 6.2 Allocated rates (R in kbps) and average SIRs (γ in dB) in the case of employing the MC approach in the proposed schemes

	Number of active MSs in the center cell							
	1	2	3	4	5	6	7	8
R	153.6	115.2	57.6	38.4	38.4	19.2	19.2	19.2
γ (no fading)	13.40	7.97	8.40	8.54	7.70	9.45	8.86	8.26
Equal SIR (γ_{eq})	15.03	8.50	8.89	9.02	7.84	9.92	9.16	8.51
γ (fading)	13.02	6.94	7.86	8.10	7.36	8.02	7.81	7.60

Table 6.3 Allocated rates (R in kbps) and average SIRs (γ in dB) in the case of employing the VSF approach in the proposed schemes

	Number of active MSs in the center cell							
	1	2	3	4	5	6	7	8
R	153.6	76.8	38.4	38.4	38.4	19.2	19.2	19.2
γ (no fading)	14.92	10.21	10.46	8.95	7.80	9.78	9.02	7.95
Equal SIR (γ_{eq})	15.03	10.27	10.65	9.02	7.84	9.92	9.16	8.51
γ (fading)	12.28	8.79	9.37	7.52	6.53	8.63	8.17	7.46

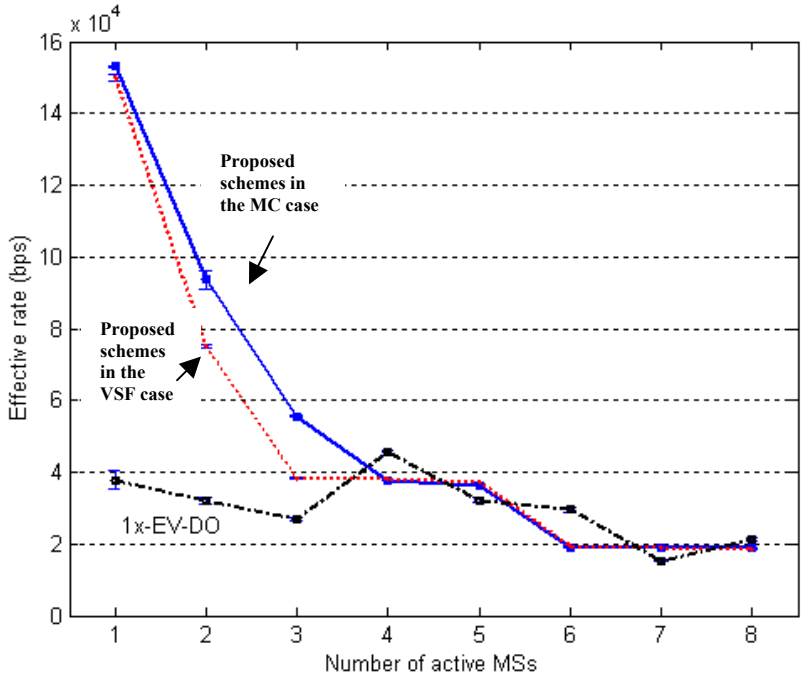

Figure 6.11 Average effective rate of each MS in the under-utilization case when the standard deviation of shadow fading is 0 dB

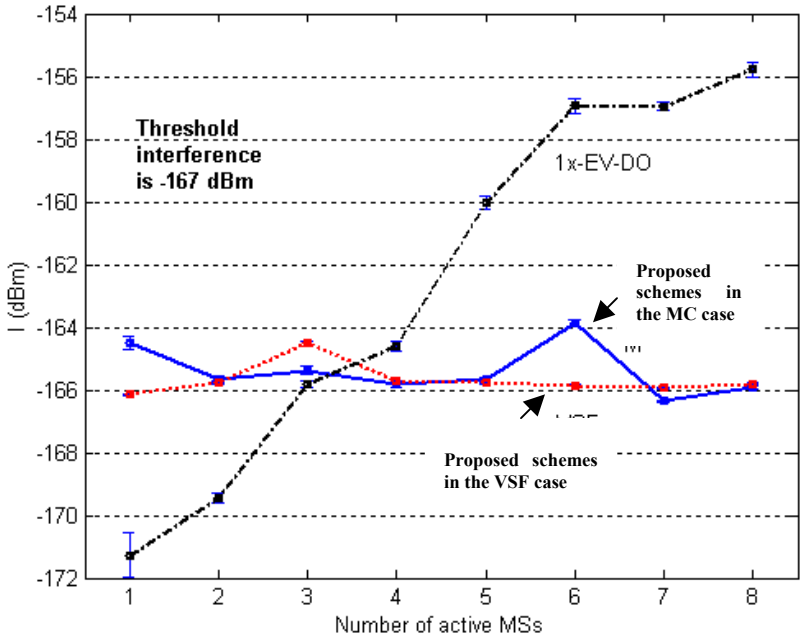

Figure 6.12 Average interference in the under-utilization case when the standard deviation of shadow fading is 0 dB

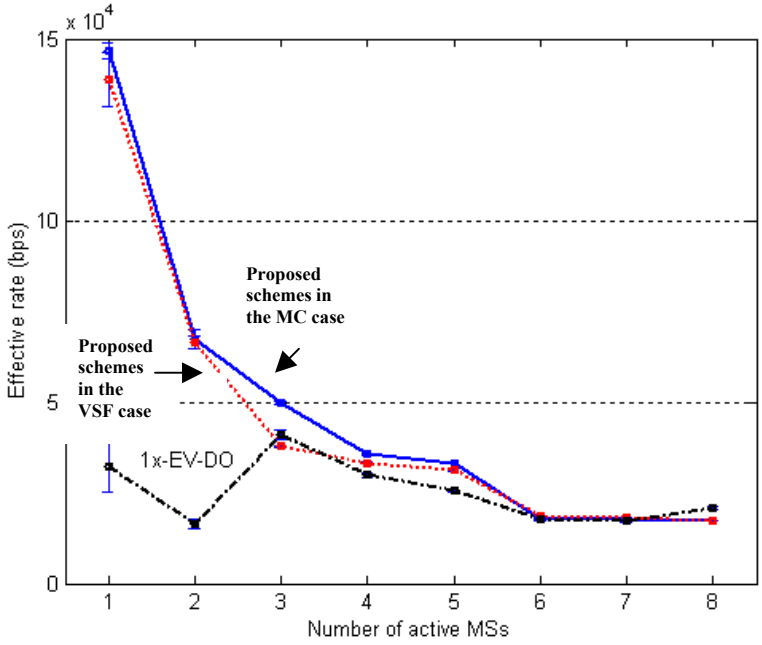

Figure 6.13 Average effective rate of each MS in the under-utilization case when the standard deviation of shadow fading is 7.5 dB

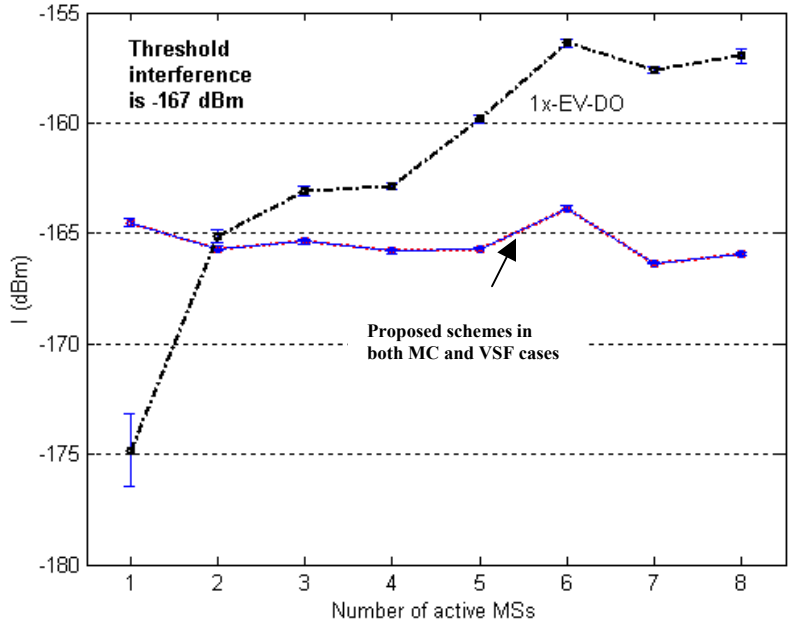

Figure 6.14 Average interference in the under-utilization case when the standard deviation of shadow fading is 7.5 dB

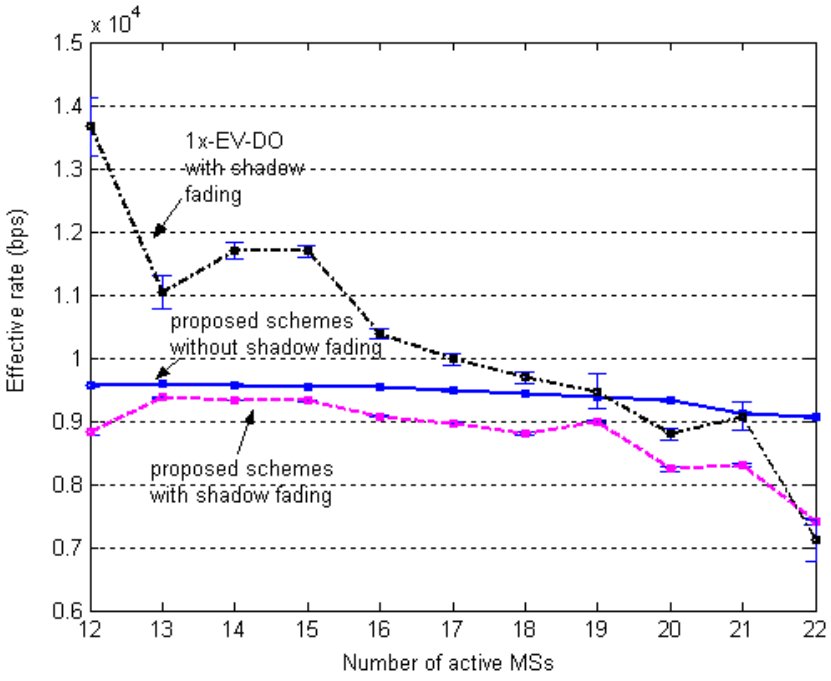

Figure 6.15 Average effective rate of each MS in the over-utilization case

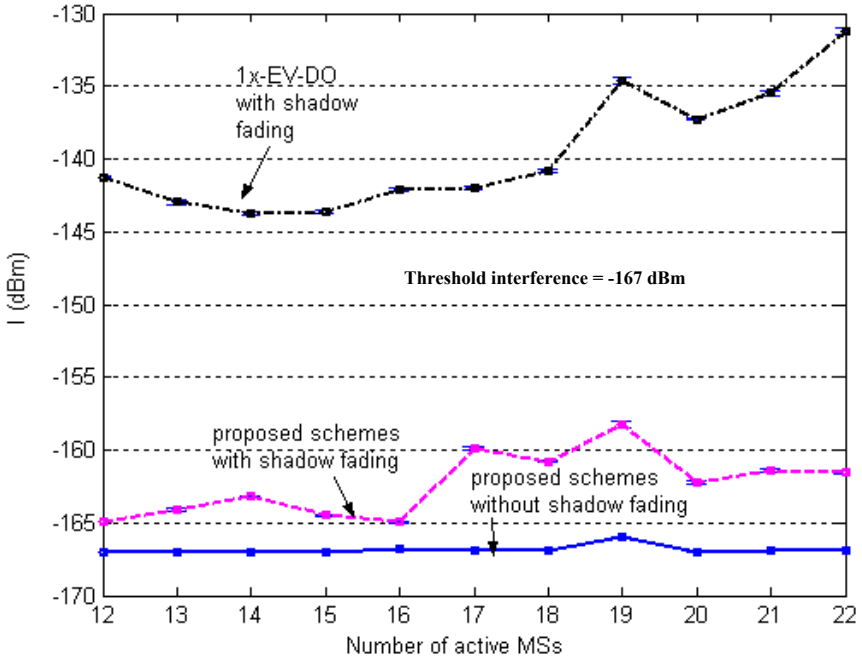

Figure 6.16 Average interference in the over-utilization case

6.3.5. Performance evaluation

This section shows the performance evaluation of the proposed rate and power control schemes compared with the 1x-EV-DO schemes. A seven-cell scenario and bursty transmission are assumed. Only VSF multi-rate approach is considered here. Four numbers of MSs in each cell are evaluated: 4, 8, 12, and 16 MSs. The response variable is the average effective rate per MS. The results in each cell are shown in the figures below. In Figure 6.17 to Figure 6.23, all MSs are assumed to moving at the same speed of 50 km/h. The proposed schemes can provide higher effective rates than the 1x-EV-DO schemes in the bursty transmission environments. When the number of MSs is close to the capacity (around 20 MSs when all of them are transmitting at 9.6 kbps and I_{max} is 1.99e-14 watts), the effective rates of both schemes are close to each other. The results of the center cell (cell no.1) in Figure 6.17 are similar to the results of other neighboring cells in Figure 6.18 to Figure 6.23 because the extra-cell interference of the center cell is not very high in this experiment.

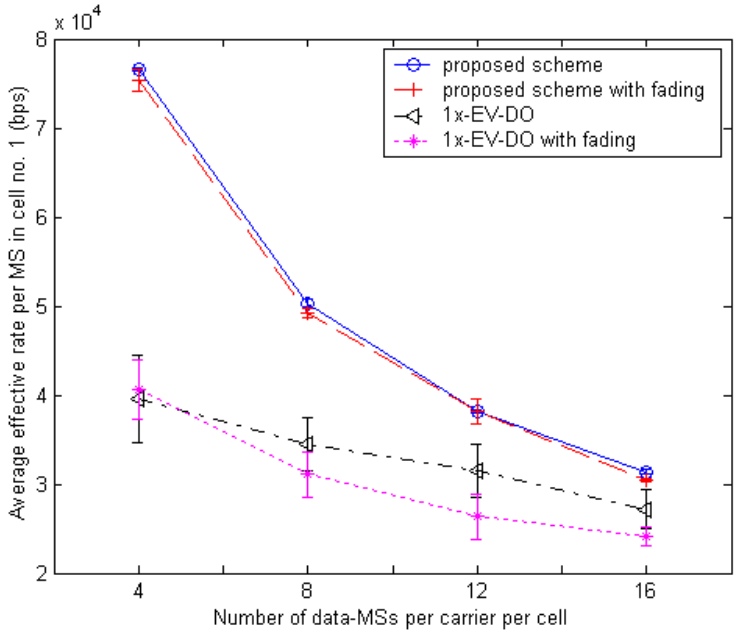

Figure 6.17 Average effective rates per MS in cell no. 1 (the centered cell) – all MS are moving at 50 kmph

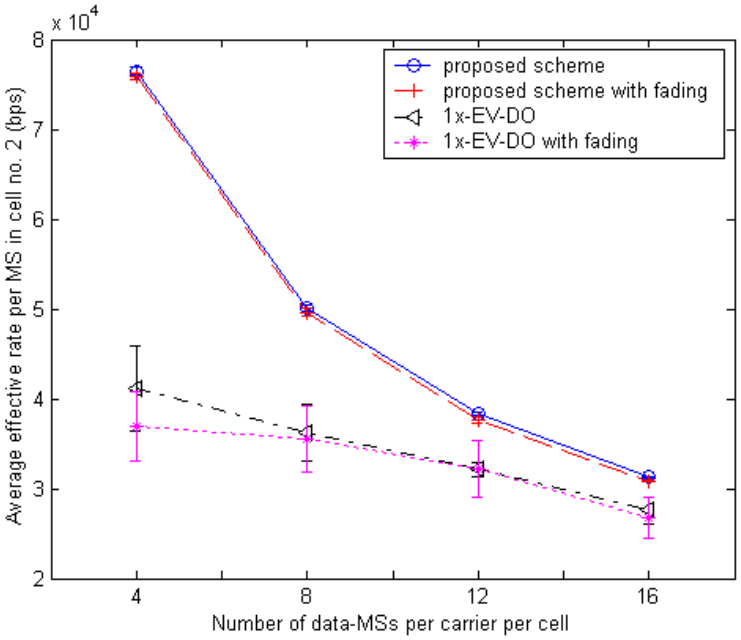

Figure 6.18 Average effective rates per MS in cell no. 2 – all MS are moving at 50 kmph

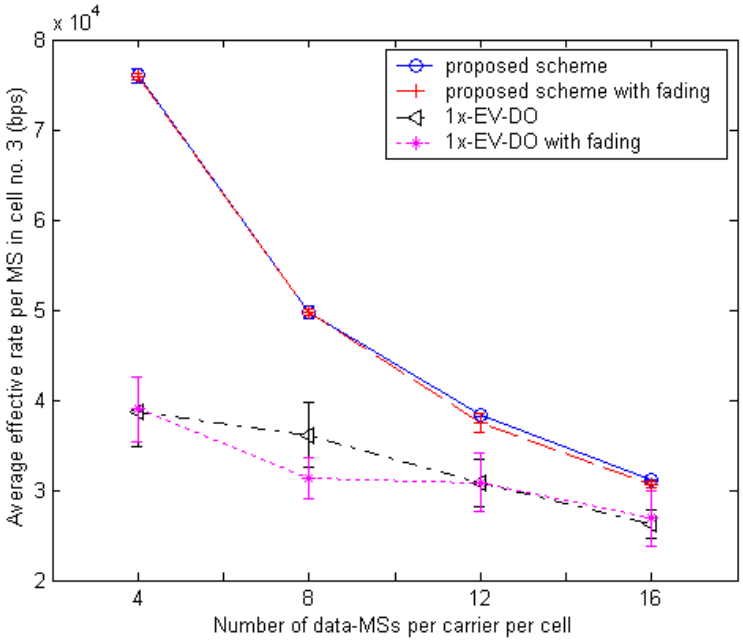

Figure 6.19 Average effective rates per MS in cell no. 3 – all MS are moving at 50 kmph

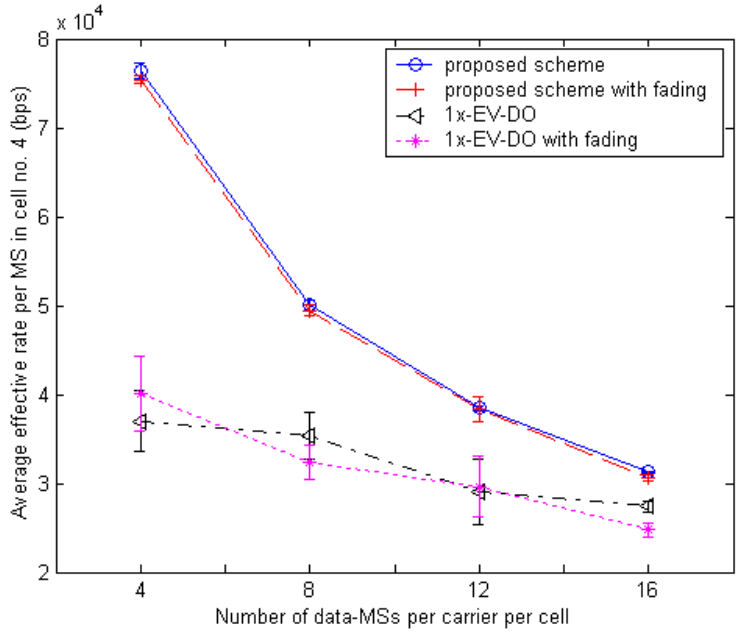

Figure 6.20 Average effective rates in cell no. 4 – all MS are moving at 50 kmph

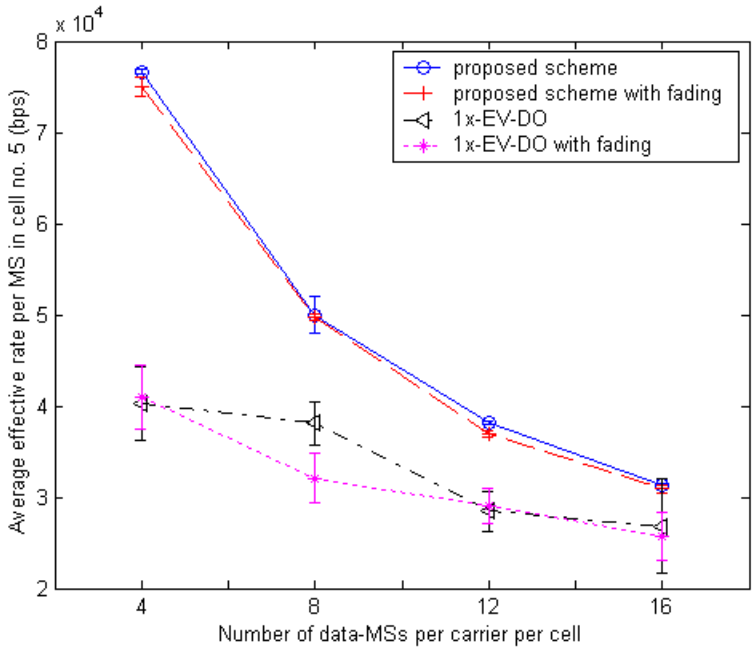

Figure 6.21 Average effective rates in cell no. 5 – all MS are moving at 50 kmph

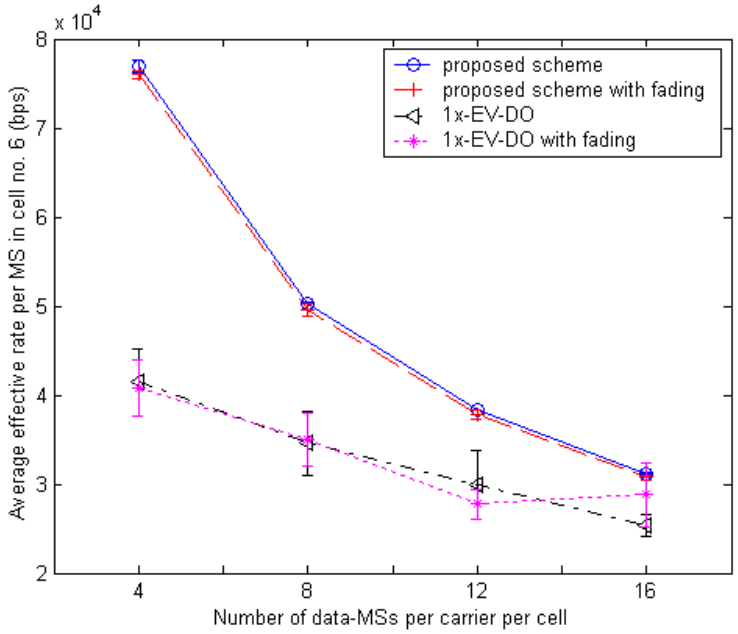

Figure 6.22 Average effective rates per MS in cell no. 6 – all MS are moving at 50 kmph

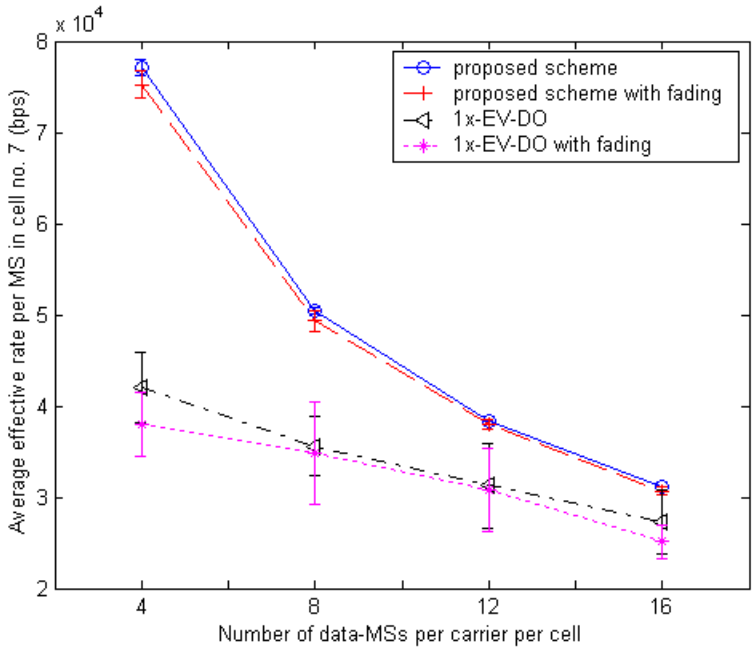

Figure 6.23 Average effective rates per MS in cell no. 7 – all MS are moving at 50 kmph

Next, the rate and power control algorithms are examined under a more realistic scenario where most of data-MSs are stationary users or pedestrians. In this evaluation, 70% of MSs are pedestrians (speeds are uniformly distributed between 0 to 5 km/h) and 30 % of MSs are high speed (uniformly distributed between 10 to 40 km/h) [85, 86]. The initial location of each MS is randomly located in each cell (the MS's location is different in each replication of the simulation). Several replications of the simulation are run (up to 20 runs) to get the 95% confidence interval. The effective rate results tested under bursty traffic environments are shown in Figure 6.24 to Figure 6.30. The results of the proposed schemes are compared with the schemes in 1x-EV-DO. The proposed schemes can provide higher effective rates than the schemes in 1x-EV-DO. When the number of MSs is larger, the effective rates of both schemes are close to each other. Additionally, these results (mixture of pedestrians and high speed moving users) are not very different from the results in the case of only high speed moving users in Figure 6.17 to Figure 6.23.

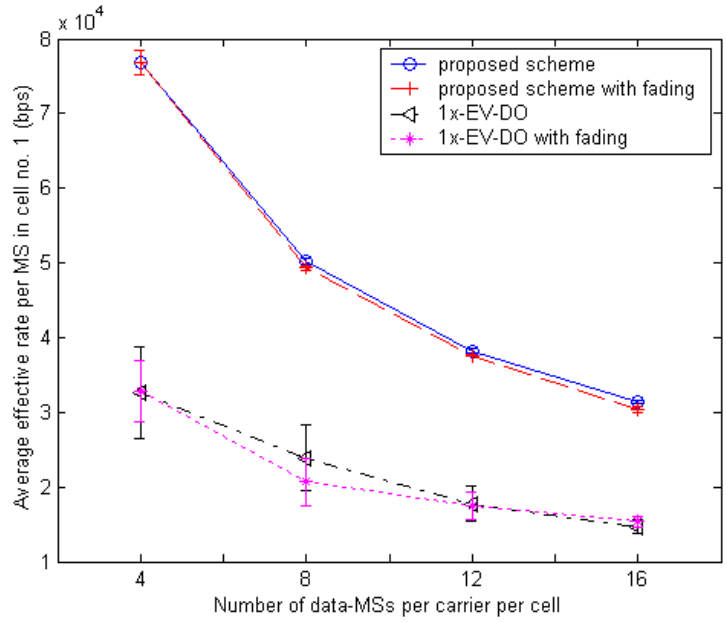

Figure 6.24 Average effective rates per MS in cell no. 1 – Mixture of pedestrians and moving MSs

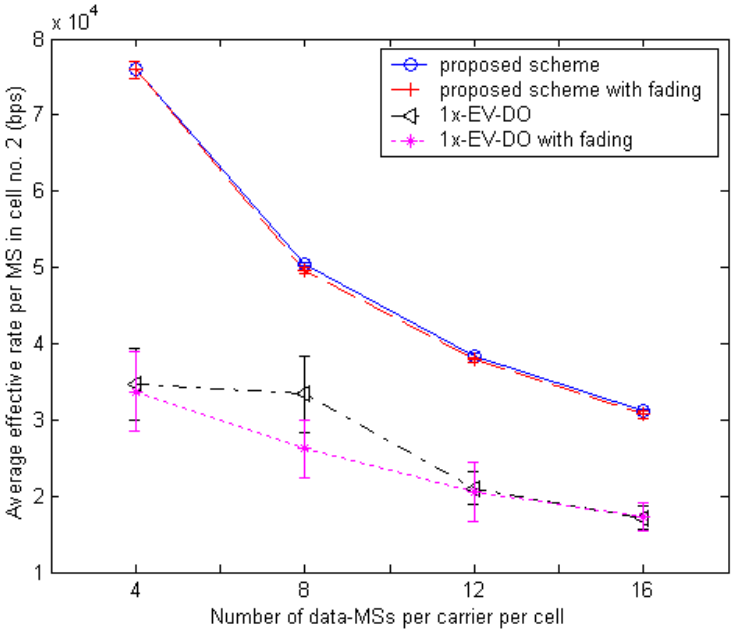

Figure 6.25 Average effective rates per MS in cell no. 2 – Mixture of pedestrians and moving MSs

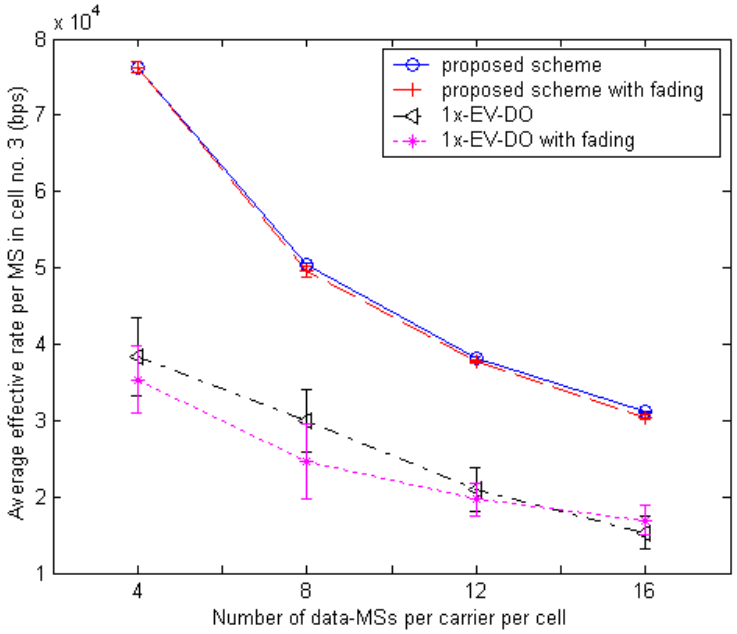

Figure 6.26 Average effective rates per MS in cell no. 3 – Mixture of pedestrians and moving MSs

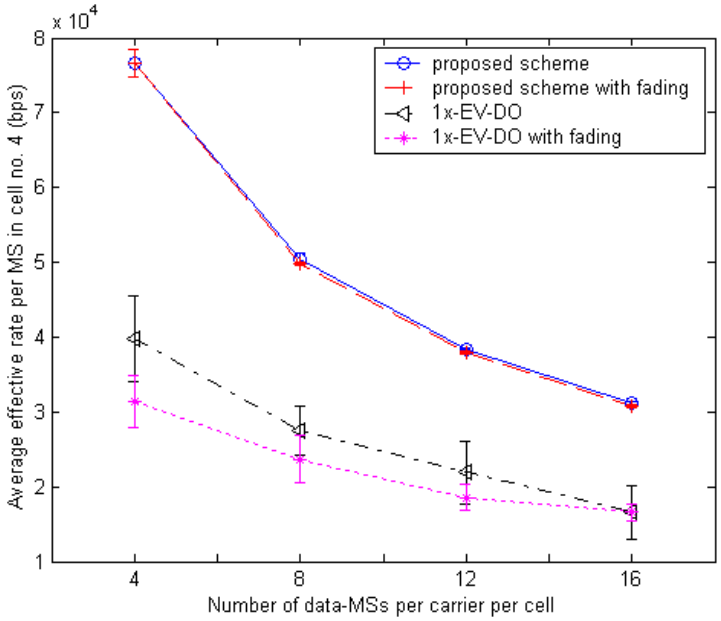

Figure 6.27 Average effective rates per MS in cell no. 4 – Mixture of pedestrians and moving MSs

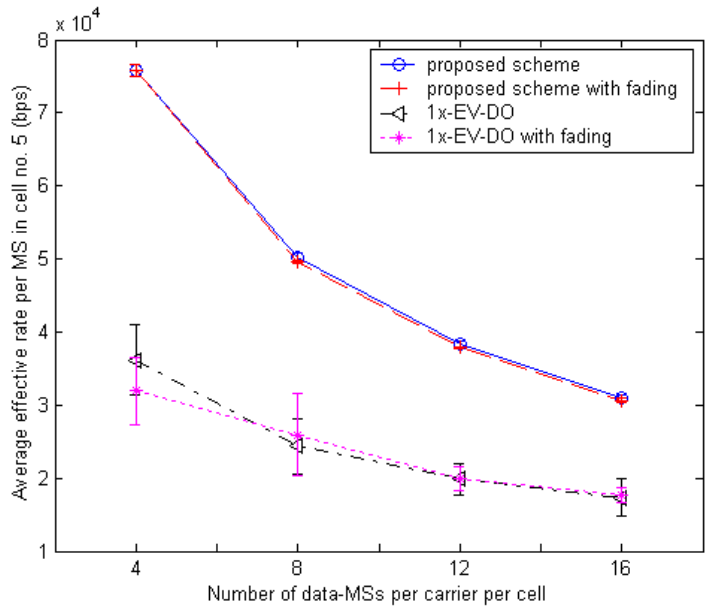

Figure 6.28 Average effective rates per MS in cell no. 5 – Mixture of pedestrians and moving MSs

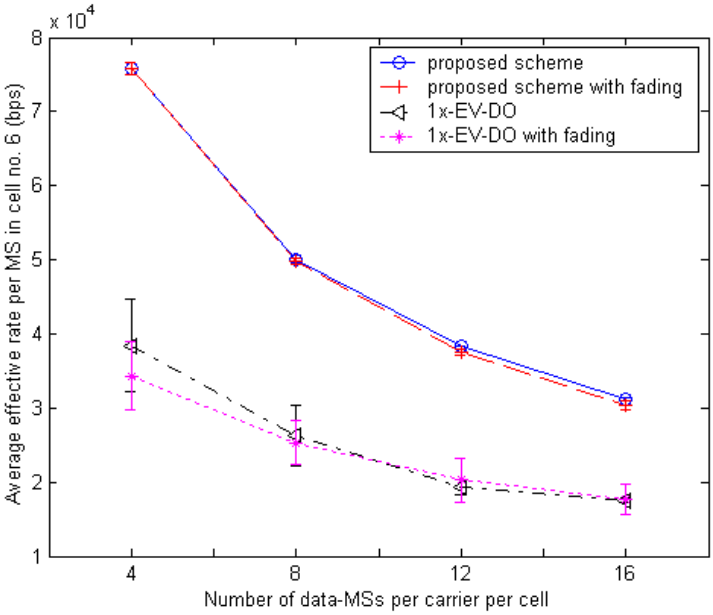

Figure 6.29 Average effective rates per MS in cell no. 6 – Mixture of pedestrians and moving MSs

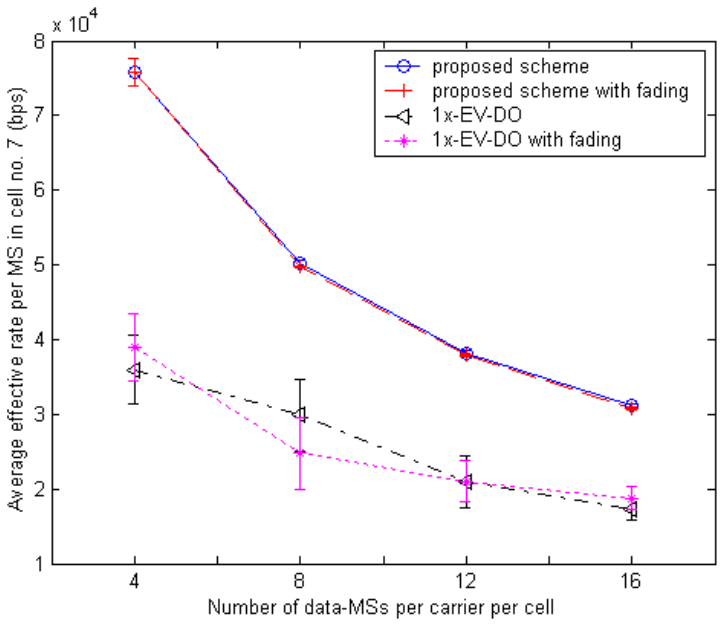

Figure 6.30 Average effective rates per MS in cell no. 7 – Mixture of pedestrians and moving MSs

6.4. CONCLUSIONS

The proposed rate and power assignments can provide high effective rates to all active MSs without causing the interference to become higher than a predefined level by implementing equal allocation and full utilization of radio resources. The proposed rate and power control schemes are examined via simulation and compared with the results from simplified analysis of equal resource allocation and full utilization. The proposed schemes can perform close to the analytical results. In addition, our approach can provide higher effective rates and SIRs while causing lower interference than the existing schemes used in 1x-EV-DO as per the simulation results. Both mobile data users and service providers can benefit from this new manner of radio resource management.

7.0 SUMMARY

Novel radio resource management (RRM) (rate assignment and power control) is studied in this dissertation. The proposed RRM scheme is distributed and it can completely utilize the available radio resources in each cell while assigning equal radio resources to each MS and maximizing each MS's throughput. Game theory is used as a basic tool in this study.

In the problem formulation using a game theoretical approach, a utility function that is a function of the effective rate and a pricing of power is employed. The first term, the effective rate, represents the data-MS's satisfaction in the sense of throughput. The second term, the pricing of power, is used to control the Nash equilibrium such that it reaches the desirable operating point. In order to eliminate the global information requirements as common knowledge for every MS, the proposed algorithms require the base station to assist in RRM by computing the appropriate rate and power. This utility function is compared with other utility functions from the literature. The proposed utility function is suitable for our approach because it is a strictly concave function and its Nash equilibrium can be varied over a wider range than other utility functions. Moreover, the Nash equilibrium of this utility function can be found in a closed form solution.

The desirable power and rate assignments are based on the idea of complete utilization and equal allocation of radio resources. The complete utilization of radio resources is specified by the maximum allowable interference level in each cell. Equal allocation of radio resources aims to assign the rate and power to each MS such that each of them obtains equal received power at the BS and the summation of all the received powers is not greater than the maximum allowable interference level. The number of active MSs at each update interval is used in the proposed RRM for assigning the amount of radio resources. However, the interference from neighboring cells is not known and it can be dynamically changing because of bursty transmissions. Therefore, the maximum allowable interference in a cell can also fluctuate. An adaptive pricing algorithm is proposed to deal with this fluctuation.

The traditional RRM scheme does not admit a high number of MSs when the signal quality is worse than a predefined level. This approach is suitable for voice but not for data. Since data communications can tolerate some transmission delay, the proposed RRM schemes can support more number of MSs than the traditional RRM schemes while providing equal radio resources to all MSs and maintaining the interference level closest to the maximum allowable level.

The proposed power control algorithm is integrated within the existing closed loop power control scheme that transmits a power feedback command from the BS to a MS to either increase or decrease its transmit power periodically. The proposed rate control scheme updates the transmission rate assigned to the MSs every time the number of active MSs is changed according to the bursty transmissions.

The evaluation of the proposed algorithms is examined in two aspects: algorithm running time and radio resource assignment performance. Two issues of the algorithm running time are studied: operation complexity and the convergence. The complexity of the algorithm can be represented by O(N), where N is the number of MSs in a cell. This complexity analysis indicates that the proposed algorithm is very simple. The convergence range of the proposed power control algorithms is derived. The convergence rates for different numbers of MSs are examined and found to be adequate. For the performance of the radio resource assignment, the proposed algorithms are examined for three cases: 1) Single rate and continuous transmission 2) Single rate and bursty transmissions 3) Multi-rate and bursty transmissions. The number of MSs is varied in each case to examine the performance under different load conditions. The response variables of signal to interference ratio (SIR) and interference are examined. The response variable of the effective rate is considered in the case of multi-rate transmissions.

In the first case, the accuracy of power control feedback command is examined. It is found that the perfect feedback power command provides ideal performance (the interference is always less than the threshold level); whereas, the 1-bit feedback power command gives acceptable performance (the interference is in the convergence range). In addition, two and seven cell scenarios are examined. Shadow fading is also considered. The simulation results are compared with the analytical results. The simulation results indicate that the proposed power control algorithms can perform closely to the analytical results. However, shadow fading that causes the radio signal fluctuations has an effect on the performance of the proposed power control algorithms (the average interference is out of convergence range) especially when the number of cells is seven and the number of MSs is higher than 25. Accordingly, the focus is restricted to a seven-cell scenario and includes the shadow fading.

In the second case, the proposed power control algorithms are modified for use in the case of bursty transmissions. The convergence analysis is provided and used for selecting the initial parameter in the adaptive pricing algorithm. The performance of the proposed power control algorithms is evaluated and compared with the traditional power control based on the fixed target SIR in a seven-cell scenario. The results show that the proposed algorithms perform closely to the best possible SIR assignments. The proposed algorithms can completely utilize the radio resources and maintain the interference level close to the predefined level. In contrast, the traditional power control under-utilizes the radio resources when the number of MSs is small.

In the third case, the rate and power control algorithms that can completely utilize the radio resources while providing equal radio resources are evaluated. Both approaches of rate adaptation techniques: variable spreading factor (VSF) and multi-code (MC) are studied in the problem formulation. From the study, we found that the formulations of the VSF approach and the MC approach are essentially the same. However, the difference is that the MC approach can provide more granularity of rate assignment than the VSF approach. The performance of the proposed schemes is evaluated and compared with the traditional schemes in 1x-EV-DO. The results show that the proposed schemes provide equal rates to all MSs; whereas, the rate control in 1x-EV-DO does not. When comparing the interference incurred at the BS, the proposed algorithms can control the interference closely to the threshold level but the schemes in 1x-EV-DO causes always more interference than the threshold level except when there are only a few active MSs. The proposed algorithms can provide higher average effective rates than the case of 1x-EV-DO when the 1x-EV-DO does not over-utilize the radio resources.

APPENDIX A

BIT ERROR RATE EXPRESSION

In the case of traditional power control, the transmit power of each MS is adjusted such that the received SIR at the BS is as close to the fixed target SIR (γ_{th}) as possible. For a given data rate R, the corresponding frame error rate (FER), and given radio propagation conditions, the target SIR that achieves this FER is fixed. Due to the changing environment, the target SIR may have to be adjusted periodically. In this study, the target SIR for the traditional power control is computed from the 1% FER requirement as follows:

$$FER = 1 - (1 - P_e)^M \tag{a.1}$$

Here M denotes the number of bits in each frame and P_e denotes the BER. Rearranging equation (a.1) we get:

$$P_e = 1 - 10^{\frac{1}{M}\log_{10}(1-FER)} \tag{a.2}$$

Figure A.1 below shows the relationship between FER and P_e at different values of M. A larger value of M can represent a higher rate when frame duration is fixed. This figure indicates that a larger M requires a higher P_e for the same level of FER.

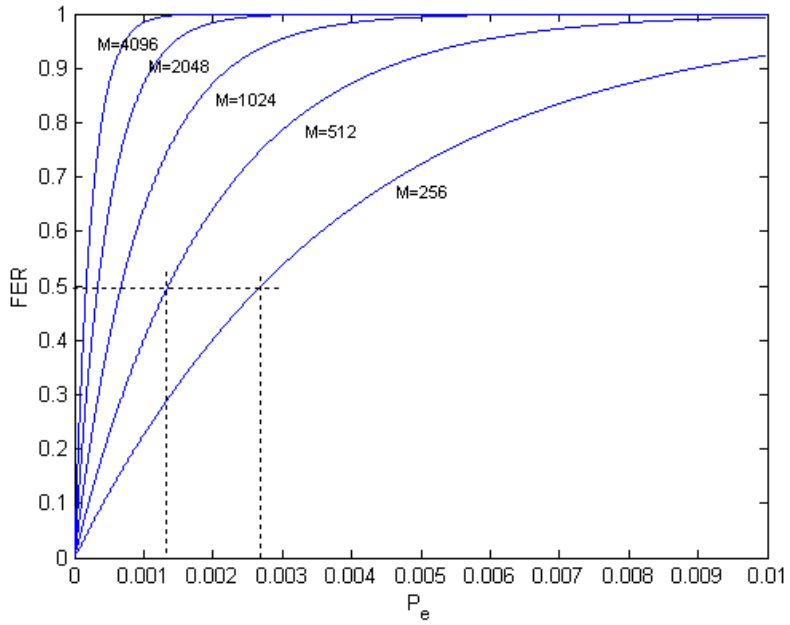

Figure A.1 *FER* and P_e relationship for different *M*

If noncoherent FSK modulation is assumed as in [14, 16], the bit error rate can be expressed as in (a.3)

$$P_e = \frac{1}{2} e^{\frac{-\gamma}{2}} \tag{a.3}$$

We can further rearrange equation (a.3) to obtain the SIR expression in term of the bit error rate as shown in (a.4).

$$\gamma = -2\ln(2P_e) \tag{a.4}$$

Substituting (a.2) into (a.4), we obtain the SIR as a function of the frame error rate and the number of bits in each frame as expressed in (a.5).

$$\gamma = -2\ln\left(2 - 2\times 10^{\frac{1}{M}\log_{10}(1-FER)}\right) \tag{a.5}$$

We use the frame format of 1x-EV-DO standard for evaluation. In 1x-EV-DO, one frame consists of 16 slots and each slot is 1.667 ms [50]. The power control update rate in this standard is 600 Hz [29]. Only the rate of 9.6 kbps is considered here. Therefore the number of bits in one frame is 1.667 ms × 16 × 9.6 kbps = 256 bits = *M*. Using *M* = 256 and FER = 0.01 in equations (a.2) and (a.5) and solving for P_e and γ_{th}

(SIR threshold) we get $P_e = 3.9345 \times 10^{-5}$ and $\gamma_{th} = 18.9$ (12.76 dB). If the rate is not 9.6 kbps, then γ_{th} is changed. This is the required target SIR if the bit error rate expression of noncoherent FSK is assumed.

In practice, the error rate of a transmitted packet is not determined by the employed modulation scheme only. The error rate is improved by signal processing techniques, error correction coding, interleaving, receiver architecture and so on [87]. The required SIR is actually lower than what is determined by the bit error rate expression of a specified modulation scheme and is quite complex to determine. A field test in IS-95 based cellular systems reports the minimum required SIR for 1% FER as 7 dB [75].

In this work, the bit error rate expression of non-coherent FSK modulation is modified to a general form such that it reflects a more realistic BER. The general form of the modified BER expression is shown in (a.6). A similar BER expression has also been employed in [70].

$$P_e = \alpha^{-1} e^{\frac{-\gamma}{\beta}} \tag{a.6}$$

The modified non-coherent FSK (Eqn. a.6) is used for the following reasons. The utility function is required to only be a function related to the user satisfaction and should represent this reasonably [69]. The realistic BER measurement in [88] also has a waterfall shape as the SIR increases. The modified non-coherent FSK form is a reasonable approximation that is mathematically tractable.

This new expression should give a bit error rate of 0.5 at SIR = 0 (not in dB), so $\alpha = 2$. Given the SIR threshold (γ_{th}), the number of bits per frame (M) and the required FER, the value of β can be solved as shown in (a.7):

$$\beta = -\gamma_{th} \times \ln\left(\alpha - \alpha 10^{\frac{1}{M}\log_{10}(1-FER)}\right) \tag{a.7}$$

If α=2, γ_{th}= 7 dB for 1 % FER and M = 256 bits for 9.6 kbps in the 1X-EV-DO systems, then β = 0.5304 from equation (a.7). The plot of the bit error rate versus SIR is shown in Figure A.2. These values of α and β are used in our performance analysis.

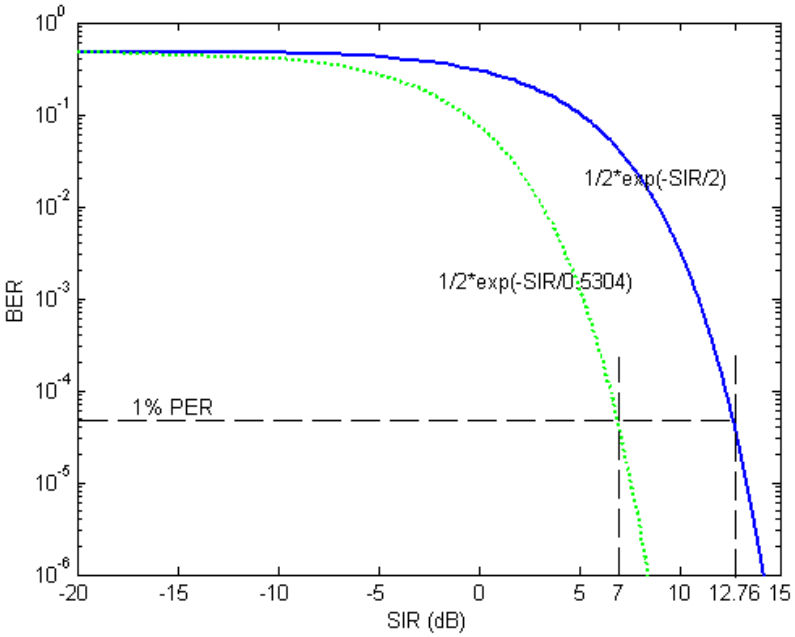

Figure A.2 BER as a function of the SIR

APPENDIX B

DERIVATION OF THE FEASIBLE RANGE OF THE PRICING COEFFICIENT

The existence of the Nash equilibrium is determined by the pricing coefficient. As long as $c_i>0$, the equilibrium always exists because the utility function in Equation (5.4) is a strict concave function [60]. However, the range of the pricing coefficient is limited by the strategy space of the transmit power defined by $\{p_{ij}: p_{ij} \in R^{+}, p_{ij} \leq p_{max}\}$. Accordingly, the feasible range of the pricing coefficient can be derived as explained below.

1) Equilibrium is exists when the equilibrium power is greater than 0 as shown in (b.1). By rearranging this equation, we can solve for c_i as shown in (b.2).

$$\hat{p}_{ij}^{r} = -\beta \frac{R_i\left(I_{ij}+\sigma^2\right)}{W} \ln\left[\alpha\beta c_i\left(\frac{I_{ij}+\sigma^2}{W}\right)\right] > 0 \tag{b.1}$$

$$c_i < \left[\alpha\beta\left(\frac{I_{ij}+\sigma^2}{W}\right)\right]^{-1} \tag{b.2}$$

2) Equilibrium exists when the equilibrium power is less than the maximum transmit power as indicated in (b.3). By rearranging this equation, we can solve for c_i as shown in (b.4).

$$\hat{p}_{ij}^{r} = -\beta \frac{R_i\left(I_{ij}+\sigma^2\right)}{W} \ln\left[\alpha\beta c_i\left(\frac{I_{ij}+\sigma^2}{W}\right)\right] \leq \overline{p} \tag{b.3}$$

$$\ln\left[\alpha\beta c_i\left(\frac{I_i+\sigma^2}{W}\right)\right] \geq \overline{p}_i\left[-\beta\frac{R_i\left(I_i+\sigma^2\right)}{W}\right]^{-1}$$

$$\alpha\beta c_i\left(\frac{I_i+\sigma^2}{W}\right) \geq \exp\left[-\frac{\overline{p}_i W}{\beta R_i\left(I_i+\sigma^2\right)}\right]$$

$$c_i \geq \frac{W}{\alpha\beta\left(I_{ij}+\sigma^2\right)} \exp\left[-\frac{\overline{p} W}{\beta R_i\left(I_{ij}+\sigma^2\right)}\right] \tag{b.4}$$

3) The exponential term in equation (b.4) is greater than zero as indicated in equation (b.5). Therefore, c_i is greater than zero, given that α and β are positive numbers. The Nash equilibrium always exists when the maximum transmit power is not zero.

$$\exp\left[-\frac{\overline{p}W}{\beta R_i\left(I_{ij}+\sigma^2\right)}\right]>0 \tag{b.5}$$

$$c_i \geq \frac{W}{\alpha\beta\left(I_{ij}+\sigma^2\right)}\exp\left[-\frac{\overline{p}W}{\beta R_i\left(I_{ij}+\sigma^2\right)}\right]>0 \tag{b.6}$$

APPENDIX C

INTRODUCTION TO GAME THEORY

Game theory is a powerful tool for modeling conflict interactions of various *objective* participants or players in a system. The result of a game theoretical analysis provides an *action* that each player should use to meet its objective requirements. A basic assumption of game theory is that each player is selfish (rational) and wants the outcome that maximizes its preference by selecting the action (strategy) appropriately based on the rules of the game. To model a problem as a game, we need players, a set of actions or strategies, and each player's payoff or utility function. The utility function maps the set of actions of all players (outcome) to a real number. The value of utility represents *a satisfaction quantity* of that set of actions. Note that the actions of one player affect the utility of all other players.

The game of *Prisoner's Dilemma* [89] as shown in Table C.1 is a classical example in game theory. Players in this game are criminals A and B. They are kept separately. A prosecutor makes an offer to each criminal: the reduction of years in jail if he confesses. Both A and B know the outcome in this conflict scenario that can be modeled as a non-cooperative game. The actions or strategies in this game are confess and deny. Table C.1 shows the payoffs or utilities as the number of years in jail for different cases of the actions by the criminals. Each criminal needs to select his strategy without knowing the opponent's decision – this is a simultaneous move game.

Table C.1 Prisoner's dilemma

A / B	Confess	Deny
Confess	**5**,5	**0**,10
Deny	**10**,0	**1**,1

If the game is played, it results in a Nash equilibrium [90]. The Nash equilibrium is the operating point where all players *do not have any incentives to unilaterally change their strategies* based on the

assumption that all players are rational. That is, the best decision for both criminals (the Nash equilibrium), in this case, is to confess.

BIBLIOGRAPHY

1. Smith, C. and D. Collins, *3G Wireless Networks*. 2002: McGraw-Hill.
2. Zander, J. and S.-L. Kim, *Radio Resource Management in Wireless Networks*. 2001: Artech House.
3. Pahlavan, K. and P. Krishanmurthy, *Principles of Wireless Networks: a Unified Approach*. 2002, New Jersey: Prentice Hall PTR.
4. Novakovic, D.M. and M.L. Dukic, *Evolution of the Power Control Techniques for DS-CDMA Toward 3G Wireless Communication Systems.* IEEE Communications Surveys, 2000: p. 2-15.
5. Jorguseski, L., et al., *Radio resource allocation in third generation mobile communication systems*, in *IEEE Communications Magazine*. 2001. p. 117-123.
6. Moustafa, M.N., et al., *QoS-Enabled Broadband Mobile Access to Wireline Networks*, in *IEEE Communications Magazine*. 2002. p. 50-56.
7. Pahlavan, K., et al., *Handoff in hybrid mobile data networks*, in *IEEE Personal Communications*. 2000. p. 34-47.
8. Esteves, E., *The High Data Rate Evolution of the cdma2000 Cellular System*, in *Multiaccess, Mobility and Teletraffic for Wireless Communications*. 2000, Kluwer Academic Publishers. p. 61-72.
9. Frodigh, M., et al., *Future-Generation Wireless Networks*, in *IEEE Personal Communications*. 2001. p. 10-17.
10. Garg, V.K., *Wireless Network Evolution 2G to 3G*. 2002: Prentice Hall.
11. Goodman, D.J. and N.B. Mandayam, *Power Control for Wireless Data*, in *IEEE Personal Communications*. 2000. p. 48-54.
12. Teerapabkajorndet, W. and P. Krishanmurthy. *A Game Theoretic Model for Power Control in Multi-rate Mobile Data Networks*. in *IEEE ICC*. 2003.
13. Sung, C.W. and W.S. Wong, *A Noncooperative Power Control Game for Multirate CDMA Data Networks.* IEEE Transaction on Wireless Communications, 2003. **2**(1): p. 186-194.
14. Saraydar, C.U., N.B. Mandayam, and D.J. Goodman, *Efficient Power Control via Pricing in Wireless Data Networks.* IEEE Transaction on Communications, 2002. **50**: p. 291-303.

15. MacKenzie, A.B. and S.B. Wicker, *Game theory and the design of self-configuring, adaptive wireless networks*, in *IEEE Communications Magazine*. 2001. p. 126-131.
16. MacKenzie, A.B. and S.B. Wicker. *Game Theory in Communications: Motivation, Explanation, and Application to Power Control*. in *IEEE Globecom*. 2001.
17. Ito, T., S. Sampei, and N. Morinaga. *A wireless packet transmission with adaptive processing gain and transmitter power control scheme for circuit-switched and packet-switched modes integrated DS/CDMA systems*. in *IEEE VTC*. 1999.
18. Lueng, K.K. and L.-C. Wang, *Integrated Link Adaptation and Power Control to Improve Error and Throughput Performance in Broadband Wireless Packet Networks.* IEEE Transaction on Wireless Communications, 2002. **1**: p. 619-629.
19. Oh, S.-J., D. Zhang, and K.M. Wasserman, *Optimal resource allocation in multiservice CDMA networks.* IEEE Transaction on Wireless Communications, 2003. **2**(4): p. 811-821.
20. Jafar, S.A. and A. Goldsmith, *Adaptive multi-rate CDMA for uplink throughput maximization.* IEEE Transaction on Wireless Communications, 2003. **2**(2): p. 218-228.
21. Xu, L., X. Shen, and J.W. Mark, *Dynamic fair scheduling with QOS constraints in multimedia wideband CDMA cellular networks.* IEEE Transactions on Wireless Communications, 2004. **3**(1): p. 60-73.
22. Bender, P., et al., *CDMA/HDR: a Bandwidth Efficient High Speed Wireless Data Service for Nomadic Users*, in *IEEE Communications Magazine*. 2000. p. 70-77.
23. Soong, A.C.K., et al., *Forward High-Speed Wireless Packet Data Service in IS-2000 -1x-EV-DV*, in *IEEE Communications Magazine*. 2003. p. 170-177.
24. Holma, H. and A. Toskala, *WCDMA for UMTS: Radio Access For Third Generation Mobile Communications*. 2000: John Wiley & Sons.
25. Pi, Z. and T. Derryberry. *CDMA2000 1x-EV-DV Reverse Link System Design*. in *IEEE WCNC*. 2003.
26. 3GPP, *Evolution of 3GPP System (Release 6)*, in *TR-T12-21.902 V6.0.0*. 2003. p. 1-16.
27. Ghosh, A., et al. *Overview of Enhanced Uplink for 3GPP W-CDMA*. in *IEEE VTC*. 2004.
28. Goodman, D.J., *Wireless Personal Communications Systems*. 1997: Addison Wiley.
29. Attar, R.A. and E. Esteves. *A Reverse Link Outer-Loop Power Control Algorithm for cdma2000 1xEV Systems*. in *IEEE ICC*. 2002.
30. Hanly, S. and D. Tse, *Power Control and Capacity of Spread-spectrum Wireless Networks.* Automatica, 1999. **35**: p. 1987-2012.
31. Zander, J., *Performance of optimum transmitter power control in cellular radio systems.* IEEE Transaction on Vehicular Technology, 1992. **41**: p. 57-62.

32. Grandhi, S.A.V., R.; Goodman, D.J.; Zander, J.;, *Centralized power control in cellular radio systems.* IEEE Transaction on Vehicular Technology, 1993. **42**(4): p. 466-468.
33. Wu, Q., *Performance of optimum transmitter power control in CDMA cellular radio systems.* IEEE Transaction on Vehicular Technology, 1999. **48**(2): p. 571-575.
34. Zander, J., *Distributed cochannel interference control in cellular radio systems.* IEEE Transaction on Vehicular Technology, 1992. **41**(3): p. 305-311.
35. Grandhi, S.A., R. Vijayan, and D.J. Goodman, *Distributed Power Control in Cellular Radio Systems.* IEEE Transaction on Communications, 1994. **42**(2/3/4): p. 226 -228.
36. Lee, T.H. and J.C. Lin, *A fully distributed power control algorithm for cellular mobile systems.* IEEE Journal on Selected Areas in Communications, 1996. **14**: p. 692-697.
37. Goodman, D.J., Z. Marantz, P. Orenstein, V. Rodriguez. *Maximizing The Throughput of CDMA Data Communications*. in *IEEE VTC*. 2003. Florida.
38. Goodman, D. and N. Mandayam, *Network assisted power control for wireless data.* Mobile Networks and Applications, 2001. **6**(5): p. 409-418.
39. Saraydar, C.U., N.B. Mandayam, and D.J. Goodman, *Pricing and Power Control in a Multicell Wireless Data Network.* IEEE Journal on Selected Areas in Communications, 2001. **19**(10): p. 1883 -1892.
40. Zander, J., *Radio Resource Management in Future Wireless Networks: Requirements and Limitations*, in *IEEE Communications Magazine*. 1997. p. 30-36.
41. Mitra, D. and J. Morrison, *A Distributed Power Control Algorithm for Bursty Transmissions on Cellular, Spread Spectrum Wireless Networks*, in *Wireless Information Networks*, J. Holtzman, Editor. 1996, Kluwer.
42. Ojanpera , T. and R. Prasad, *Wideband CDMA for Third Generation Mobile Communications*. 1998: Artech House.
43. Nanda, S., K. Balachandran, and S. Kumar, *Adaptation Techniques in Wireless Packet Data Services*, in *IEEE Communication Magazine*. 2000.
44. Chung, Y.-u., et al. *An efficient reverse link data rate control scheme for 1xEV-DV system*. in *IEEE VTC*. 2001.
45. Knisely, D.N., et al., *Evolution of wireless data services: IS-95 to cdma2000*, in *IEEE Communication Magazine*. 1998. p. 140-149.
46. Kumar, S. and S. Nanda, *High data-rate packet communications for cellular networks using CDMA: algorithms and performance.* IEEE Journal on Selected Areas in Communications, 1999. **17**: p. 472-492.

47. I, C.-L. and S. Nanda. *Load and interference based demand assignment (LIDA) for integrated services in CDMA wireless systems*. in *IEEE Globecom*. 1996.
48. So, J.-W., S.-S. Choi, and D.-H. Cho. *Efficient Resource Allocation Scheme for Reverse High Speed Operation in cdma2000 System*. in *IEEE VTC*. 2001.
49. Etemad, K., *Enhanced random access and reservation scheme in CDMA2000*, in *IEEE Personal Communications*. 2001. p. 30-36.
50. Chakravarty, S., R. Pankaj, and E. Esteves. *An Algorithm for Reverse Traffic Channel Rate Control for cdma2000 High Rate Packet Data Systems*. in *IEEE Globecom*. 2001.
51. Oh, S.J. and V. Vanghi. *HDR (1x-EV-DO) Reverse Link Throughput with Fast Rate Control*. in *IEEE WCNC*. 2002.
52. Fiorini, A. *Uplink user bitrate adaptation for packet data transmissions in WCDMA*. in *IEEE PIMRC*. 2000.
53. Koo, C., B. Bae, and J. Jung. *An Efficient Reverse Link Control Scheme for 3G Mobile Communication Systems*. in *IST*. 2002.
54. Yao, S. and E. Geraniotis. *Optimal power control law for multimedia multirate CDMA systems*. in *IEEE VTC 46th*. 1996.
55. Ulukus, S. and L.J. Greenstein. *Throughput maximization in CDMA uplinks using adaptive spreading and power control*. in *IEEE ISSSTA*. 2000.
56. Rodriguez, V., D.J. Goodman and Z. Marantz. *Power and Data Rate Assignment for Maximal Weighted Throughput in 3G CDMA: A Global Solution with Two Classes of Users*. in *IEEE WCNC*. 2004. Atlanta.
57. Rodriguez, V., and D.J. Goodman. *Power and Data Rate Assignment for Maximal Weighted Throughput in 3G CDMA*. in *IEEE ICC*. 2003. Alaska.
58. Feng, N., N.B. Mandayam, and D.J. Goodman. *Joint Power and Rate Optimization for Wireless Data Services Based on Utility Functions*. in *CISS*. 1999.
59. Recktenwald, G., *Numerical Methods with MATLAB Implementation and Application*. 2000, New Jersey: Prentice Hall.
60. Rosen, J.B., *Existence and Uniqueness of Equilibrium Points for Concave N-Person Games.* Econometrica, 1965. **3**(3): p. 520-534.
61. Chih-Lin, I. and K.K. Sabnani. *Variable spreading gain with adaptive control for true packet switching wireless network*. in *IEEE ICC*. 1995.
62. Chih-Lin, I. and R.D. Gitlin. *Multicode CDMA wireless personal networks*. in *IEEE ICC*. 1995.
63. Yang, S.C., *CDMA RF System Engineering*. 1 ed. 1998, Boston: Artech House. 280.
64. Sundaram, R.K., *A First Course in Optimization Theory*. 1996: Cambridge University Press. 357.

65. Teerapabkajorndet, W. and P. Krishnamurthy. *A Power Control Algorithm for Bursty Transmissions in Multi-cell Wireless Data Networks*. in *AlgorithmS for Wireless And mobile Networks (A-SWAN) in conjunction with the international conference on Mobiquitous*. 2004. Boston, USA.
66. Teerapabkajorndet, W. and P. Krishanmurthy. *Modeling Power Control Using Game Theory for the Reverse Link in CDMA Systems*. in *MPRG/Virginia Tech Symposium*. 2003.
67. Teerapabkajorndet, W. and P. Krishnamurthy. *Rate and Power Control on a Reverse Link for Multi-cell Mobile Data Networks*. in *IEEE/ACM MSWIM*. 2004. Venice, Italy.
68. Teerapabkajorndet, W. and P. Krishanmurthy. *A Power Control Algorithm based on Game Theory for Multi-cell Wireless Data Networks*. in *IEEE Adaptive Wireless Networks (AWiN)*. 2004. Texas, USA.
69. Xiao, M., N.B. Shroff, and E.K.P. Chong, *A utility-based power-control scheme in wireless cellular systems.* IEEE/ACM Transactions on Networking, 2003. **11**: p. 210-221.
70. Kim, J.B. and M.L. Honig, *Resource Allocation for Multiple Classes of DS-CDMA Traffic.* IEEE Transaction on Vehicular Technology, 2000. **49**(2): p. 506-518.
71. Nisan, N. and A. Ronen, *Algorithmic mechanism design.* Games and Economic behavior, 2001. **35**: p. 166-196.
72. Nisan, N. *Algorithms for Selfish Agents Mechanism design for distributed computation*. in *Symposium on Theoretical Aspects of Computer Science (STACS)*. 1999.
73. Cruz, J.B., *Leader-Follower Strategies for Multilevel Systems.* IEEE Transaction on Automatic Control, 1978. **23**(2): p. 244-254.
74. Korilis, Y.A., A.A. Lazar, and A. Orda, *Achieving Network Optima Using Stackelberg Routing Strategies.* IEEE/ACM Transactions on Networking, 1997. **5**(1): p. 161-173.
75. Padovani, R., *Reverse Link Performance of IS-95 Based Cellular Systems*, in *IEEE Personal communications*. 1994. p. 28-34.
76. Kim, D., *On the Convergence of Fixed-Step Power Control Algorithms with Binary Feedback for Mobile Communication Systems.* IEEE Transaction on Communications, 2001. **49**(2): p. 249-252.
77. Gudmundson, M., *Correlation model for shadow fading in mobile radio systems.* IEEE Electronoics Letters, 1991. **27**(23): p. 2145-2146.
78. Zonoozi, M.M. and P. Dassanayake. *Shadow fading in Mobile Radio Channel*. in *IEEE PIMRC*. 1996.
79. Jeong, D.G. and W.S. eon, *Congestion Control Schemes for Reverse Link Data Transmission in Multimedia CDMA Systems.* IEEE Transaction on Vehicular Technology, 2003. **52**(6): p. 1489-1496.

80. Janevski, T., *Traffic analysis and design of wireless IP networks*. 2003, MA: Artech House. 368.
81. Das, K. and S.D. Morgera, *Interference and SIR in Integrated Voice/Data Wireless DS-CDMA Networks-A Simulation Study*. IEEE Journal on Selected Areas in Communications, 1997. **15**(8): p. 1527-1538.
82. Ding, L. and J.S. Lehnert, *An Uplink Power Control Based on Truncated Channel Inversion for Data Traffic in a Cellular CDMA System.* IEEE Transactions on Vehicular Technology, 2001. **50**(3): p. 854-866.
83. Mandyam, G. and J. Lai, *Third-generation cdma systems for enhanced data services*. 2002, San Diego, California: Academic Press. 275.
84. Chih-Lin, I., et al. *Performance of multi-code CDMA Wireless Personal Communications Networks*. in *IEEE VTC*. 1995.
85. Kourtis, S. and R. Tafazolli. *Cell Dimensioning under General User Mobility*. in *IEE 3G Mobile Communication Technologies*. 2001.
86. Markoulidakis, J.G. and G.L. Lyberopoulos, *Mobility Modeling in Third Generation Mobile Telecommunications Systems*, in *IEEE Personal Communications*. 1997. p. 41-56.
87. Viterbi, A.J., *CDMA Principles of Spread Spectrum Communication*. 1 ed. 1995: Addison Wesley Longman. 245.
88. Ottoson , T. and A. Svensson, *Multi-rate performance in DS/CDMA Systems*, in *Technical Report no. 14, ISSN 0283-1260*. 1995, Dept. of Information Theory, Chalmers University of Technology: Goteborg, Sweden.
89. Fudenberg, D. and J. Tirole, *Game Theory*. 1992, Cambridge: The MIT Press.
90. Nash, J., *Non-Cooperative Games.* Annals of Mathematics, 1951. **54**: p. 286-295.